Some remarks on SPEEDY AGCM

(ver. 41.5 [ver41])

Followed by some examples of teleconnections research with SPEEDY

Thanks to Martin King for initially developing this part

Local thermodynamic equilibrium

The 'parcel' size of such a mixture if gases (e.g. atmosphere) could be in the order of mm for theoretical description and use of local thermodynamics equilibrium, or in the order of 100 km for numerical models of climate.

'Infinitesimal' Parcel of air

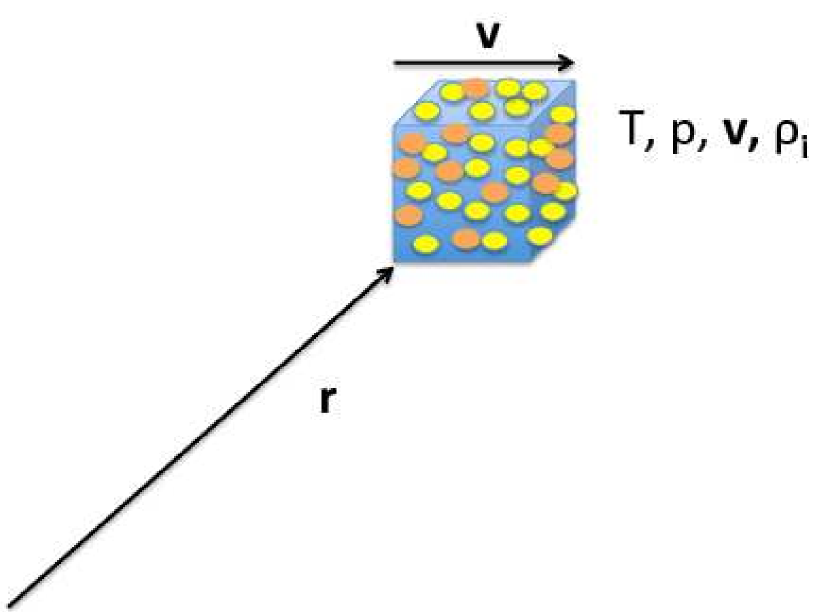

Note that this absolutely does not imply global thermodynamic equilibrium; indeed, the contrary is the case

Non-Hydrostatic Equations for Atmosphere (well known to some extent)

$$\rho \frac{d\mathbf{v}}{dt} = -\nabla p - 2\rho \boldsymbol{\Omega} \times \mathbf{v} - \rho \nabla \phi - \nabla \cdot \mathbf{F}$$

Momentum or Navier-Stokes Eqs.

$$\frac{\partial \rho}{\partial t} + \nabla \cdot (\rho \mathbf{v}) = 0$$

Mass balance or continuity Eq.

$$c_p \frac{dT}{dt} - \alpha \frac{dp}{dt} = Q - L_c \frac{dq}{dt}$$

Energy or thermodynamics Eq.
including latent heat release by cond.

$$\rho \frac{dq}{dt} = S$$

Eqs. for any important mass fraction
that we may want to distinguish and follow,
here water vapor, S=diffusion,
phase changes, evaporation at surface

$$p = \rho R T$$

Perfect Gas Law

This system of partial differential equations is coupled and nonlinear, has to be solved on the computer by discretizing. Processes circled in red are unresolved, sometimes not well known and need to be parameterized.

Sometimes we can be lucky to be able to simplify the Eqs, otherwise..number crunching!

ICTP The Abdus Salam International Centre for Theoretical Physics

Note that whenever there is a monotonic relationship between a variable andt he height z, then we can introduce a new vertical coordinate using this varible as independent height variable. For the atmosphere, the pressure is such a quantity due to hydrostatic balance, which is very well fulfilled for large-scale flows.

Basic equations

Thermo-Hydrodynamic equations in pressure coordinate system

$$\frac{d\mathbf{v}}{dt} = -f\mathbf{k} \times \mathbf{v} - \nabla\Phi + \mathbf{F} \quad , \qquad \text{Momentum} \qquad (1)$$

where $\mathbf{v} = \mathbf{i}u + \mathbf{j}v$.

$$\frac{dT}{dt} = \frac{RT}{c_p p}\omega + \frac{Q}{cp} \quad , \qquad \text{Energy} \qquad (2)$$

where $\omega = dp/dt$ (called the 'omega' vertical velocity), R is the gas constant, Q is the diabatic heating.

$$\frac{\partial\Phi}{\partial p} = -\frac{RT}{p} \quad . \qquad \text{Hydrostatic} \qquad (3)$$

$$\nabla \cdot \mathbf{v} + \frac{\partial\omega}{\partial p} = 0 \ . \qquad \text{Continuity} \qquad (4)$$

$$\frac{dq}{dt} = S \quad , \qquad \text{Moisture} \qquad (5)$$

Basic equations

However, the equations used in SPEEDY are posed in the $\sigma = p/p_s$ coordinate system (very similar) [Bourke, 1974, A multi-level spectral model I. formulation and hemispheric integrations, Monthly Weather Review, 102, pp.687-701.]

$$\frac{d\mathbf{v}}{dt} = -f\mathbf{k}\times\mathbf{v} - \nabla\Phi - RT\nabla p_s + \mathbf{F}, \qquad \text{Momentum} \qquad (6)$$

$$\frac{dT}{dt} = \frac{RT}{c_p}\left(\frac{\dot\sigma}{\sigma} - \frac{\partial\dot\sigma}{\partial\sigma} - \nabla\cdot\mathbf{v}\right) + \frac{Q}{cp} \quad , \qquad \text{Energy} \qquad (7)$$

$$\frac{d\ln p_s}{dt} = -\nabla\cdot\mathbf{v} - \frac{\partial\dot\sigma}{\partial\sigma} \qquad \text{Continuity} \qquad (8)$$

$$\frac{\partial\Phi}{\partial\sigma} = -\frac{RT}{\sigma} \quad . \qquad \text{Hydrostatic} \qquad (9)$$

$$\frac{dq}{dt} = S \quad , \qquad \text{Moisture} \qquad (10)$$

Basic equations

Alternatively to **v** we can use the vorticity ($\xi = \mathbf{k} \cdot \nabla \times \mathbf{v}$) and divergence $D = \nabla \cdot \mathbf{v}$ equations by applying $\mathbf{k}\nabla\times$ and $\nabla\cdot$ to the horizontal momentum equations, and $\xi = \nabla^2\psi$, $D = \nabla^2\chi$, and inverting the ∇^2*operator*, which is easy in spectral space (see later), thus deriving equations for ψ and χ.

The physiology of SPEEDY:

1. Dynamical core—equations of motion in spectral form

Streamfunction

$$\psi = a^2 \sum_{m=-J}^{+J} \sum_{l=|m|}^{|m|+J} \psi_l^m Y_l^m$$

Velocity potential

$$\chi = a^2 \sum_{m=-J}^{+J} \sum_{l=|m|}^{|m|+J} \chi_l^m Y_l^m$$

Temperature

$$T = \sum_{m=-J}^{+J} \sum_{l=|m|}^{|m|+J} T_l^m Y_l^m$$

ln(p_{surf})

$$q = \sum_{m=-J}^{+J} \sum_{l=|m|}^{|m|+J} q_l^m Y_l^m$$

where $Y_l^m = P_l^m(\sin\phi)e^{im\lambda}$.

The prognostic variables, are vorticity $\xi = \nabla^2\psi$, divergence $D = \nabla^2\chi$,

Temperature T and logarithm of surface pressure, ln(surface presssure).

N.B. For simplicity of presentation here, I will only use *q* to illustrate the method, to read more details including meanings of symbols, see Bourke, 1974, A multi-level spectral model I. formulation and hemispheric integrations, Monthly Weather Review, 102, pp.687-701.

Spectral Triangular Truncation

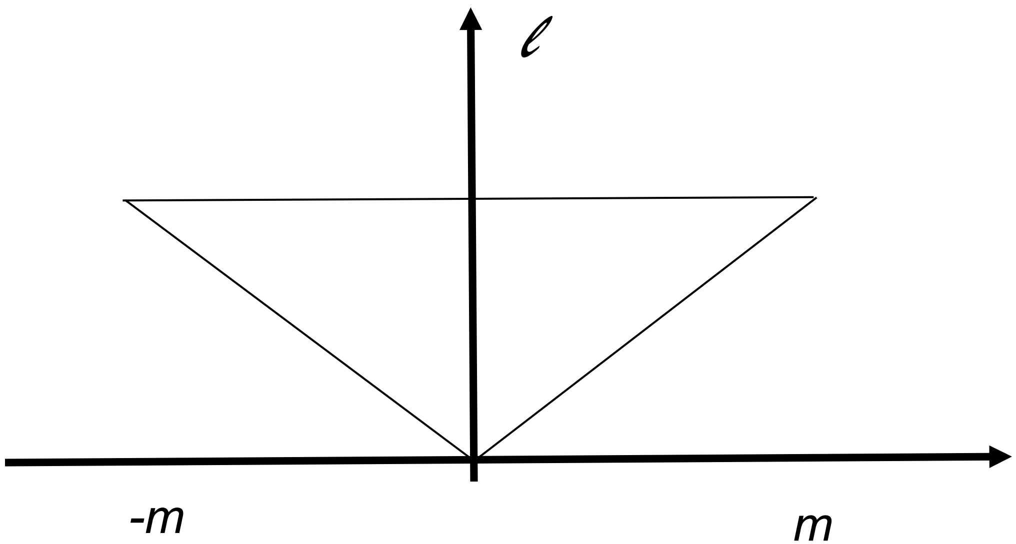

$$\psi = \sum_{m=-J}^{J} \sum_{l=|m|}^{J} \psi_l^m Y_l^m$$

where

$$Y_l^m = P_l^m \sin(\phi) e^{im\lambda}$$

Associated Legendre Polynomial

l - *m* nodal zeros

m wave numbers

Spectral tendencies for the *expansion coefficients* can be derived.

related to vorticity, see Eq.(28) in Bourke, 1974.

$$-l(l+1)\frac{\partial \psi_l^m}{\partial t} = \ldots$$

related to divergence, see Eq.(29) in Bourke, 1974.

$$-l(l+1)\frac{\partial \chi_l^m}{\partial t} = \ldots$$

related to temperature, see Eq.(30) in Bourke, 1974.

$$\frac{\partial T_l^m}{\partial t} = \ldots$$

etc.......

Time integration

Leapfrog scheme with filters in SPEEDY for the vector of prognostic variables A may be expressed as

$$A^{t+1} = A^{t-1} + 2\Delta t \, f\left(A^{t+1}, A^{t-1}\right) \tag{18}$$

with Robert filter to suppress the computational mode and semi-implicit treatment of gravity waves. Since A^{t+1} is also present on the rhs of Eq. 18 it has to be found by gaussian elimination.

N.B. See Bourke, 1974 (ref. above).

Continuing... the physiology of SPEEDY:

2. Physical parameterizations.

Parameterizations are computed in grid-point space. To have an idea of how a parameterization work, here only the convection scheme is described in detail. For details of other schemes look at Appendix to ver. 41 available on the SPEEDY webpage.

From the primitive variables, U, V, T, Q, Φ and p_{surf} additional diagnostics variables are calculated:

saturation specific humidity: Q^{sat}

relative humidity: RH

dry static energy: $SE = c_p T + \Phi$

moist static energy: $MSE = SE + L_c Q$

saturation moist static energy: $MSS = SE + L_c Q^{sat}$

Atmospheric layers in SPEEDY (T30)

$\sigma = p / p_0$

Total no of DOF:

~ 900 * 39 ≈ 35000

$\sigma = 0.$			$\sigma' = d\sigma/dt = 0$
$\sigma = 0.025$ (30 hPa)	------------------------	ζ, D, T, Φ	
	Stratosphere		σ'
$\sigma = 0.095$ (100 hPa)	------------------------	ζ, D, T, Φ	
			σ'
$\sigma = 0.200$ (200 hPa)	------------------------	ζ, D, T, S_h, Φ	
			σ'
$\sigma = 0.340$ (300 hPa)	------------------------	ζ, D, T, S_h, Φ	
	"free"		σ'
$\sigma = 0.510$ (500 hPa)	------------------------	ζ, D, T, S_h, Φ	
	troposphere		σ'
$\sigma = 0.685$ (700 hPa)	------------------------	ζ, D, T, S_h, Φ	
			σ'
$\sigma = 0.835$ (850 hPa)	------------------------	ζ, D, T, S_h, Φ	
			σ'
$\sigma = 0.950$ (925 hPa)	-------- PBL --------	ζ, D, T, S_h, Φ	
$\sigma = 1.$		p_0	$\sigma' = d\sigma/dt = 0$

Equivalent potential temperature and moist static energy

The basic stability criterium for many convective scheme, and in particular for the SPEEDY scheme is the vertical moist static energy gradient, which is identical to a criterion on equivalent potential temperature. We consider changes of equivalent potential temperature θ_e and Moist Static Energy MSE with height

$$c_p d\ln\theta_e = c_p d\theta + \frac{L_c}{T}dq = \frac{c_p}{T}dT - \frac{R}{p}dp + \frac{L_c}{T}dq, \tag{20}$$

where q is the specific humidity, T temperature, p the pressure, R the gas constant of dry air, θ is the potential temperature of dry air and L_c is the latent heat of condensation. We multiply this with T we get

$$\frac{c_p T}{\theta_e}d\theta_e = c_p dT - \frac{RT}{p}dp + L_c dq, \tag{21}$$

Equivalent potential temperature and moist static energy

Using the hydrostatic approximation $dp = -\rho g dz$

$$\frac{c_p T}{\theta_e} d\theta_e = c_p dT + gdz + L_c dq := dSE + L_c dq := dMSE. \quad (22)$$

The criterion for instability a model grid point is then

$$\frac{\partial \theta_e}{\partial z} < 0, \text{ thus } \frac{\partial MSE}{\partial z} < 0 \quad (23)$$

For practical purposes, we assume that saturation is present wherever a parcel is lifted, therefore the criterion for instability is

$$\frac{\partial MSS}{\partial z} < 0 \quad (24)$$

This last criterion implies also that boundary layer relative humidity exceeds a minimum threshold. Also

$$\frac{\partial SE}{\partial z} = c_p \frac{\partial T}{\partial z} + g > 0 \quad \text{for statically stable atmosphere.} \quad (25)$$

Tendencies due to convection

The tendencies due to convection at level k for specific humidity q and Temperature T or Static Energy SE, are

$$\left.\frac{\partial q_k}{\partial t}\right|_{conv} = \frac{g\Delta F_k^q}{\Delta p_k} \quad , \tag{17}$$

$$\left.\frac{\partial T_k}{\partial t}\right|_{conv} = \frac{g\Delta F_k^{SE}}{c_p\Delta p_k} \quad , \tag{18}$$

where $\Delta F_k^{q,SE}$ represent the flux convergences for each layer for upward and downward fluxes

$$\Delta F_k^{q,SE} = (F_{k+h}^{u;q,SE} - F_{k-h}^{u;q,SE}) + (F_{k+h}^{d;q,SE} - F_{k-h}^{d;q,SE}) \quad , \tag{19}$$

a. Convection

An updraft of saturated and unstable air from the PBL to a top-of-convection (TCN) level in middle or top of troposphere.

Compensating large-scale descending motion.

Entrainment into updraft occurs in lower troposphere above PBL. Detrainment only in TCN level.

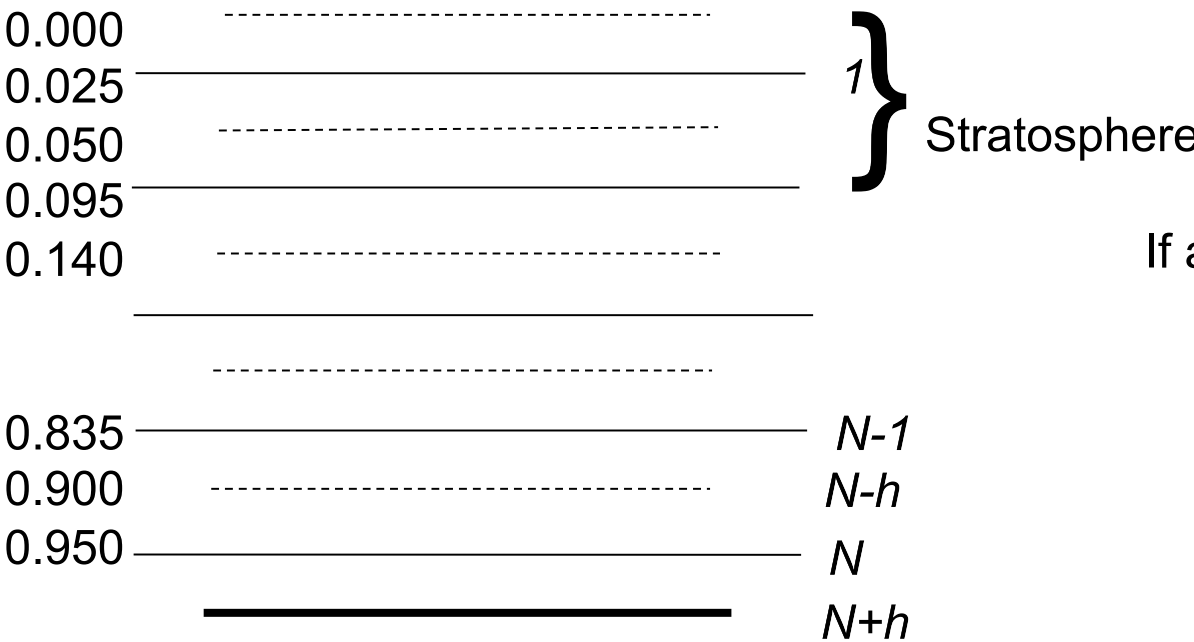

Conditions for activation:

$$RH_{N,N-1} > RH_{cnv}$$

and, for 1<k<N-1,

If a level k+h exists such that

$$MSS_N > MSS_{k+h}$$

Physical Parameterizations: Convection scheme

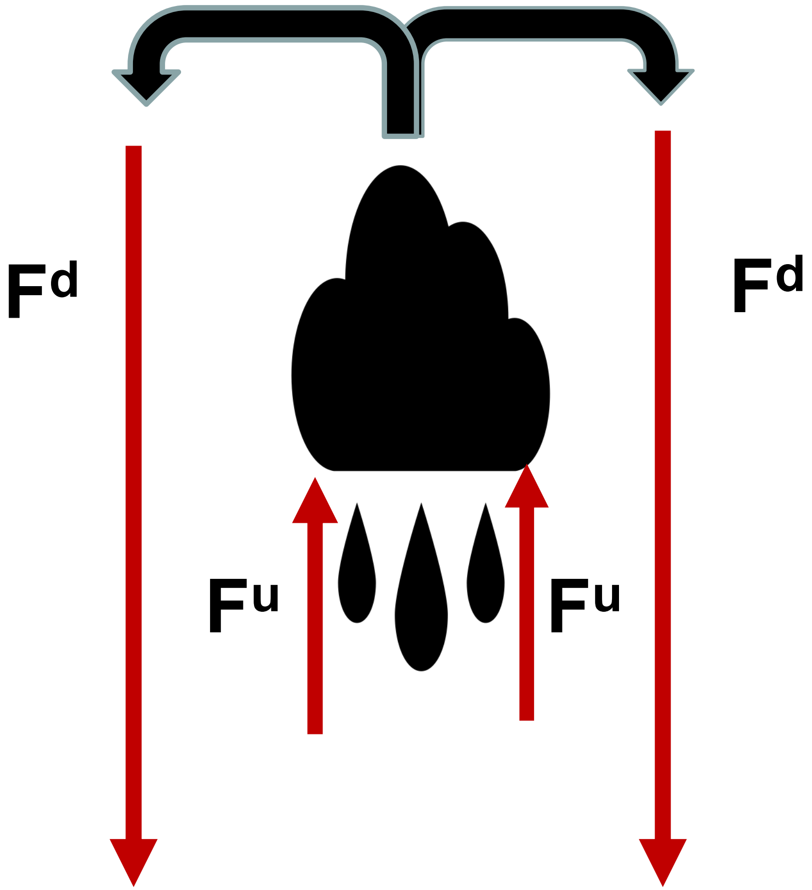

This 'represents' a model gridbox

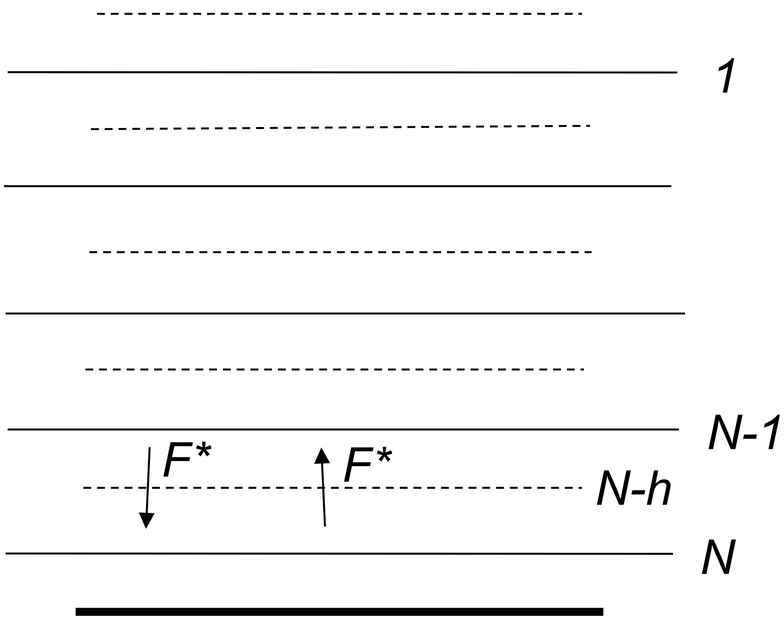

$$ {}^{u}F^{m}_{N-h} = {}^{d}F^{m}_{N-h} = F^{*} $$

$$ {}^{u}F^{Q}_{N-h} = F^{*} \cdot Q^{sat}_{N} \qquad {}^{d}F^{Q}_{N-h} = F^{*} \cdot Q_{N-h} $$

$$ {}^{u}F^{SE}_{N-h} = F^{*} \cdot SE_{N} \qquad {}^{d}F^{SE}_{N-h} = F^{*} \cdot SE_{N-h} $$

To find F*, we use

$$ \left(\frac{\partial Q_N}{\partial t}\right)_{cnv} = -\frac{gF^{*}\left(Q^{sat}_{N} - Q_{N-h}\right)}{\Delta p_N} = -\frac{Q_N - Q_{thr}}{\tau_{cnv}} $$

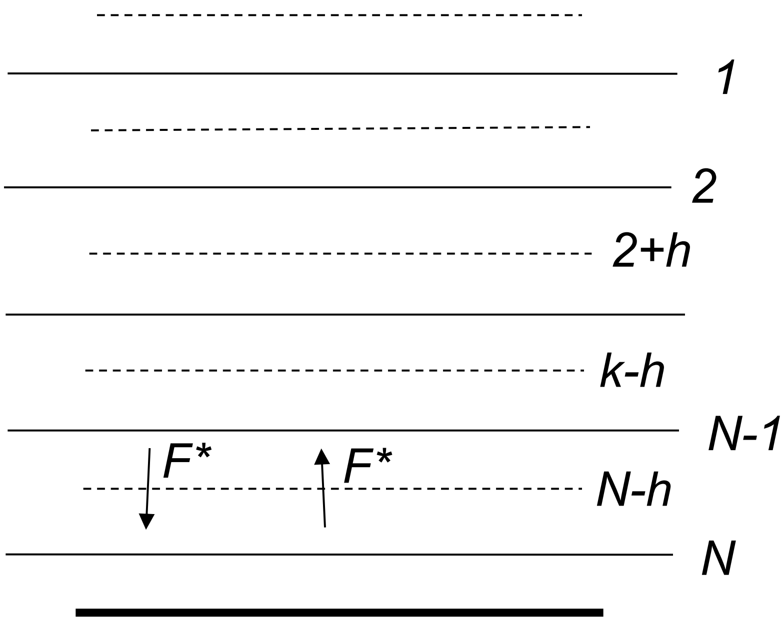

Now we have the necessary fluxes at N-h...

An entrainment flux is calculated

$$E^m_{N-1} = \varepsilon(\sigma_{N-1})F^m_{N-h}$$

Then fluxes at k-h are calculated:

$$F^m_{k-h} = F^m_{N-h} + E^m_{N-1}$$

$${}^uF^Q_{k-h} = {}^uF^Q_{N-h} + E^m_{N-1}Q_{N-1}$$

$${}^dF^Q_{k-h} = F^m_{k-h}Q_{k-h}$$

$${}^uF^{SE}_{k-h} = {}^uF^{SE}_{N-h} + E^m_{N-1}SE_{N-1}$$

$${}^dF^{SE}_{k-h} = F^m_{k-h}SE_{k-h}$$

And hence going up all the half-levels until, and including, TCN-h (for the diagram here TCN=2).

Basic properties of convection scheme

We want derive some basic properties of the convection scheme in SPEEDY, assuming no Entrainment $E_k^m = 0$.
For the moisture flux we have in this case at the top level of convection k_0

$$\Delta F_{k_0}^q = F^* \left(q_N^{sat} - q_{k_0+h} \right) - P_{cnv} \quad , \tag{21}$$

and for all other levels $k \neq N$ the is only the downward flux convergence contribution

$$\Delta F_k^q = F^* \left(q_{k-h} - q_{k+h} \right) \ < \ 0 \quad , \tag{22}$$

meaning the effect is always a drying of the atmosphere (due to environmental sinking).

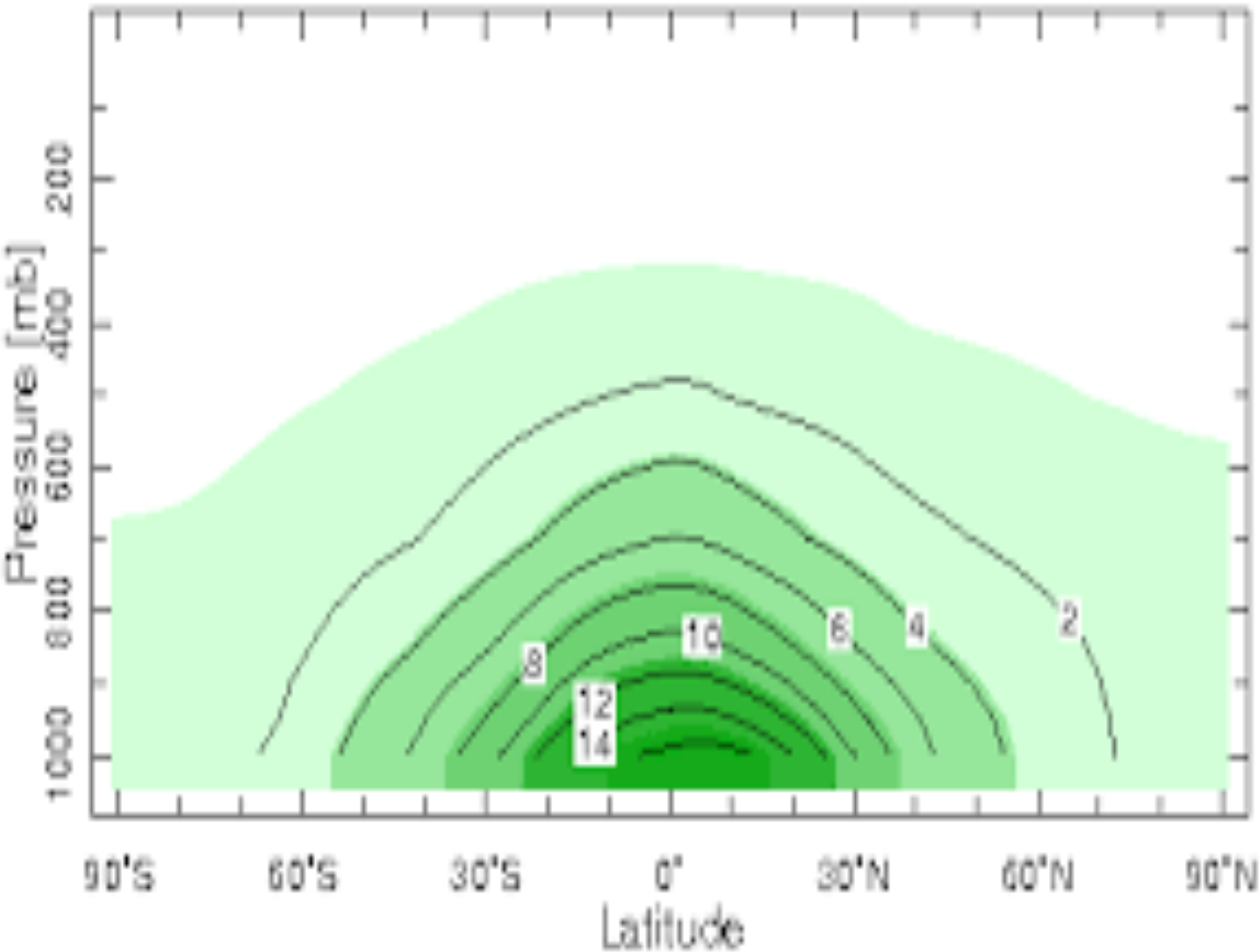
Pressure [mb]
200
400
600
800
1000
2
4
6
8
10
12
14
90°S
60°S
30°S
0°
30°N
60°N
90°N
Latitude

Basic properties of convection scheme

Instead at $k = N$ we have

$$\Delta F_N^q = F^* \left(q_{N-h} - q_N^{sat} \right) \; < \; 0 \quad , \tag{23}$$

It follows that for the sum of all layers below the top

$$\sum_{k=k_0+1}^{N} \Delta F_k^q = F^* \left(q_{k_0+h} - q_N^{sat} \right) < 0 \quad . \tag{24}$$

Comparing Eqs. 24 with 21 we see that the top level exchanges moisture with the levels below, and that

$$\sum_{k=k_0}^{N} \Delta F_k^q = -P_{cnv} = \sum_{k=k_0}^{N} \frac{\Delta p_k}{g} \frac{\partial q_k}{\partial t} < 0 \quad , \tag{25}$$

the properly vertically integrated moisture tendency due to convection.

Basic properties of convection scheme

Similarly we have for the Static Energy (SE) fluxes
For the moisture flux we have in this case at the top level of convection k_0

$$\Delta F_{k_0}^{SE} = F^* \left(SE_N - SE_{k_0+h} \right) + L_c P_{cnv} \quad , \tag{26}$$

and for all other levels $k \neq N$ the is only the downward flux convergence contribution

$$\Delta F_k^{SE} = F^* \left(SE_{k-h} - SE_{k+h} \right) \ > \ 0 \quad , \tag{27}$$

meaning the effect is always a warming of the atmosphere (due to environmental sinking), and therefore also stabilizing the atmosphere because typically $\partial SE / \partial z$ is largest in upper troposphere.

Basic properties of convection scheme

Instead at $k = N$ we have

$$\Delta F_N^{SE} = F^* \left(SE_{N-h} - SE_N\right) \ > \ 0 \quad , \tag{28}$$

It follows that for the sum of all layers below the top

$$\sum_{k=k_0+1}^{N} \Delta F_k^{SE} = F^* \left(SE_{k_0+h} - SE_N\right) > 0 \quad . \tag{29}$$

Comparing Eqs. 29 with 26 we see that the top level exchanges energy with the levels below, and that

$$\sum_{k=k_0}^{N} \Delta F_k^{SE} = L_c P_{cnv} = \sum_{k=k_0}^{N} \frac{c_p \Delta p_k}{g} \frac{\partial T_k}{\partial t} > 0 \quad , \tag{30}$$

the properly vertically integrated temperature tendency due to convection.

b. Other schemes (no less important but I don’t have time to describe them in details here):

Large-scale condensation: Where relative humidity exceeds heigh-dependent thresholds, specific humidity is relaxed (represents ‘raining’) to the corresponding threshold on a 4hr timescale . The released latent heat is converted to dry static energy.

Clouds: Cloud cover and thickness are diagnosed from relative and absolute humidity.

Shortwave radiation: Two spectral bands. Reflected at cloud top and ‘earth’ surface. Cloud albedo is related to cloud cover. SW transmissivities of model layers are functions of layer thickness, specific humidity.

Longwave radiation: Four spectral bands. One for atmospheric infrared window, one for CO2 and two for water vapour.

Surface fluxes of momentum and energy: Defined by bulk aerodynamic formulas with different exchange coefficients from land and sea.

Vertical diffusion: Redistribution of dry static energy and moisture between two lowest layers in conditional instability. Water vapour diffusion. Diffusion of dry static energy if lapse rate exceeds the dry adiabatic limit.

https://www.ictp.it/research/esp/mod

Global Model: SPEEDY

A simplified GCM developed at ICTP

SPEEDY is a simplified GCM developed at ICTP by Franco Molteni and Fred Kucharski.

The ICTP AGCM (nicknamed SPEEDY, for "Simplified Parameterizations, privitivE-Equation DYnamics") is based on a spectral dynamical core developed at the Geophysical Fluid Dynamics Laboratory. It is a hydrostatic, s-coordinate, spectral-transform model in the vorticity-divergence form, with semi-implicit treatment of gravity waves.

- SPEEDY 8-layer (version 40) description (pdf)
- Description of a previous SPEEDY 5-layer model (version 23)
- Articles published at the ICTP using SPEEDY
- SPEEDY 8-layer (version 40) climatology verification

Typical performance on a Pentium 4 (3.40GHz) processor: 1 year of simulation can be run in 12 min.

For reference, please cite:

Molteni F (2003) Atmospheric simulations using a GCM with simplified physical parametrizations. I. Model climatology and variability in multi-decadal experiments. Clim Dyn 20: 175-191
and
Kucharski F, Molteni F, and Bracco A (2006) Decadal interactions between the western tropical Pacific and the North Atlantic Oscillation. Clim Dyn 26: 79-91

For downloading SPEEDY, please contact: kucharsk@ictp.it (Fred Kucharski)

In the following a collection of experimentation with the SPEEDY model
(sometimes coupled to different ocean models)

lets call it

SPEEDY Parade

Some should be easily to be repeated, some are
related to older versions coupled to diverse ocean models;

I can stop at any time should you get bored....

The Abdus Salam
International Centre
for Theoretical Physics

Example 1: Atlantic SST impacts on South Asian summer monsoon, and on the ENSO-monsoon teleconnection

Barimalala R, Bracco A, Kucharski F. 2011. The representation of the south tropical Atlantic teleconnection to the Indian Ocean in the AR4 coupled models. Clim. Dyn. 38: 1147–1166, doi: 10.1007/s00382-011-1082-5.

Hari, V., Pathak, A. & Koppa, A. 2020. Dual response of Arabian Sea cyclones and strength of Indian monsoon to Southern Atlantic Ocean. Clim Dyn. https://doi.org/10.1007/s00382-020-05577-9

Kucharski F, Bracco A, Yoo JH, Molteni F. 2007. Low-frequency variability of the Indian monsoon – ENSO relationship and the tropical Atlantic: The 'weakening' of the 1980s and 1990s. *J. Clim.* **20**: 4255–4266, doi: 10.1175/JCLI4254.1.

Kucharski F, Bracco A, Yoo JH, Molteni F. 2008. Atlantic forced component of the Indian monsoon interannual variability. *Geophys. Res. Lett.* **35**: L04706, doi: 10.1029/2007GL033037.

Kucharski F, Bracco A, Yoo JH, Tompkins AM, Feudale L, Ruti P, Dell'Aquila A. 2009. A Gill – Matsuno-type mechanism explains the tropical Atlantic influence on African and Indian monsoon rainfall. *Q. J. R. Meteorol. Soc.* **135**: 569–579, doi: 10.1002/qj.406.

Losada T, Rodriguez-Fonseca B, Polo I, Janicot S, Gervois S, Chauvin F, Ruti P. 2010. Tropical response to the Atlantic Equatorial mode: AGCM multimodel approach. *Clim. Dyn.* **35**: 45 – 52, doi 10.1007/s00382-009- 0624-6.

Pottapinjara V, Girishkumar MS, Ravichandran M, Murtugudde R. 2014. Influence of the Atlantic zonal mode on monsoon depressions in the Bay of Bengal during boreal summer. *J. Geophys. Res. Atmos.* **119**: 6456 – 6469, doi: 10.1002/2014JD021494.

Pottapinjara V, Girishkumar MS, Sivareddy S, Ravichandran M MR. 2015. Relation between the upper ocean heat content in the equatorial Atlantic during boreal spring and the Indian monsoon rainfall during June–September. *Int. J. Climatol.* **36**: 2469–2480, doi: 10.1002/joc.4506.

Syed FS, Kucharski F. 2016. Statistically related coupled modes of South Asian summer monsoon interannual variability in the tropics. *Atmos. Sci. Lett.* **17**: 183–189, doi: 10.1002/asl.641.

Yadav RK. 2009. Role of equatorial central Pacific and northwest of North Atlantic 2-metre surface temperatures in modulating Indian summer monsoon variability. *Clim. Dyn.* **32**: 549–563.

Yadav RK. 2017. On the relationship between east equatorial Atlantic SST and ISM through Eurasian wave. *Clim. Dyn.* **48**: 281–295, doi: 10.1007/s00382- 016-3074-y

Yadav, R.K., Srinivas, G. & Chowdary, J.S. 2018. Atlantic Niño modulation of the Indian summer monsoon through Asian jet. *npj Clim Atmos Sci* **1,** 23. https://doi.org/10.1038/s41612-018-0029-5.

Sabeerali, C. T., Ajayamohan, R. S., Bangalath, H. K., & Chen, N. (2019). Atlantic Zonal Mode: An emerging source of Indian summer monsoon variability in a warming world. *Geophysical Research Letters*, 46, 4460– 4467. https://doi.org/10.1029/2019GL082379

Sources of Monsoon Variability?

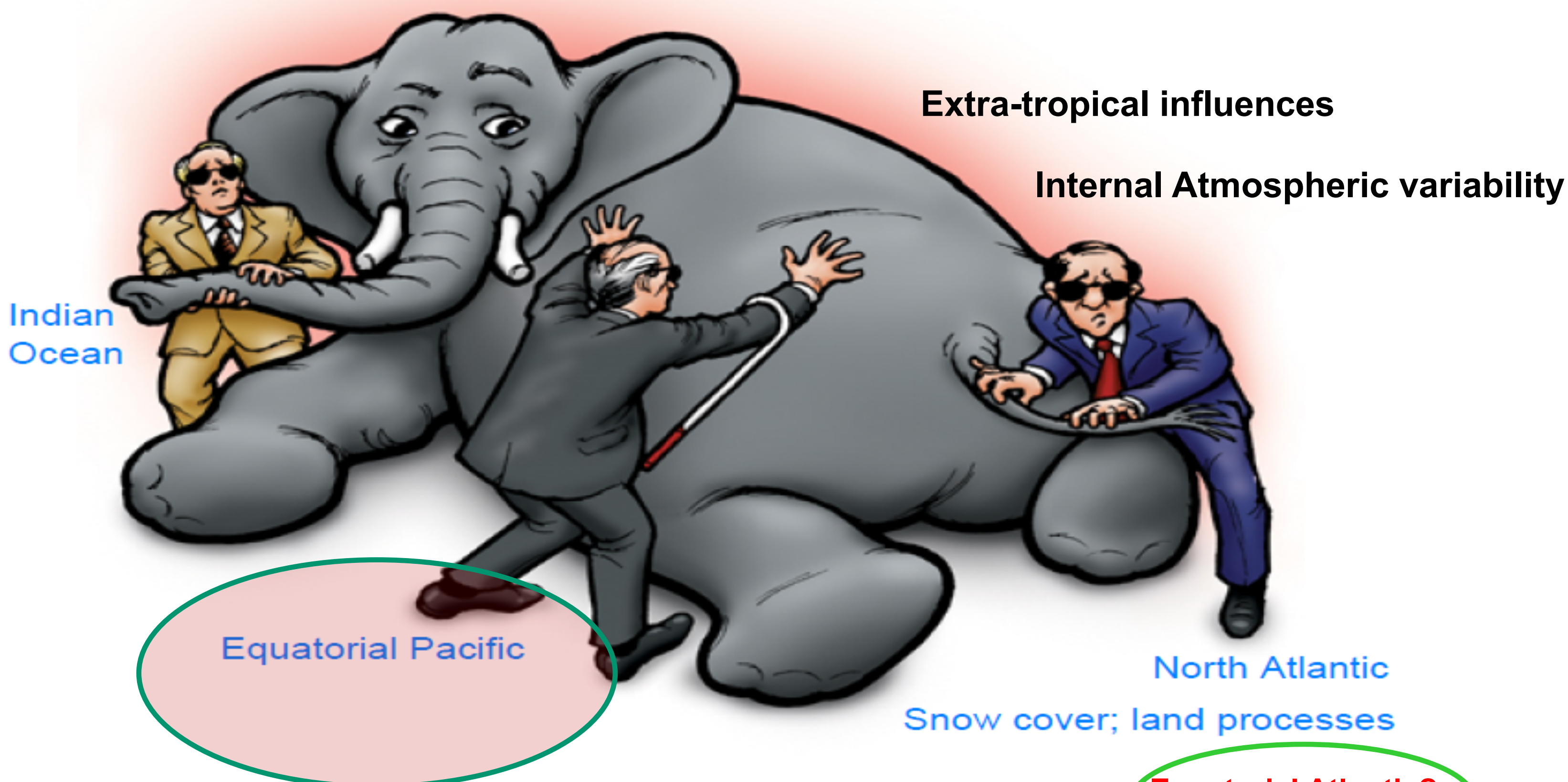

Equatorial Atlantic?

Probably many many more processes…..

Slide taken from presentation of Mark Cane at TTA 2008 at ICTP

The Abdus Salam International Centre for Theoretical Physics

The India Rainfall - ENSO connection

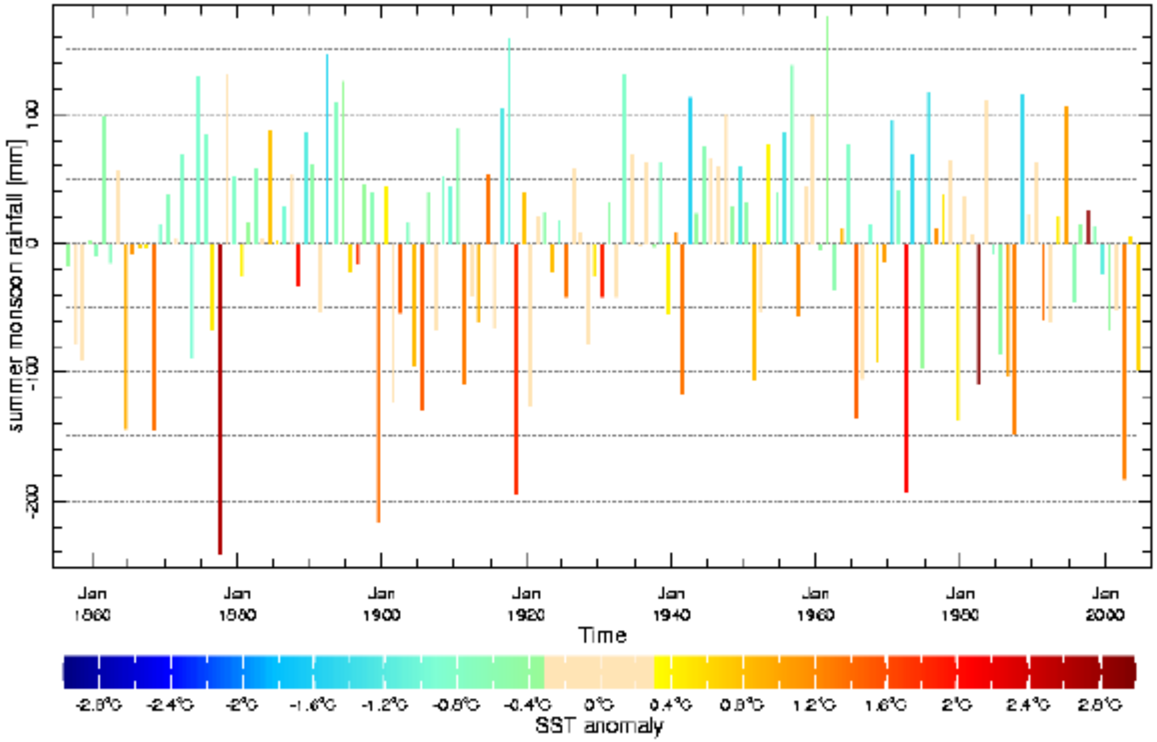

Rainfall Data: Indian Institute of Tropical Meteorology (IITM).

SST Data: Kaplan NINO3 index from Optimal Smoother analysis of MOHSST5 monthly sea surface temperature anomalies.

Slide taken from presentation of Mark Cane at TTA 2008 at ICTP

The Abdus Salam International Centre for Theoretical Physics

Interannual SST standard deviation

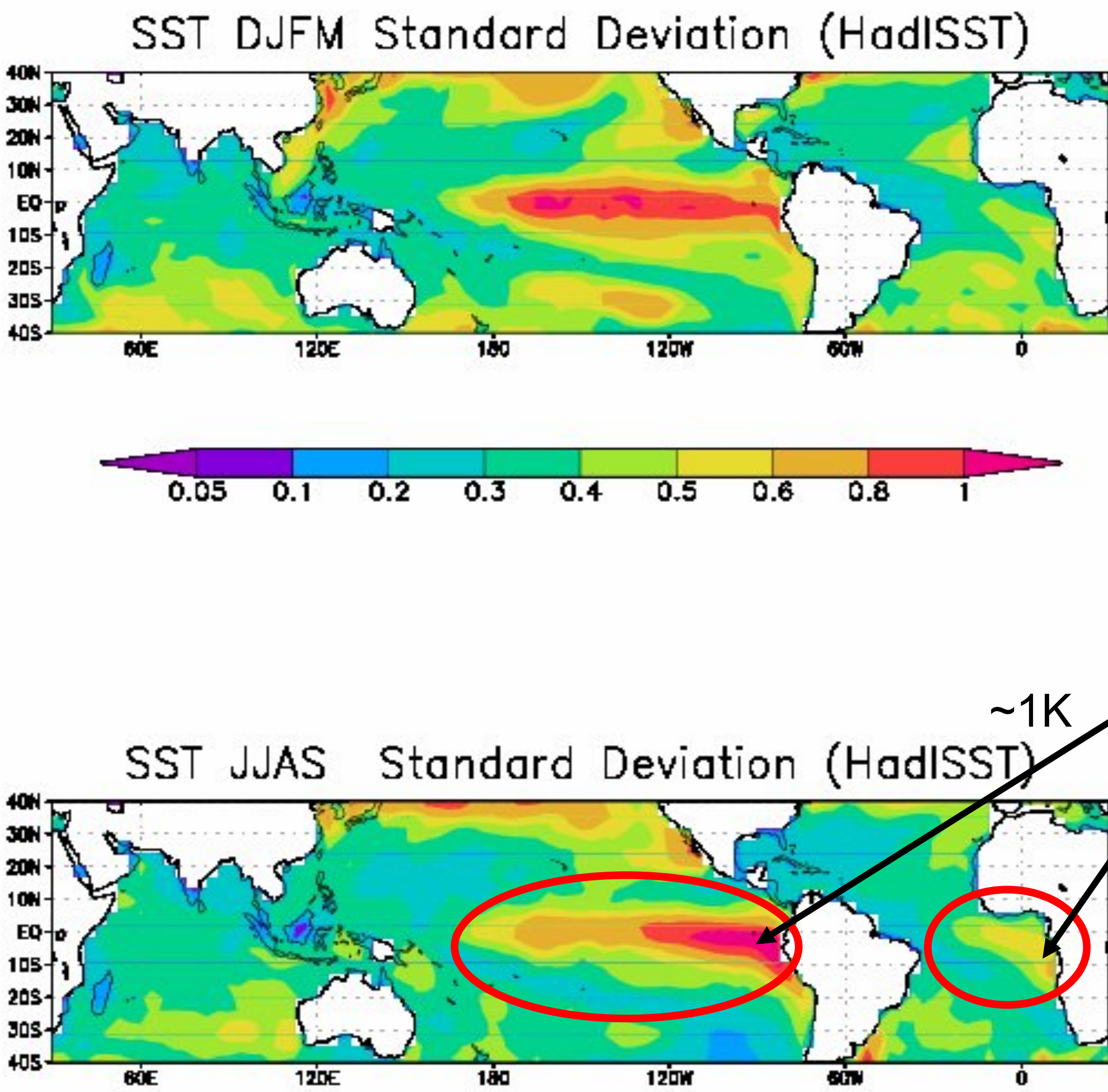

DJFM

In JJAS, two distinct Maxima in STDEV

~1K

~0.5 K

JJAS

Goliath

David

The Abdus Salam
International Centre
for Theoretical Physics

Contrasting Eastern Pacific and tropical Atlantic influences on rainfall.

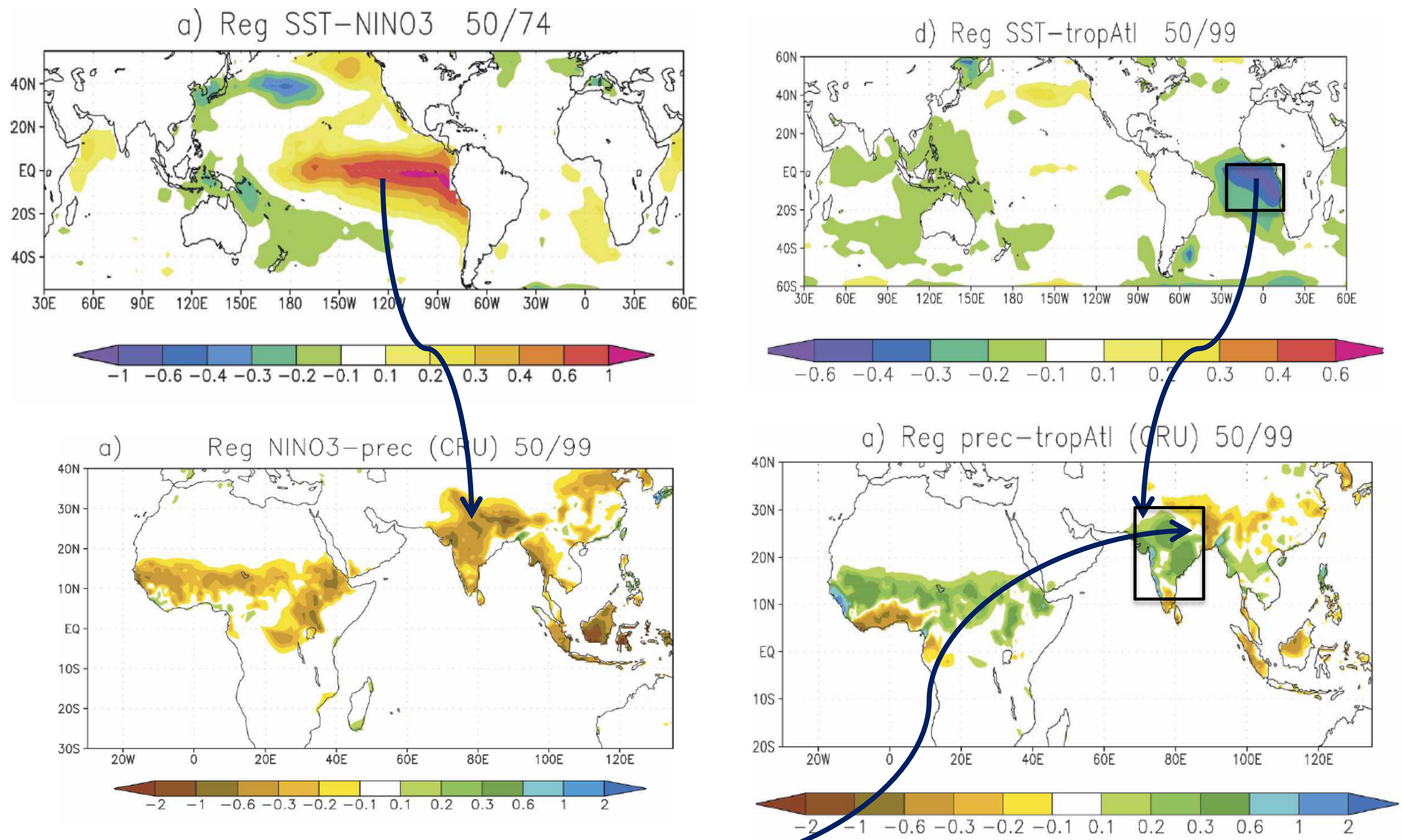

There are some interesting regional features, too!

Warm anomalies in Eq. Pacific and Atlantic have broadly very similar influences on Asian (and African) Monsoon!

From: Kucharski et al. (2007), J. Climate, 20, 4255-4266 lead-lag correlations:

Results from SPEEDY
-MICOM

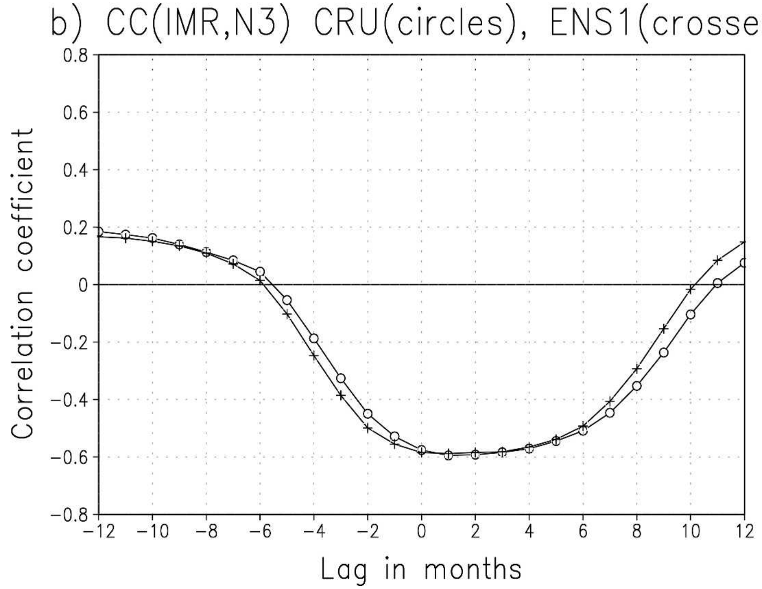

Nino3 index versus IMR

In the following we
want to understand
the physical mechanism
for the Atlantic impact

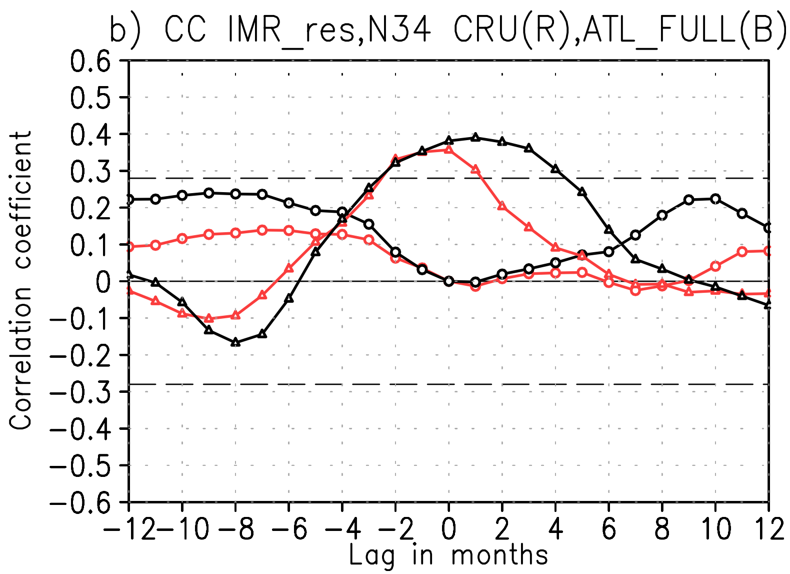

- South Tropical Atlantic
Index versus IMR

- Figures from Kucharski et al., 2007 (JClim) and 2008 (GRL)

ENSO regression

1950/1974

1975/1999

Difference

The fact that the during ENSO the 2 basins are anticorrelated in recent the 1980’s and 1990’s could have contributed to a weakening of the ENSO-ISM relationship, because with the same sign they cause a similar response, meaning that in opposite phases they may interfere destructively

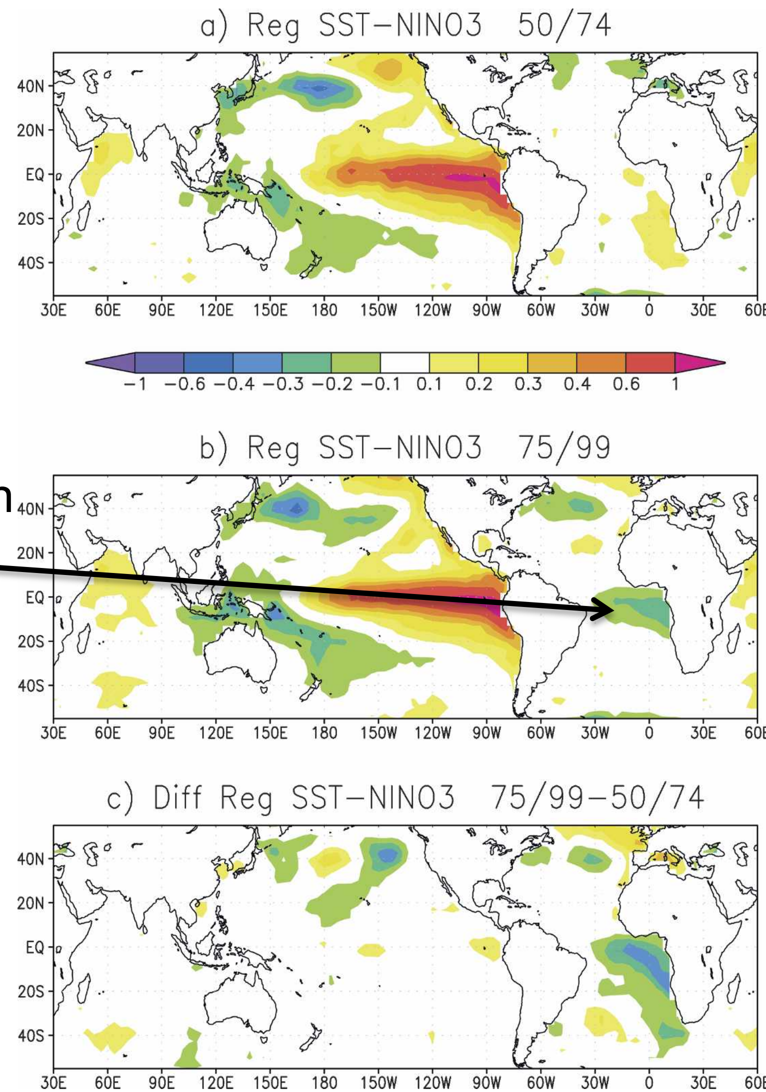

FIG. 4. Regressions and regression differences of SSTs onto the Niño-3 index: (a) 1950–74, (b) 1975–99, (c) 1975–99 − 1950–74 difference of regressions. Units are K.

- Figure from Kucharski et al., 2007 (JClim)

Nino3.4 index regression rainfall and wind differences

obs Model

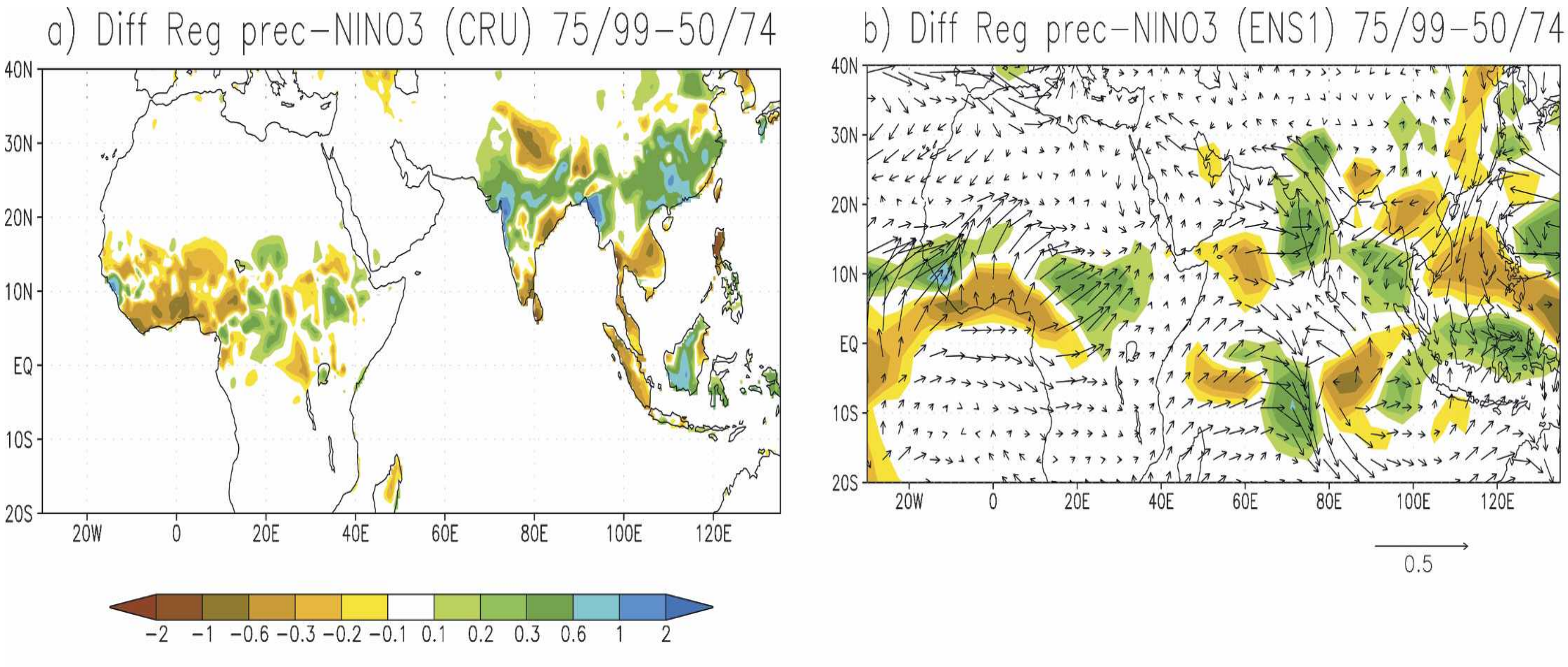

Regression differences indicating a weakening of the ENSO-Monsoon relationship

- Figure from Kucharski et al., 2007 (JClim)

STA index regression on rainfall and wind

obs

Model

SST

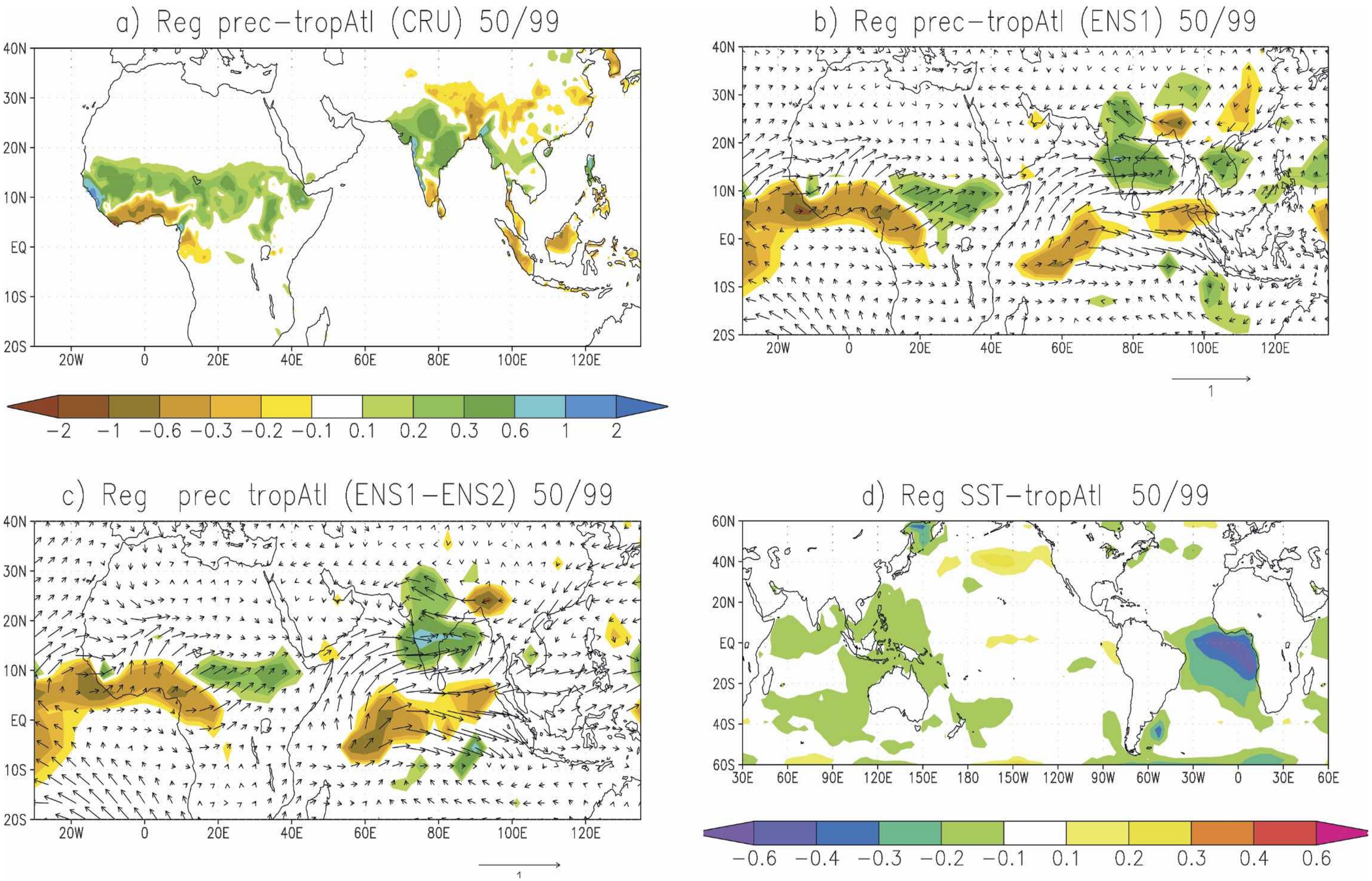

- Figure from Kucharski et al., 2007 (JClim)

The Abdus Salam International Centre for Theoretical Physics

Sliding correlation between Nino3 index and ISMR

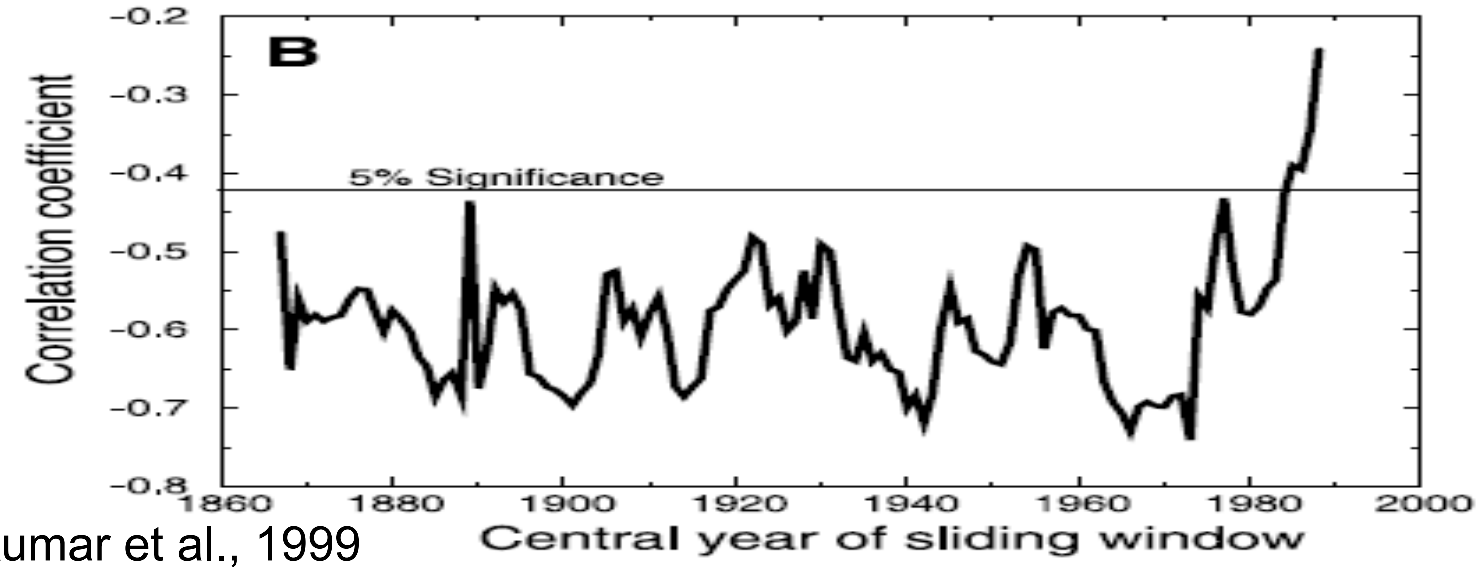

From: Kumar et al., 1999

Sliding correlation between Atl3 index and ISMR

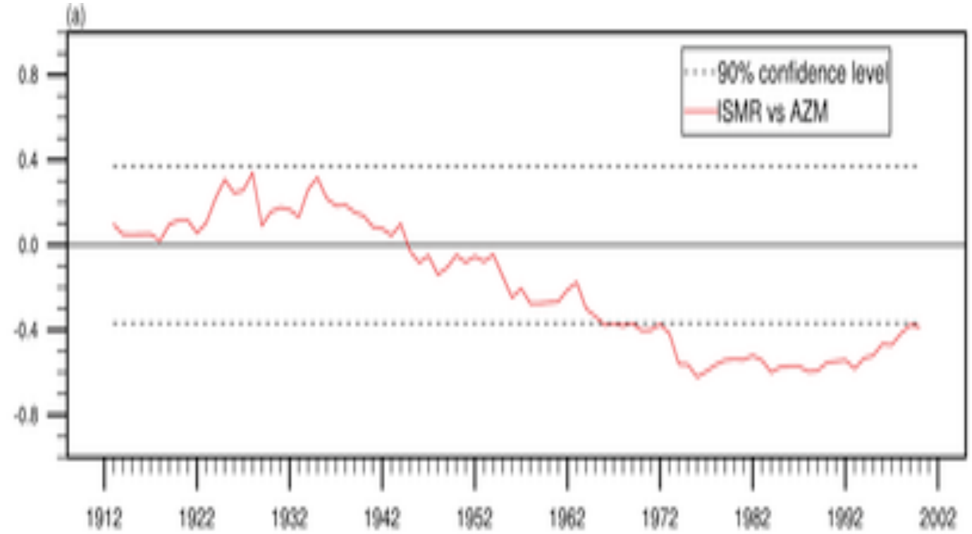

From: Sabeerali et al., GRL, 2019

The Abdus Salam International Centre for Theoretical Physics

The mechanism: A Gill-type response; possibly enhanced by compensating sinking in Western Pacific

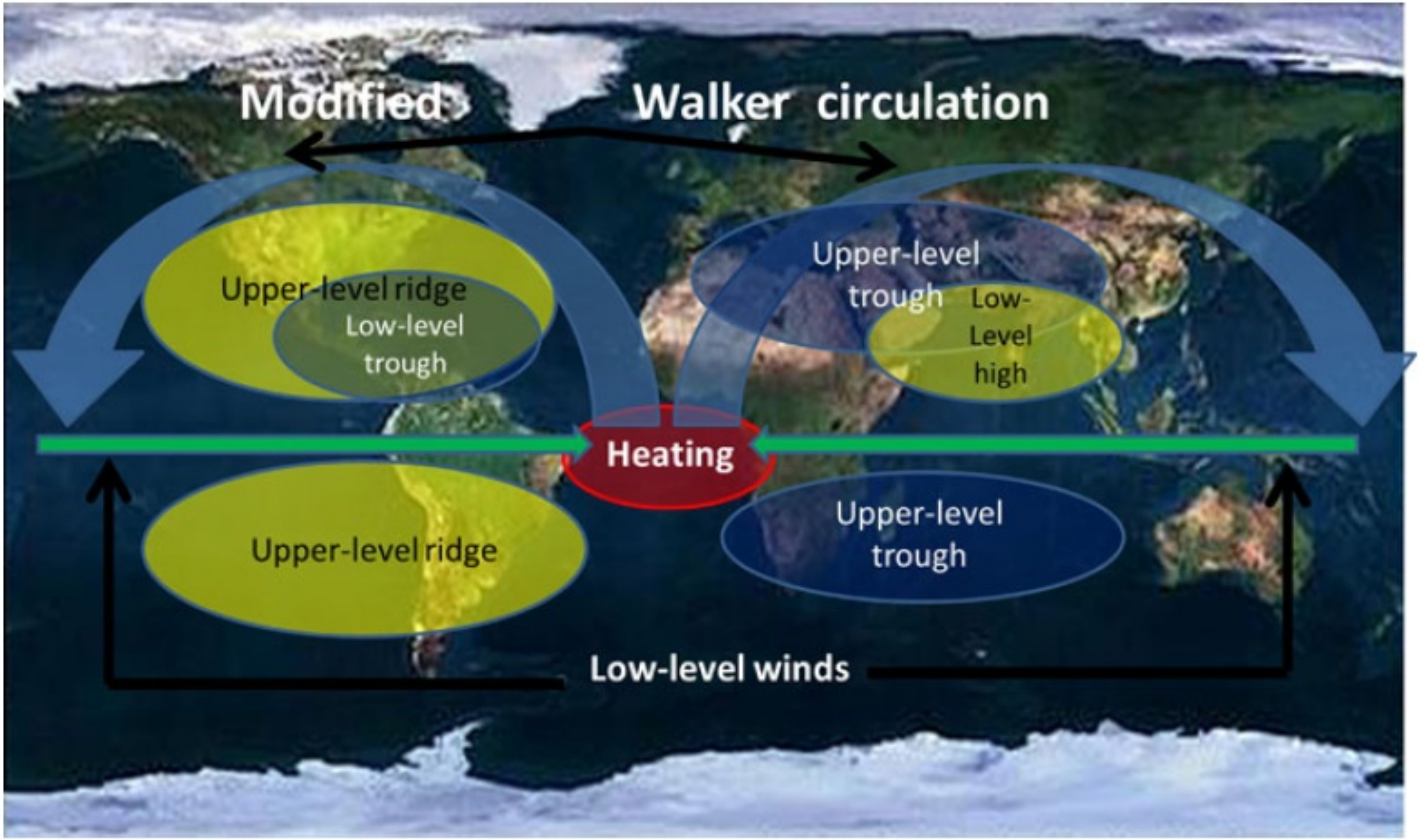

Figure from Barimalala et al., 2011

Evaluate parcel properties with respect to its environment

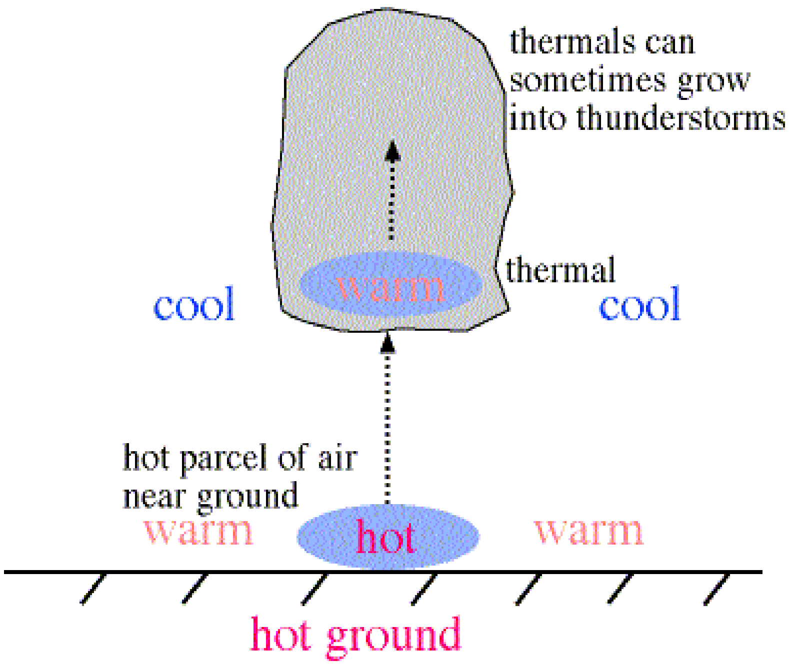

ρ, p, T

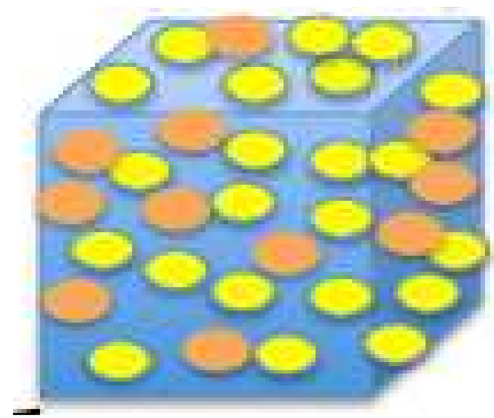

$\rho_{env}, p_{env}, T_{env}$

Buoyancy forces:

$$\frac{\partial w}{\partial t} = -\frac{\rho'}{\bar{\rho}} g \qquad \rho' = \rho - \rho_{env}$$

This is done in convective parameterization schemes in GCMs.
We will see later how this exactly works in SPEEDY

Source: appollo.lsc.vsc.edu

Environment Criterion for instability of moist (saturated) air:

(Environment quantities indicates with a bar)

$$\frac{\partial \overline{T}}{\partial z} <= -\frac{g}{c_p} \frac{\left(1 + \frac{L_{lv}\overline{m}_{vs}}{RT}\right)}{\left(1 + \frac{L_{lv}^2\overline{m}_{vs}}{c_p\overline{T}^2 R_v}\right)}$$

~ -0.6 k/100m

for dry air: -1K/100m

Note that this is equivalent to:

$$\frac{\partial \overline{\theta}_e}{\partial z} <= 0$$

Temperature has to decrease with height faster than the critical limit.
Such a situation may be favored by high surface temperatures!

Source: appollo.lsc.vsc.edu

For small-scale air parcel scale motions (~ 1km): A parcel of rising air always cools

$$\frac{dT}{dt} = -w\frac{g}{c_p}\frac{\left(1+\frac{L_{lv}m_{vs}}{RT}\right)}{\left(1+\frac{L_{lv}^2 m_{vs}}{c_p T^2 R_v}\right)}.$$

Assuming adiabatic ascent; no heat exchange with its environment while rising

Note that as long as water vapor in parcel is not saturated we have m_{sv}=0, and therefore the parcel cools as $-wg/c_p$.

Further, it can be shown that due to the decreasing temperature as a parcel rises the relative humidity increases until condensation occurs (Clausius-Clapeyron):

$$RH = \frac{p_v}{p_{vs}} = \frac{m_v}{m_{vs}}$$

$$\frac{dRH}{dt} = -\frac{m_v}{m_{vs}^2}\frac{dm_{vs}}{dt} > 0$$

Note that there is a huge asymmetry between a rising and a sinking parcel:

A rising parcel loses all its water vapor (to rainwater that fall out) if rising high enough, whereas a sinking parcel will evaporate the little cloud water it may hold.

Therefore, the net effect of these rising and sinking parcels induced by static instability will be an increase of atmospheric heating!

Reflection: The process of a rising parcel with condentational heating and following sinking would be reversible (i.e. entropy conserving) if no rain is falling out! It's the rain falling out that make is irreversible and entropy producing (just as luv-lee effect, see below)!

The Abdus Salam
International Centre
for Theoretical Physics

For large-scale motions (~ 100-1000km) this means (e.g. model like SPEEDY):

$$c_p \frac{dT}{dt} - \frac{RT}{p}\frac{dp}{dt} = -L_{lv}\frac{dm_v}{dt} > 0$$

First law of thermodynamics
Heat release by condensation of rising parcels; done by convection scheme

$$\left(\frac{\partial T}{\partial t} + u\frac{\partial T}{\partial x} + v\frac{\partial T}{\partial y}\right)_p - S_p\omega = \frac{Q}{cp} \quad ,$$

Re-formulated in pressure coordinates

Stability parameter:

$$S_p = (\Gamma_d - \Gamma)/(\rho g)$$

Always positive
in large scales

Lapse-rate definition:

$$-dT/dz = \Gamma$$

$$\Gamma_d = g/cp$$

In tropical regions, horizontal gradients and local time changes are small compared to the other terms in the Thermodynamic Equation, therefore we have approximately:

$$\cancelto{\sim 0}{\left(\frac{\partial T}{\partial t} + u\frac{\partial T}{\partial x} + v\frac{\partial T}{\partial y}\right)_p} - S_p\omega = \frac{Q}{cp} \quad ,$$

$$-S_p\omega \approx S_p\rho g w \approx \frac{Q}{c_p}$$

$$\boxed{w \approx \frac{Q}{c_p}\frac{1}{S_p\rho g}} \; .$$

Also anomalous:

$$\boxed{\Delta w \approx \frac{\Delta Q}{c_p}\frac{1}{S_p\rho g}}$$

This means whenever there is convective heat release, we can expect that this heating is compensated by large-scale rising motion!

The Abdus Salam International Centre for Theoretical Physics

Unstable condition – negative static stability

$\Gamma_d < \Gamma_{env}$

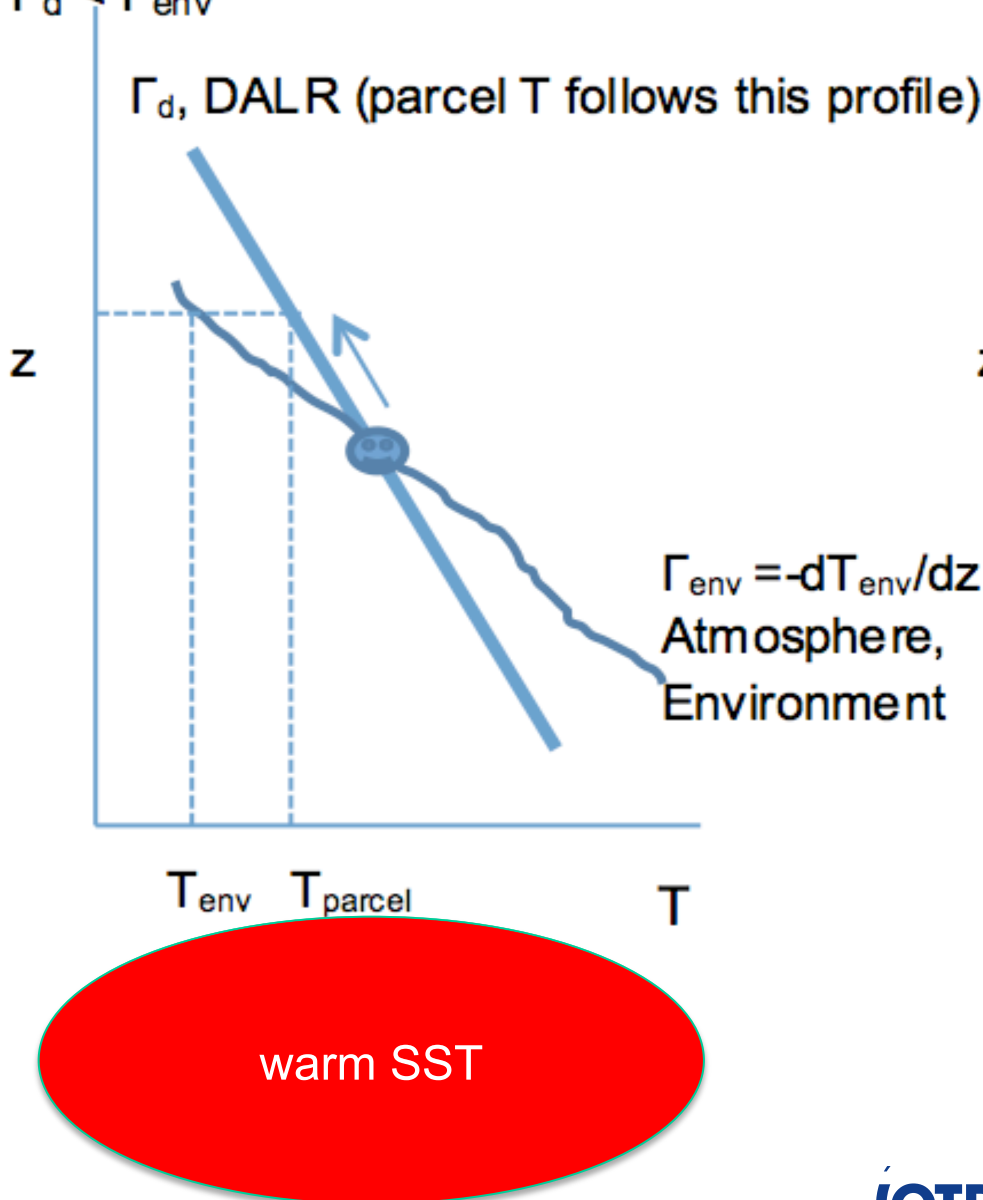

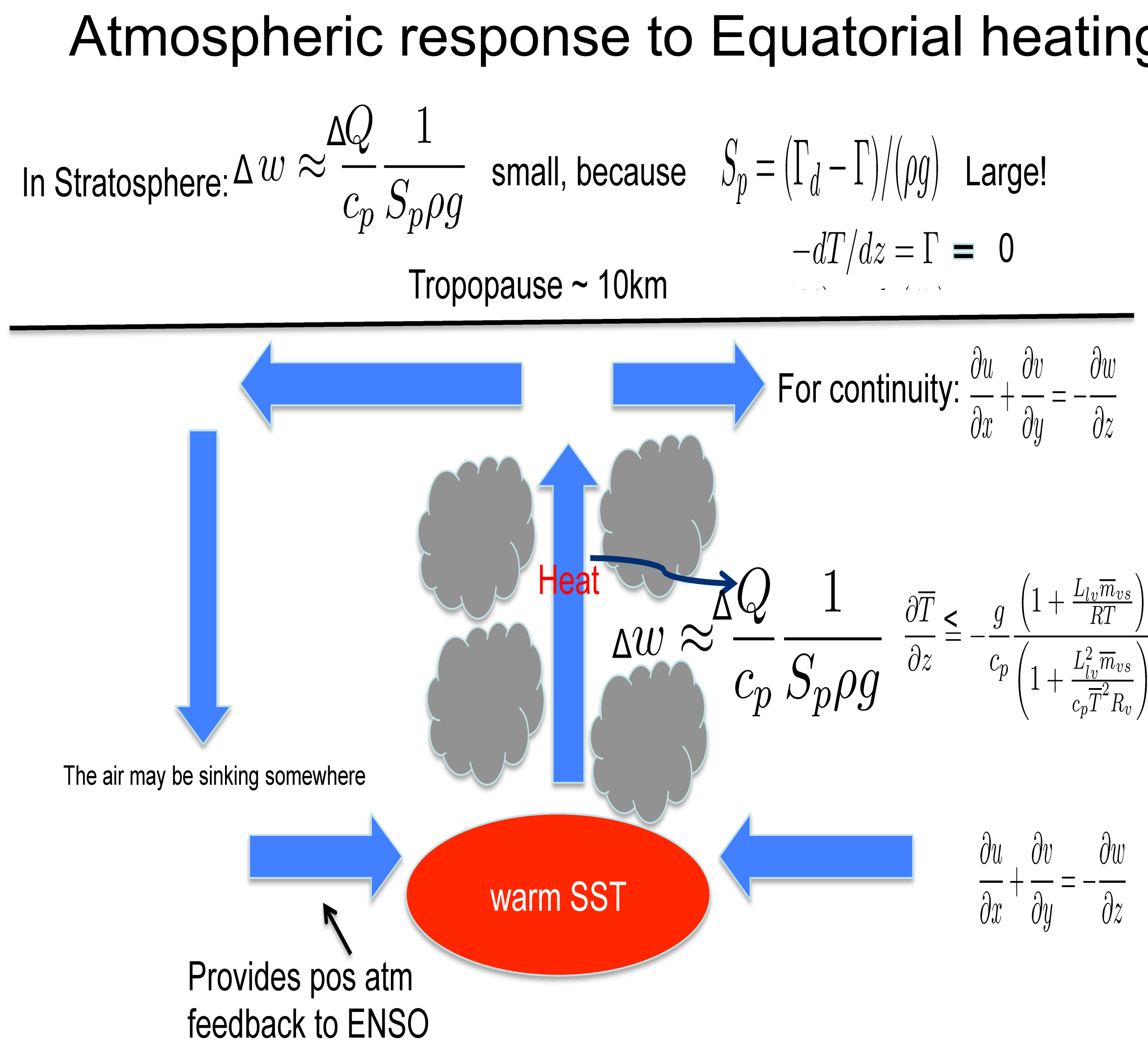

Figure 23: Large-scale adjustments to diabatic convective heating.

Many AGCM simulations have confirmed the tropical Atlantic Indian monsoon teleconnection; here results from a very idealised setting: Aquaplanet

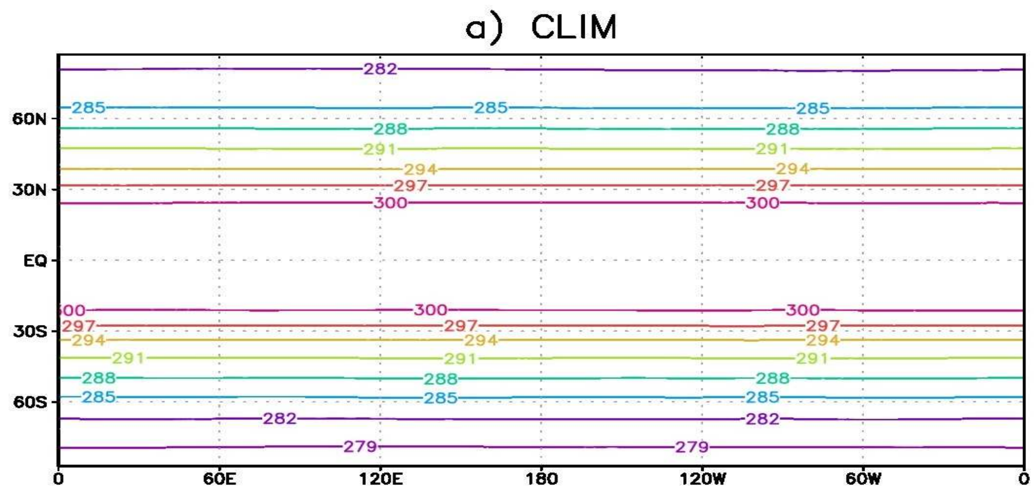

A zonally symmetric world made of water, no mountains!

SST

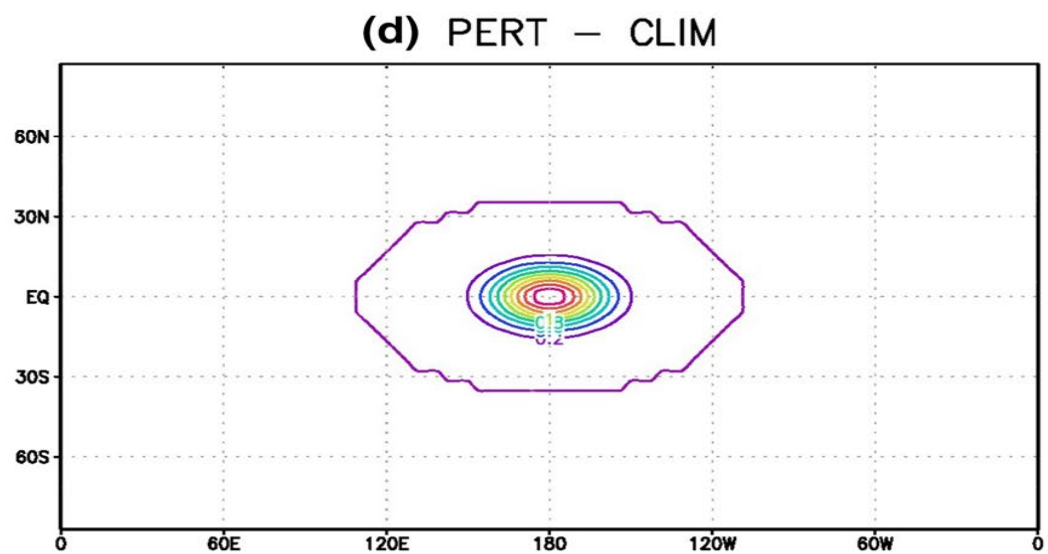

AGCM aquaplanet simulations; 2 K SST perturbation added to symmetric mean state SSTs

Hamouda & Kucharski (2018) , Ekman pumping mechanism driving precipitation anomalies in response to equatorial

Understanding the upper-level response (note response is baroclinic and changes sign in lower levels)

$$\xi_g = \frac{\partial v_g}{\partial x} - \frac{\partial u_g}{\partial y} \qquad \frac{d_g \xi_g}{dt} = -f\left(\frac{\partial u_a}{\partial x} + \frac{\partial v_a}{\partial y}\right) - \beta v_g$$

approximate vorticity equation; again gradients are small in tropics

$$\xi_g = \nabla^2 \psi$$

$$\boxed{\beta v_\psi = -f_0\left(\frac{\partial u_\chi}{\partial x} + \frac{\partial v_\chi}{\partial y}\right)}$$

Sverdrup balance in tropics (Rodwell & Hoskins)

$$\mathbf{v}_\chi = \nabla \chi \qquad \mathbf{v}_\psi = \mathbf{k} \times \nabla \psi$$

Note that responses are baroclinic; i.e. change sign with height

200 hPa Velocity Potential χ

(c) Response Chi 200 hPa PERT – CLIM

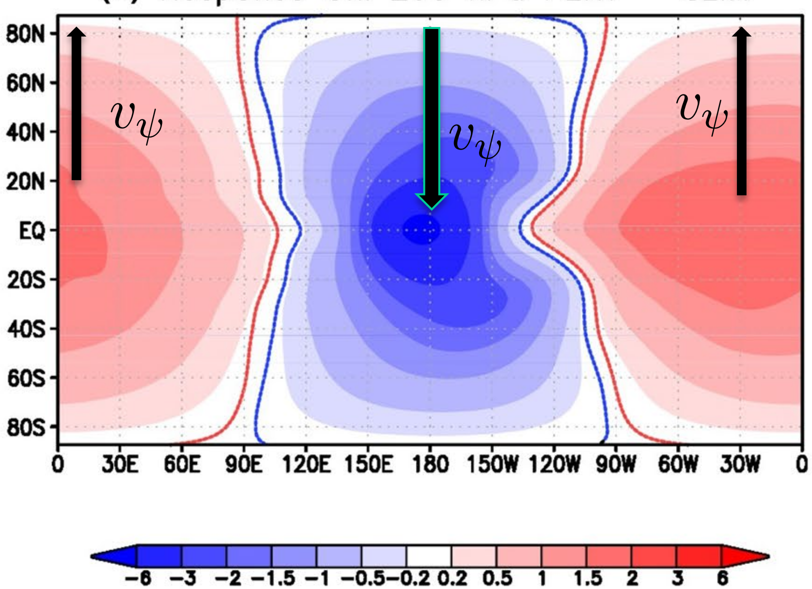

200 hPa Eddy Streamfunction Ψ

(d) Response eddy Psi 200 hPa PERT – CLIM

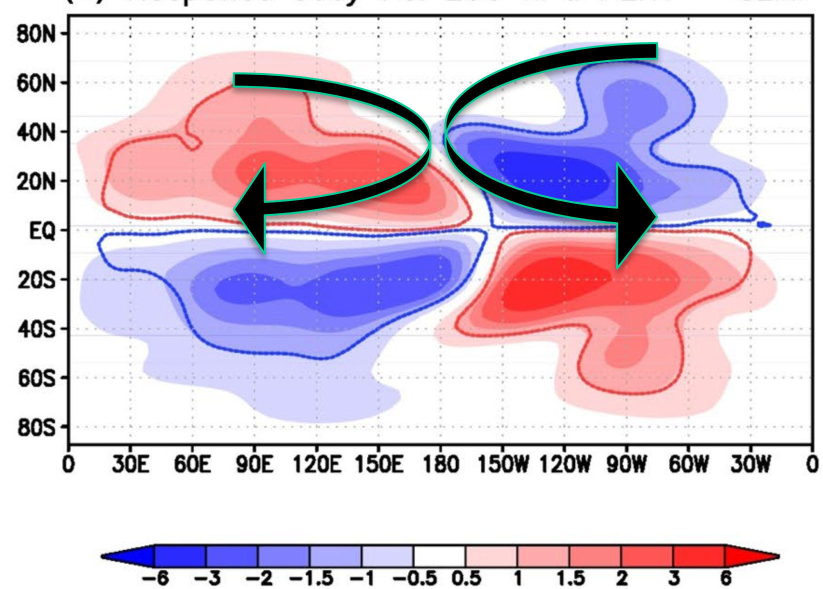

Hamouda & Kucharski (2018) , Ekman pumping mechanism driving precipitation anomalies in response to equatorial

One mechanism for vertical velocity and rainfall changes is the already discussed compensating upper-level convergence

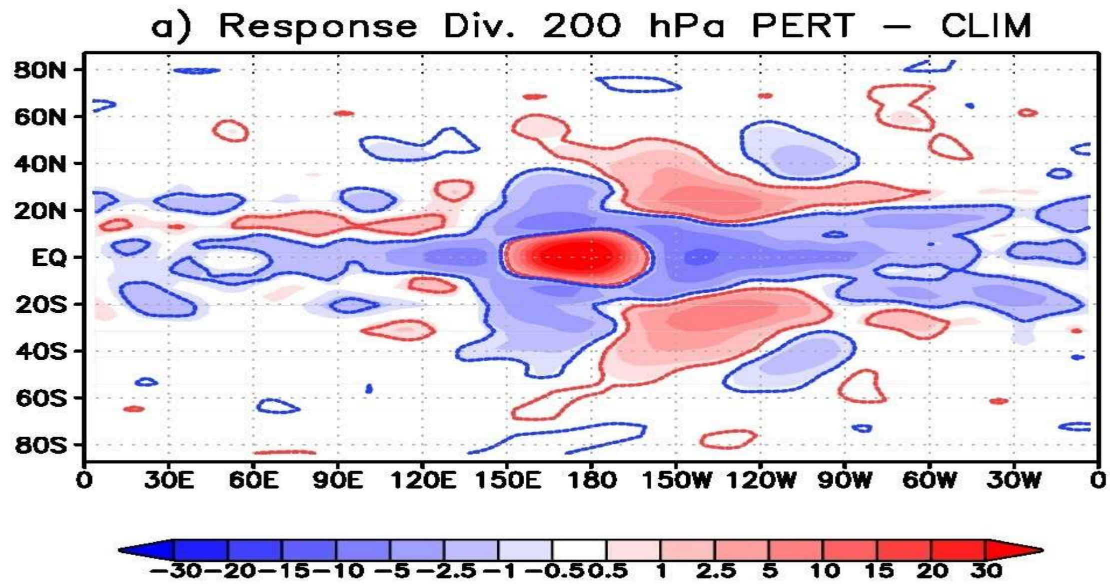

But structure does not fit so nicely with rainfall!

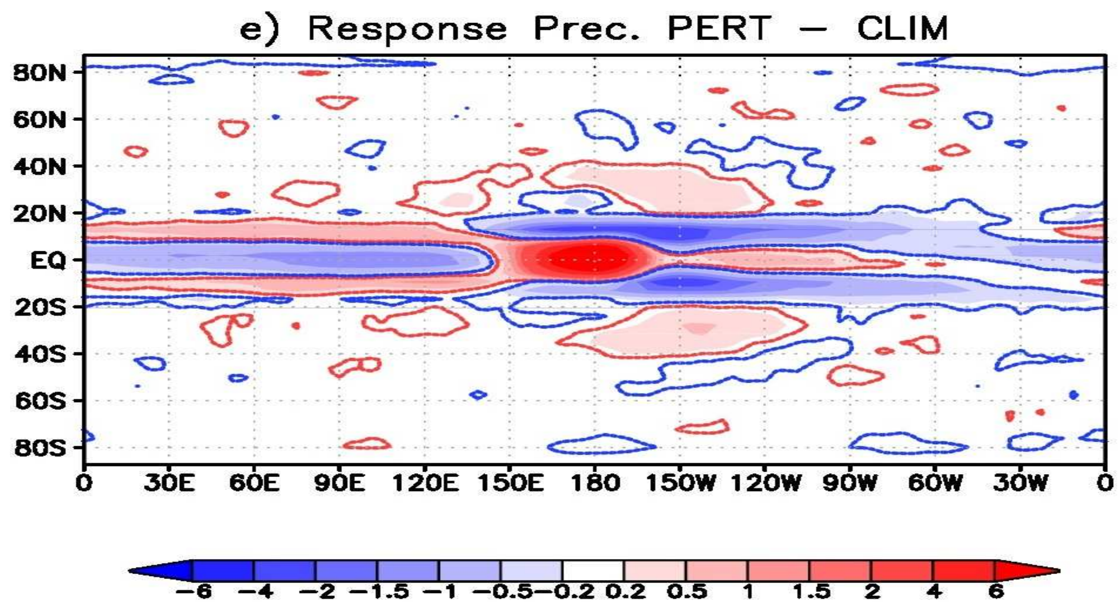

Hamouda & Kucharski (2018) , Ekman pumping mechanism driving precipitation anomalies in response to equatorial

Surface zonal wind

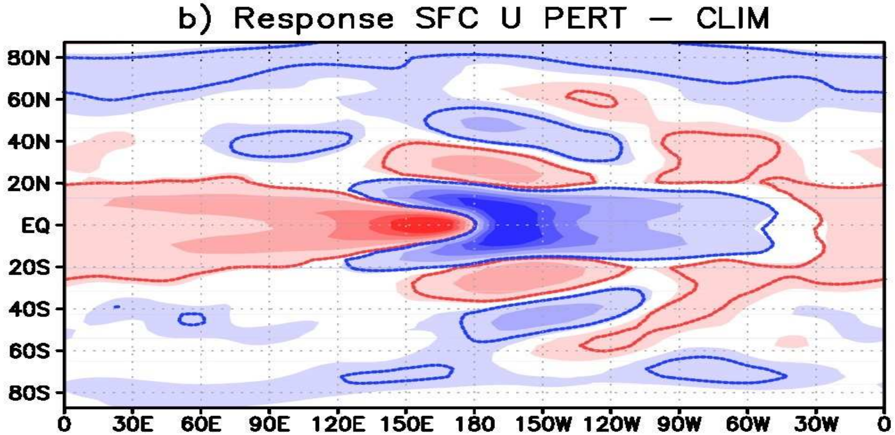

The low-level response

$$\xi_g = \cancel{\frac{\partial v_g}{\partial x}}^{\sim 0} - \frac{\partial u_g}{\partial y}$$

Ekman pumping

Note: $-S_p\omega \approx S_p \rho g w$

$$w(De) = \xi_g \sqrt{\frac{K_m}{2f}}$$

Omega

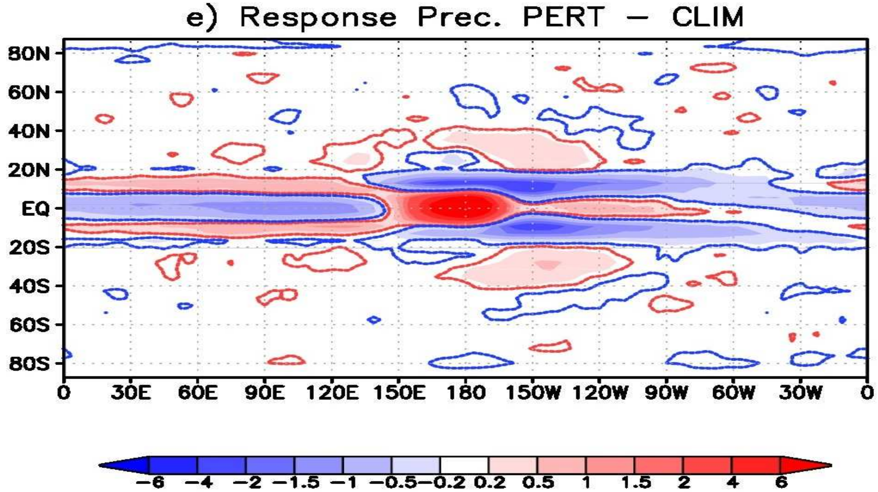

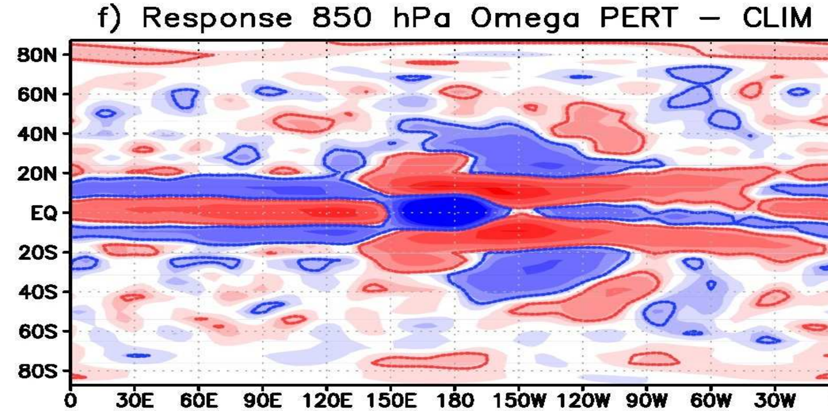

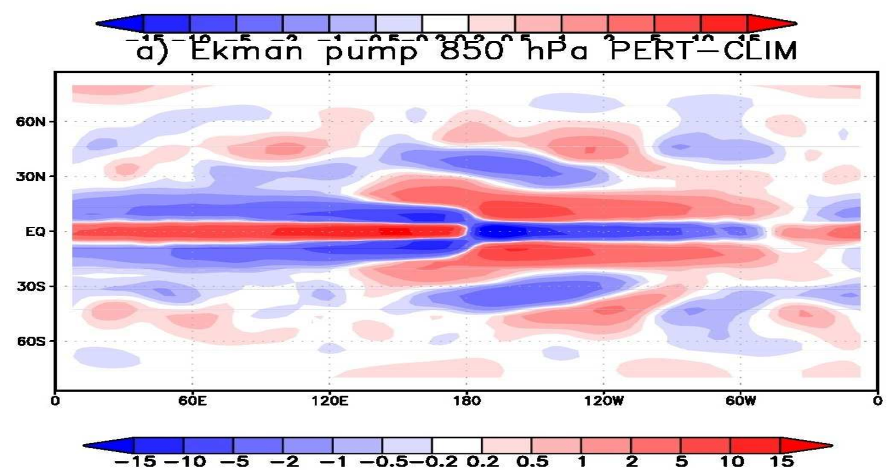

Note that also: $$\Delta w \approx \frac{\Delta Q}{c_p} \frac{1}{S_p \rho g}$$

Always holds! But sometimes ΔQ or rainfall is not the cause for the results of vertical motions!

The mechanism: A Gill-type response; possibly enhanced by compensating sinking in Western Pacific

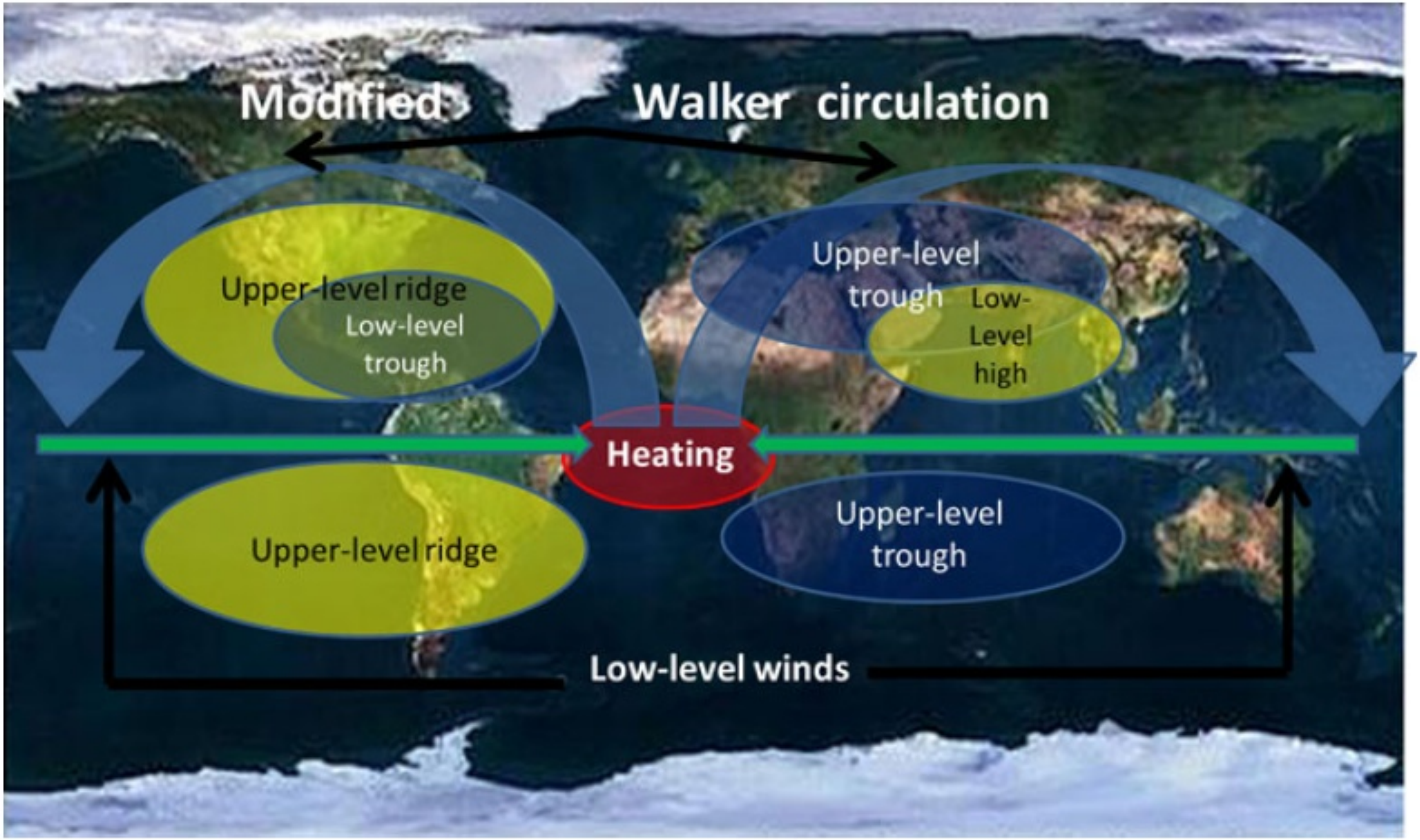

Figure from Barimalala et al., 2011

The Abdus Salam International Centre for Theoretical Physics

Example 2: Decadal Monsoon variability

Indian summer monsoon time series CRU (red), observed SST forced (black) and Indian Ocean forced (green)

Indian Monsoon Index

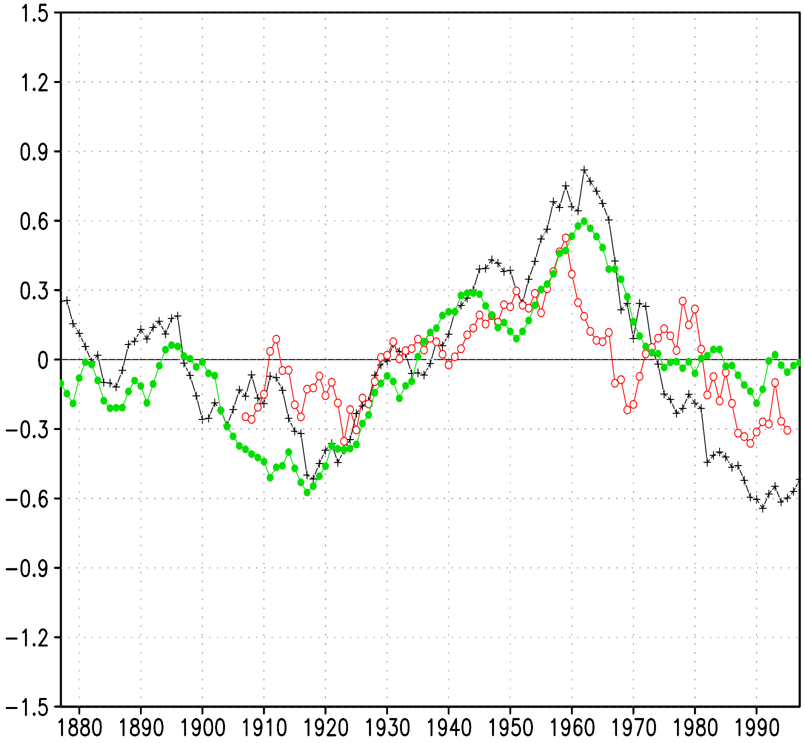

PC1 CRU, PC2 Model

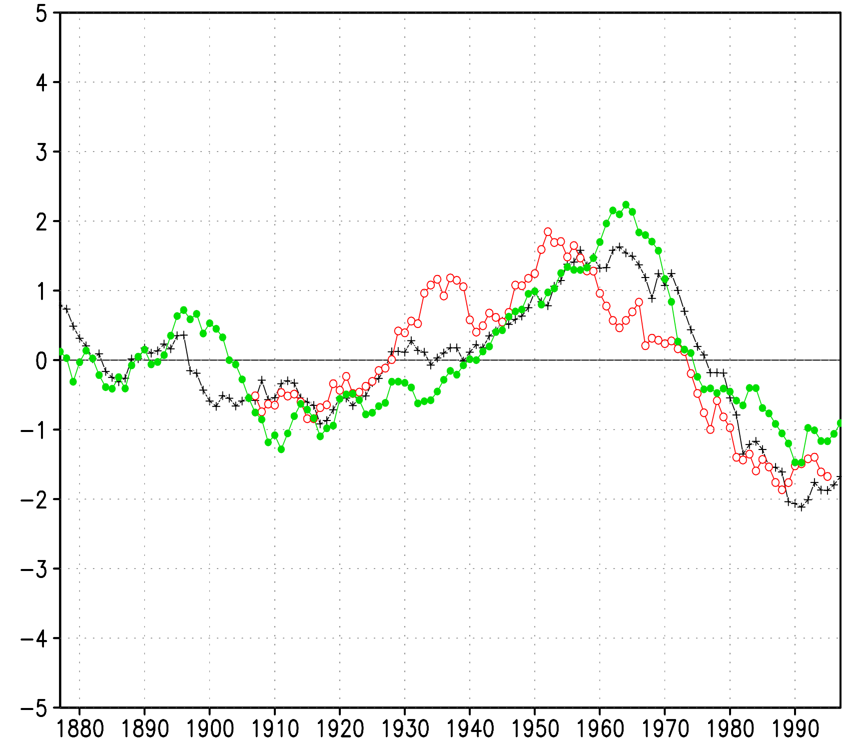

From: Kucharski et al., 2006, GRL, VOL. 33, L03709, doi:10.1029/2005GL025371

The Abdus Salam International Centre for Theoretical Physics

Regressions of PCs on SSTs

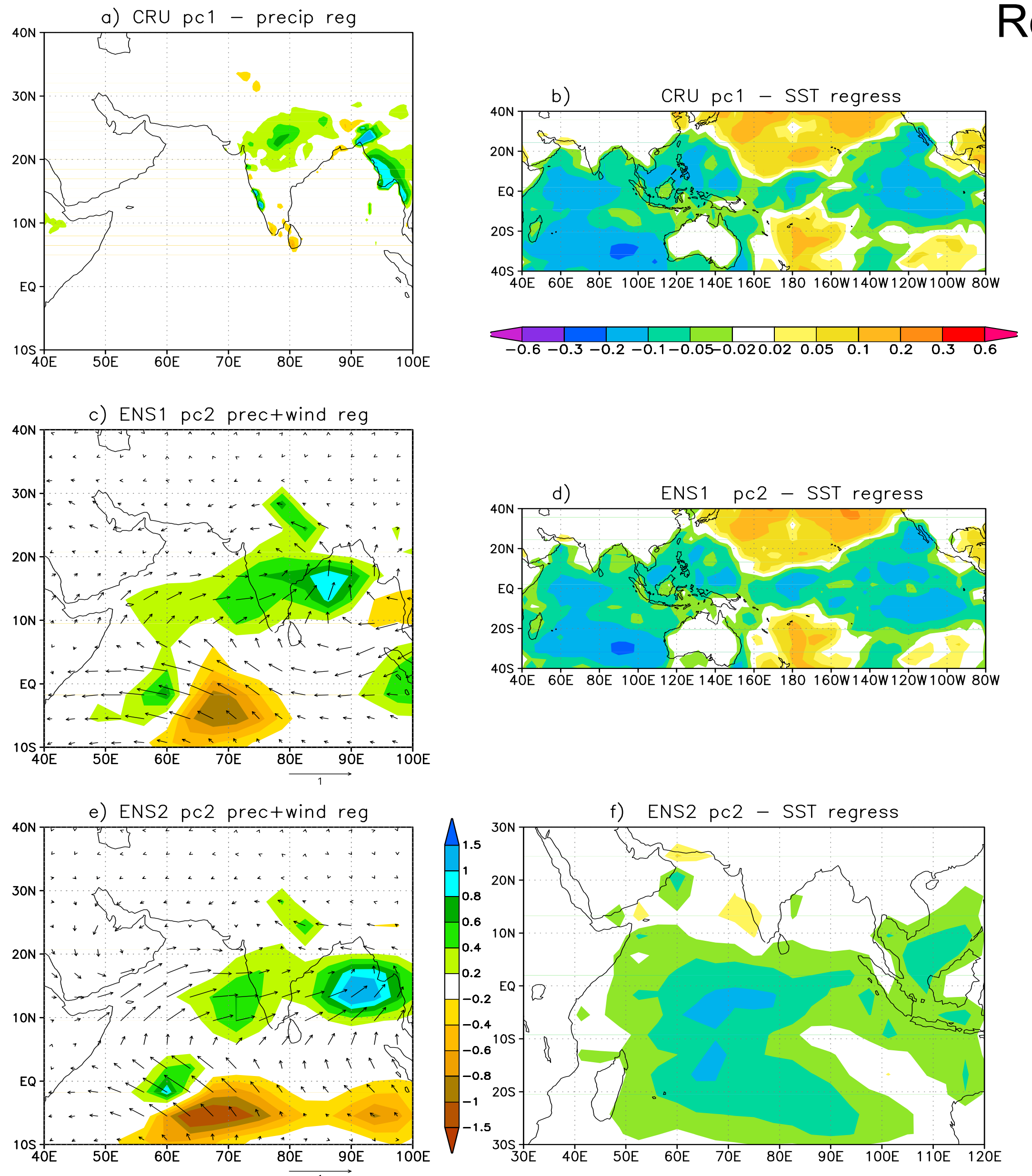

CRU PC1

Global SST forced PC2

Indian Ocean SST forced PC2

From: Kucharski et al., 2006, GRL, VOL. 33, L03709, doi:10.1029/2005GL025371

Example 3: Indian Ocean Dipole forcing of East Africa short rains

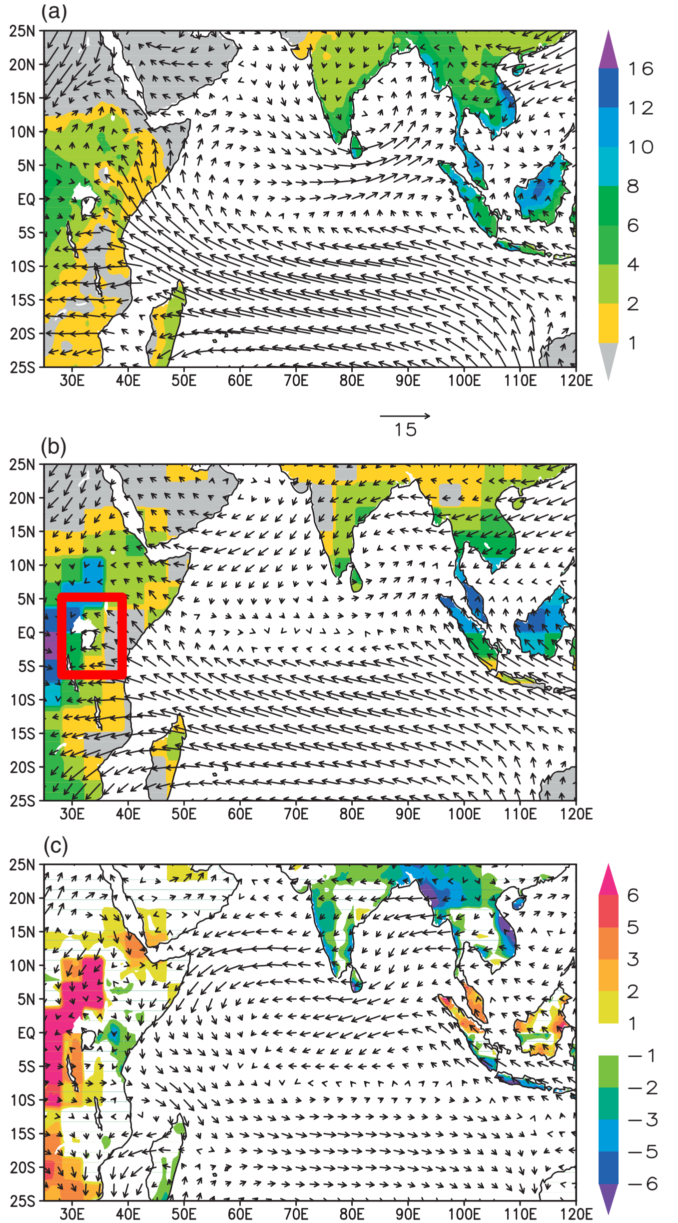

Figure 1. SON rainfall climatology (shaded) and 925 hPa winds: (a) CRU rainfall

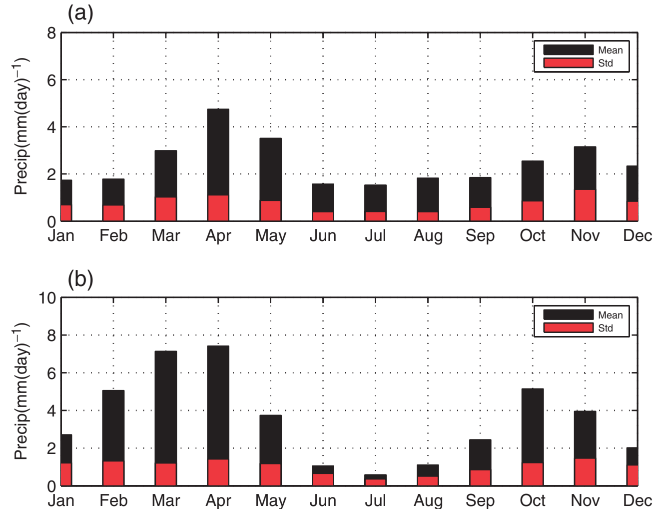

Figure 2. Climatology of the East African short rains averaged over (5°S–5°N, 30–40°E) along with monthly standard deviation derived from (a) observation results and (b) the AO.ICTPAGCM simulation; rainfall units are given in mm (day)$^{-1}$.

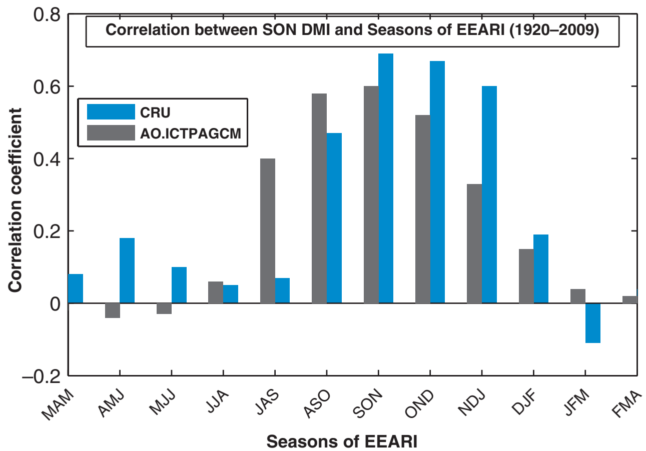

Figure 3. Time-lagged correlation between the seasonal mean annual cycle of EEARI and SON mean DMI during the period 1920–2009. Rainfall is derived from CRU observations and the AO.ICTPAGCM experiment, whereas the DMI is from ERSSTv3b.

CC between SON DMI and EEARI

From Bahaga et al., *Q. J. R. Meteorol. Soc.* 141: 16 - 26, January 2015 A DOI:10.1002/qj.2338

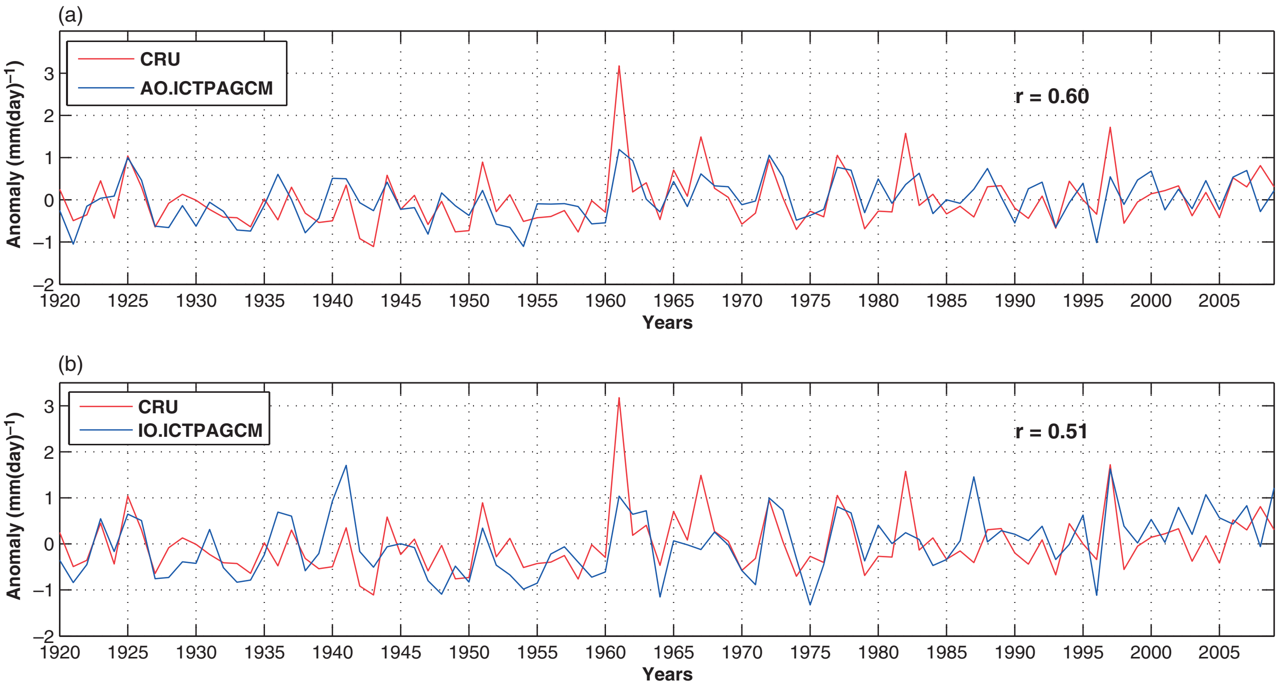

Figure 4. Interannual variability of the seasonal mean rainfall anomaly for SON over Equatorial East Africa (5°S–5°N, 30–40°E) since 1920. Plotted in blue is the rainfall derived from (a) AO-ICTPAGCM and (b) IO-ICTPAGCM simulations; red is the observed rainfall resulting from CRU. All rainfalls are given in mm day^{-1}.

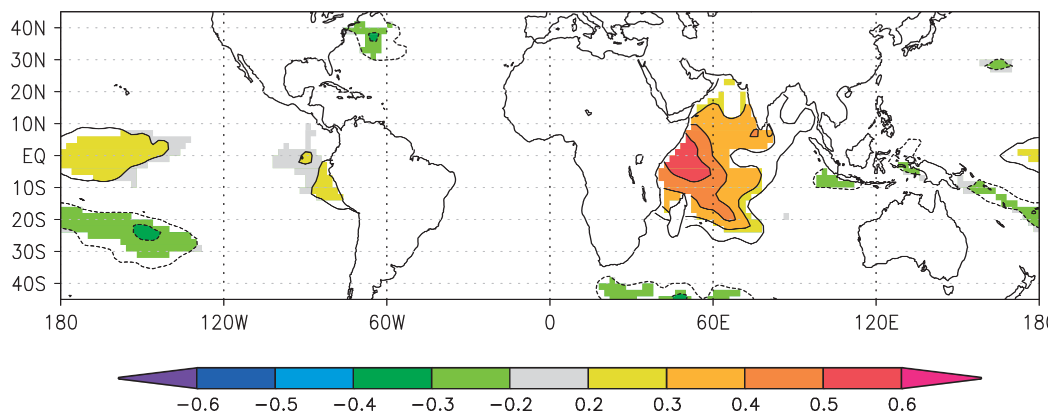

Figure 5. Concurrent correlations between the SON short rains index derived from the AO.ICTPAGCM experiment and SON season SST computed from ERSSTv3b. Shaded contours are statistically significant at least 95% confidence level.

From Bahaga et al., *Q. J. R. Meteorol. Soc.* 141: 16 – 26, January 2015 A DOI:10.1002/qj.2338

<u>Example 4:</u> Change of ENSO-Northwest India winter precipitation relationship

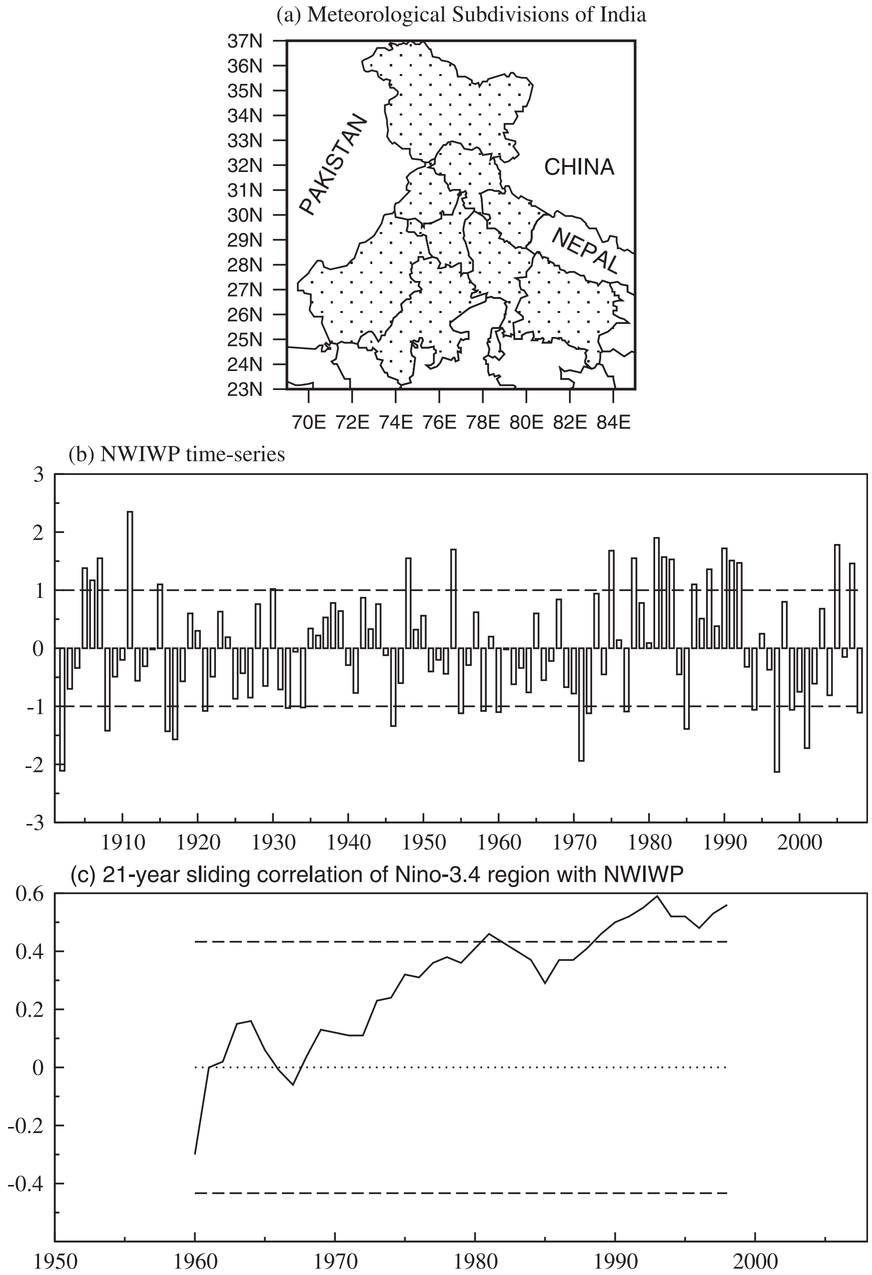

NWIWP index

Correlation of NWIWP with Nino3.4 index

From: Yadav et al., J Climate 2010,DOI: 10.1175/2009JCLI3202.1

The Abdus Salam International Centre for Theoretical Physics

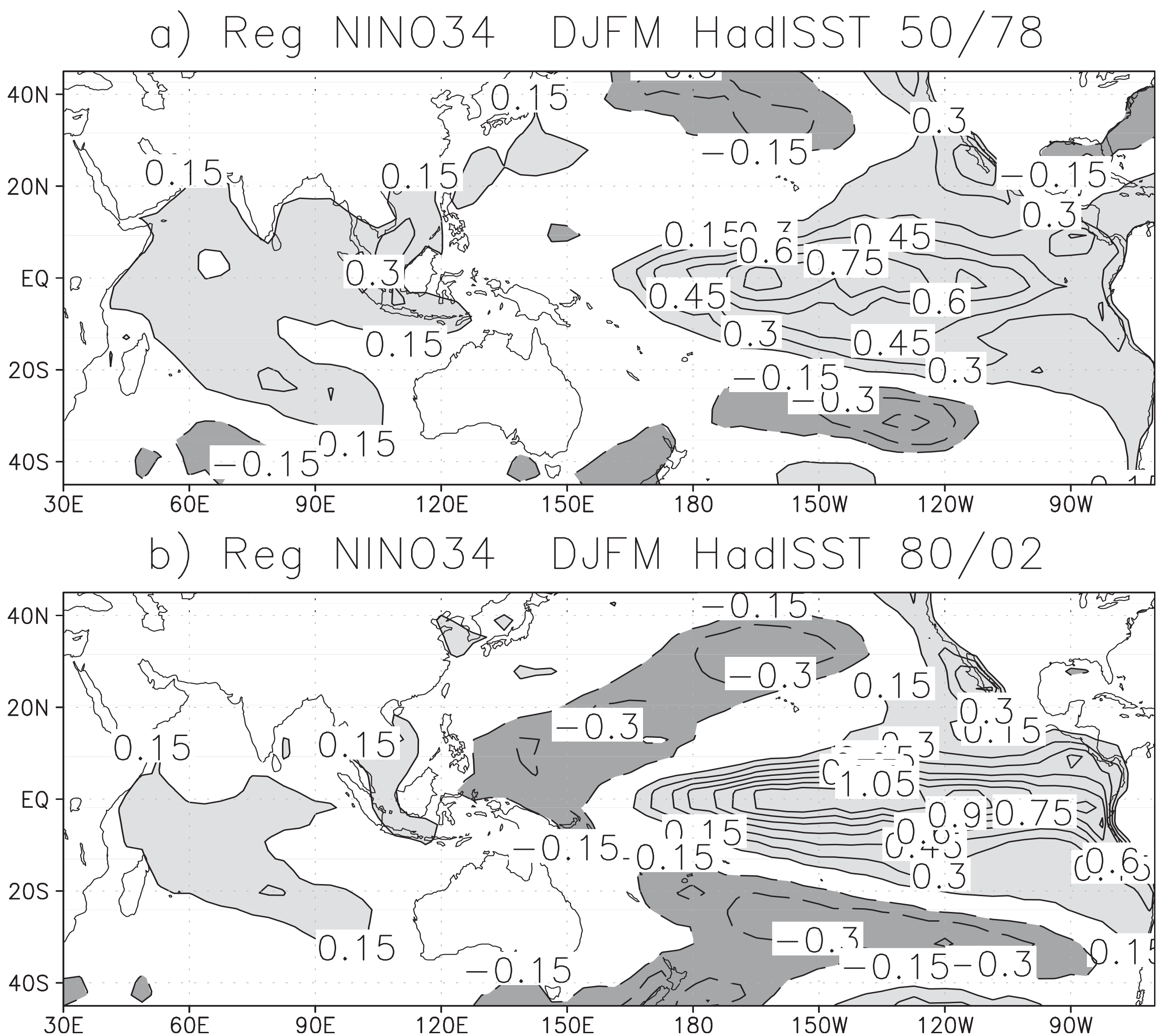

FIG. 6. Regression of observed SSTs (K) onto Niño-3.4 index for (a) 1950–1978 and (b) 1980–2002.

DJFM SST regression on Nino3.4 index for

1950/1978

1980-2002

From: Yadav et al., J Climate 2010,DOI: 10.1175/2009JCLI3202.1

The Abdus Salam International Centre for Theoretical Physics

Regression of DJFM SLP and 200 hPa height onto Nino3.4 index for

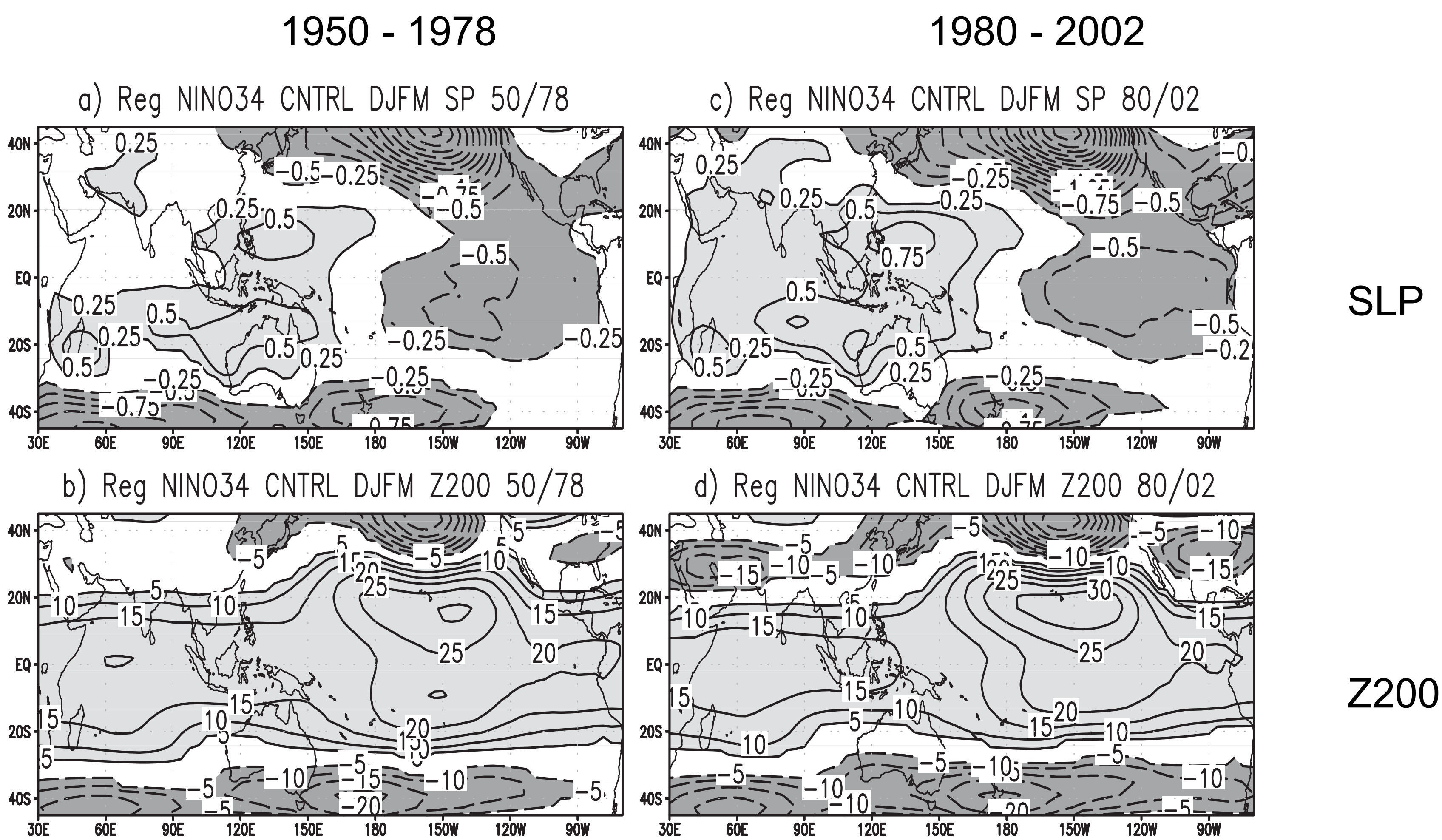

FIG. 7. Regression onto the Niño-3.4 index of modeled (CNTRL): (a) surface pressure (hPa) 1950–78, (b) 200-hPa geopotential height (m) 1950–78, (c) surface pressure (hPa) 1980–2002, (d) 200-hPa height (m) 1980–2002.

From: Yadav et al., J Climate 2010,DOI: 10.1175/2009JCLI3202.1

The Abdus Salam International Centre for Theoretical Physics

Signal variance/Total variance of DJFM 200 hPa height

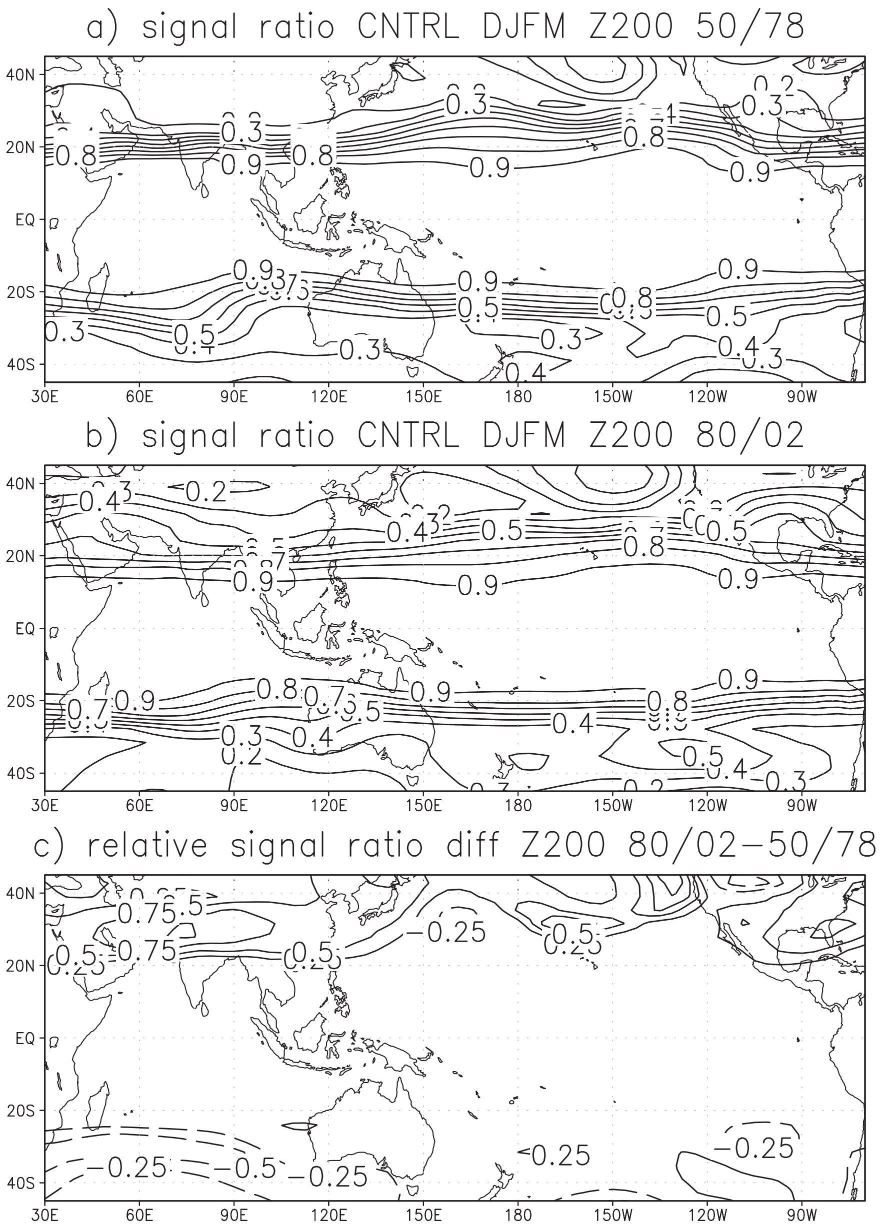

1950 - 1978

1980 - 2002

Difference

(1950 - 1978) minus (1980 – 2002)

FIG. 9. Ratio of forced variance (derived from the ensemble mean of CNTRL) to total variance: (a) 1950–78, (b) 1980–2002, and (c) difference of (b) and (a) divided by the mean of (a) and (b).

From: Yadav et al., J Climate 2010,DOI: 10.1175/2009JCLI3202.1

The Abdus Salam International Centre for Theoretical Physics

Regression of DJFM 200 hPa vel pot and eddy streamfunction height onto Nino3.4 index for

1950 - 1978 | 1980 - 2002

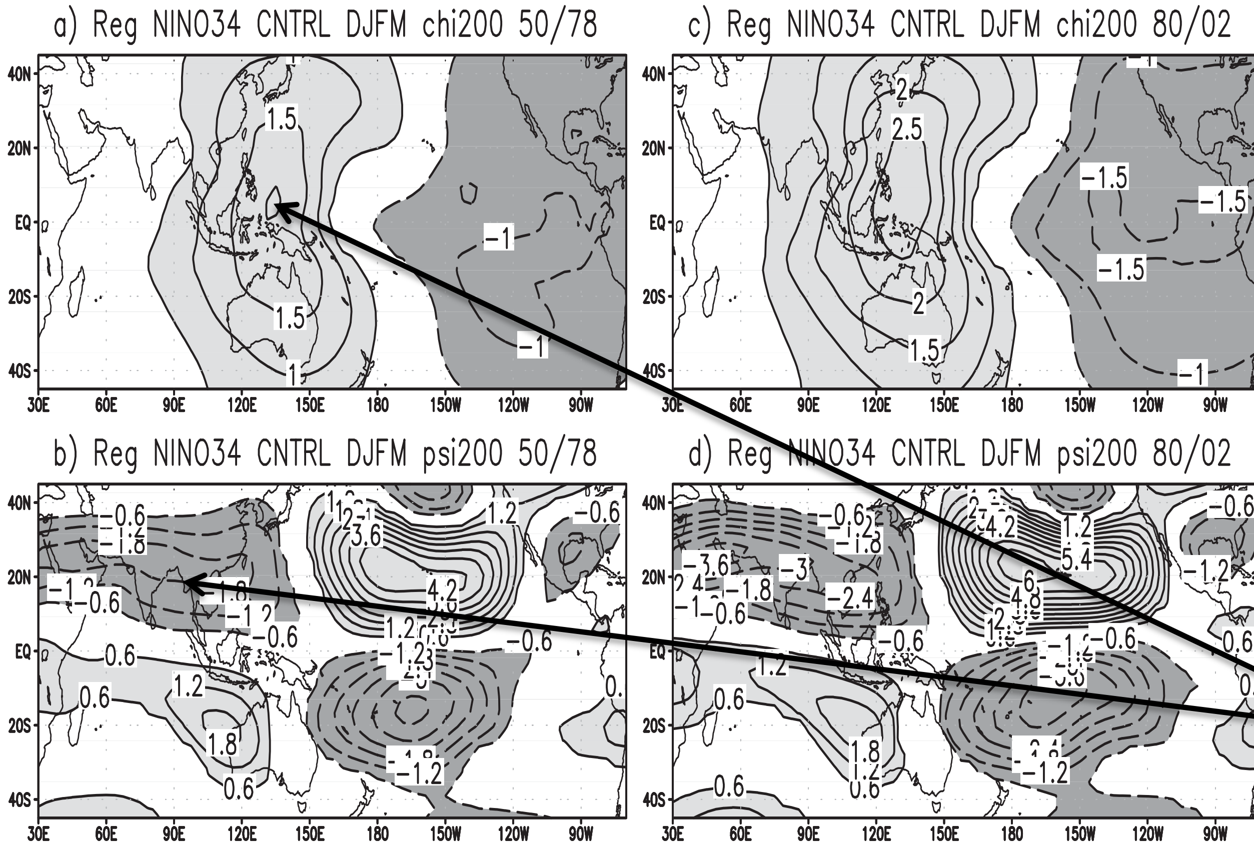

200 hPa velocity potential

200 hPa eddy streamfunction

Remember Sverdrup balance!

FIG. 11. Regression onto the Niño-3.4 index of modeled (CNTRL): (a) 200-hPa velocity potential 1950–78, (b) 200-hPa eddy streamfunction 1950–78, (c) 200-hPa velocity potential 1980–2002, and (d) 200-hPa streamfunction 1980–2002 (units are 10^6 m^2 s^{-1}).

From: Yadav et al., J Climate 2010,DOI: 10.1175/2009JCLI3202.1

Understanding the upper-level response (note response is baroclinic and changes sign in lower levels)

$$\xi_g = \frac{\partial v_g}{\partial x} - \frac{\partial u_g}{\partial y} \qquad \frac{d_g \xi_g}{dt} = -f\left(\frac{\partial u_a}{\partial x} + \frac{\partial v_a}{\partial y}\right) - \beta v_g$$

approximate vorticity equation; again gradients are small in tropics

$$\xi_g = \nabla^2 \psi$$

$$\boxed{\beta v_\psi = -f_0\left(\frac{\partial u_\chi}{\partial x} + \frac{\partial v_\chi}{\partial y}\right)}$$

Sverdrup balance in tropics (Rodwell & Hoskins)

$$\mathbf{v}_\chi = \nabla \chi \qquad \mathbf{v}_\psi = \mathbf{k} \times \nabla \psi$$

Note that responses are baroclinic; i.e. change sign with height

200 hPa Velocity Potential χ

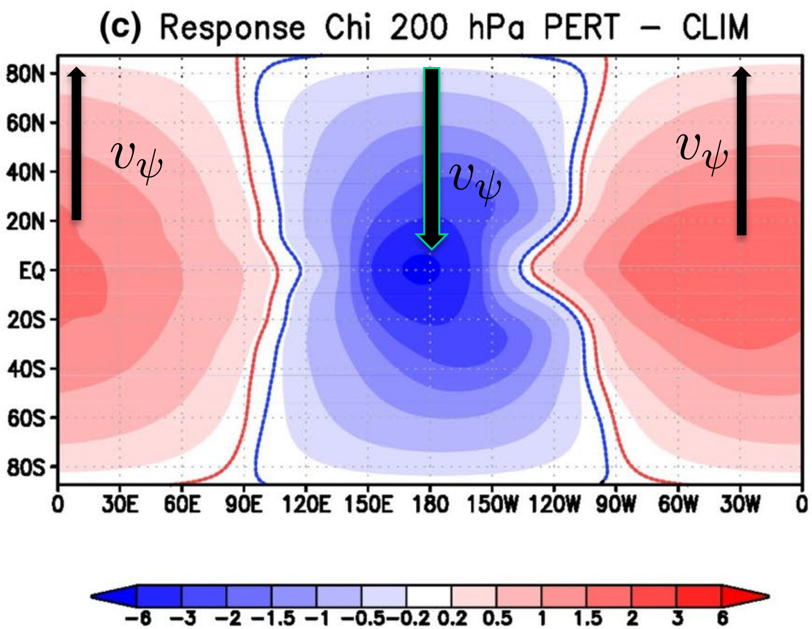

200 hPa Eddy Streamfunction Ψ

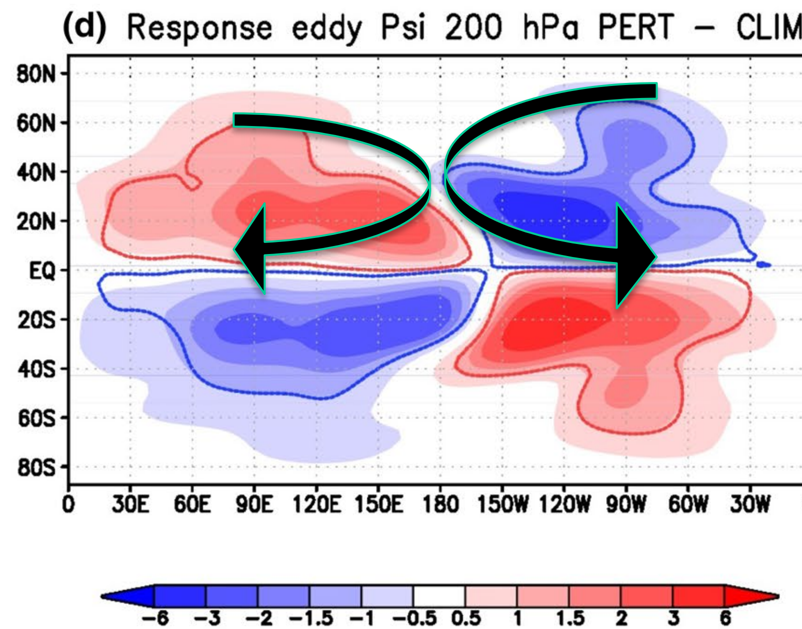

Hamouda & Kucharski (2018) , Ekman pumping mechanism driving precipitation anomalies in response to equatorial

Example 5: Delayed ENSO impact on European spring precipitation

First EOF of late spring precipitation

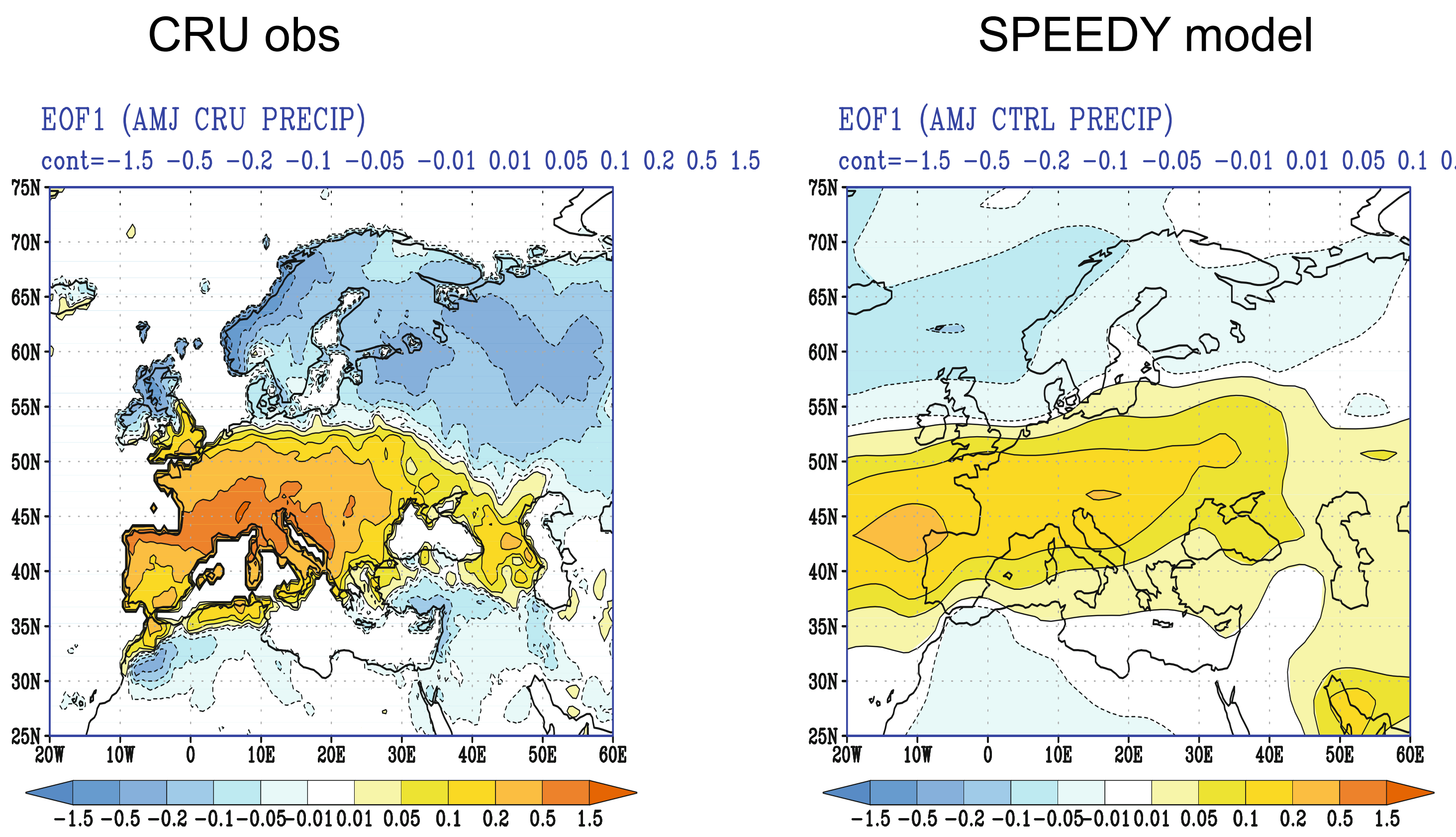

Fig. 3 First EOF mode of spring (AMJ) precipitation over the NAE region for: **a** CRU data and **b** CTRL experiment. Contours every 0.01, 0.05, 0.1, 0.2, 0.5 and 1.0

From: Herceg-Bulic' et al., 2010, Clim Dyn, DOI 10.1007/s00382-011-1151-9

The Abdus Salam International Centre for Theoretical Physics

Corr of first EOF with

CRU obs

SPEEDY presc SST

SPEEDY presc SST +mxl

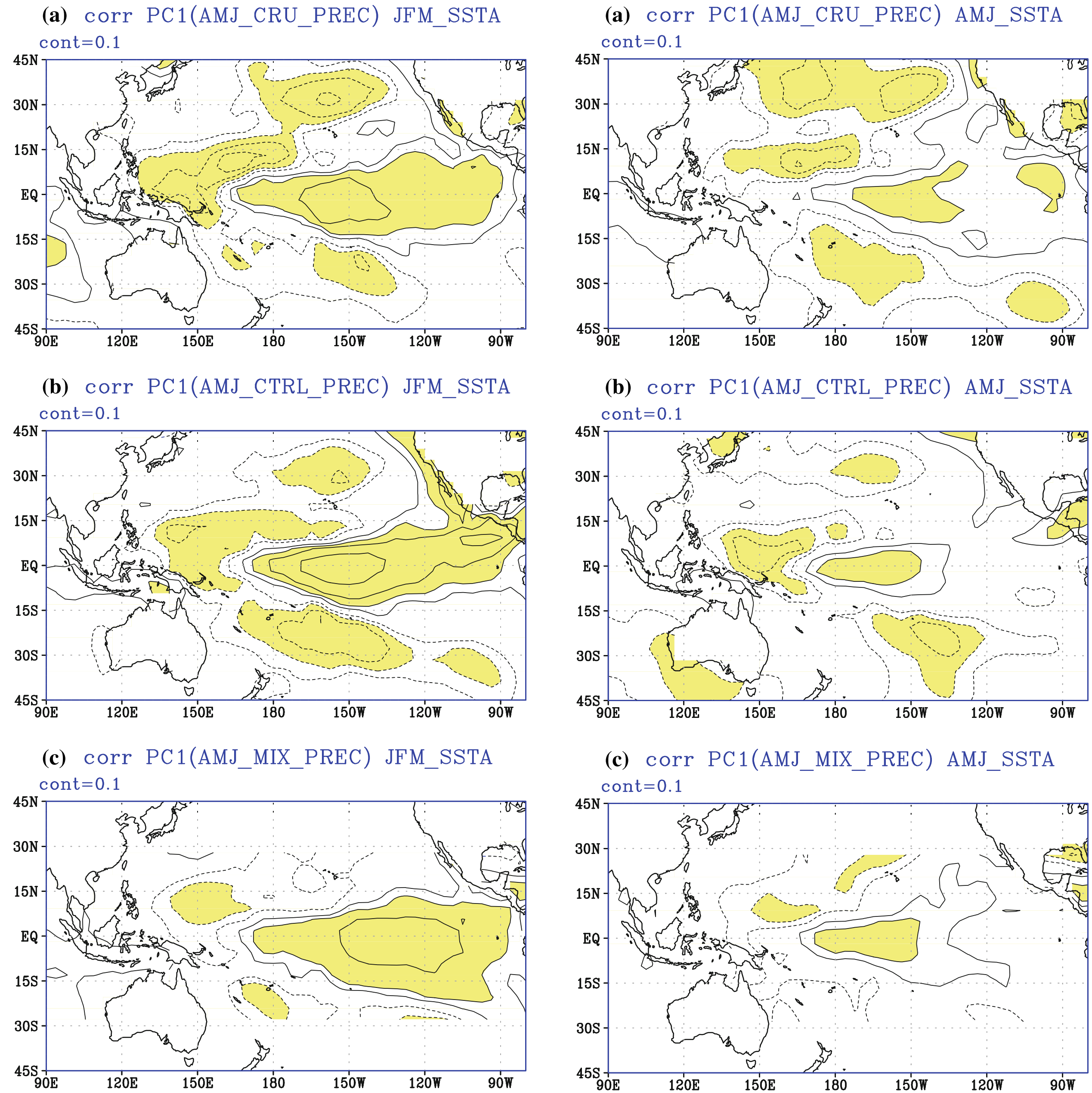

From: Herceg-Bulic' et al., 2010, Clim Dyn, DOI 10.1007/s00382-011-1151-9

ST anomalies.
d. Correlations
are *shaded*

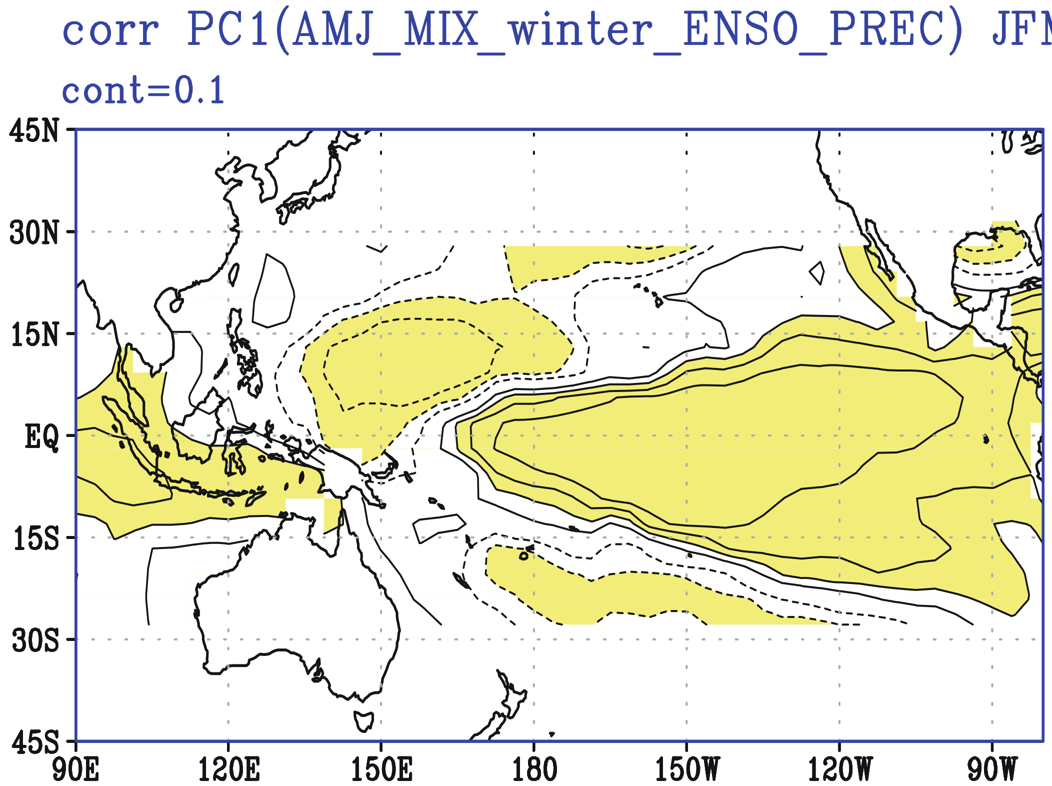

Corr of first EOF with

SPEEDY + presc SST winter + mxl

Prescribing observed SSTs from October to March, and mixed-layer in North Atlantic region

From: Herceg-Bulic' et al., 2010, Clim Dyn, DOI 10.1007/s00382-011-1151-9

Warm | Cold | ENSO SLP composites

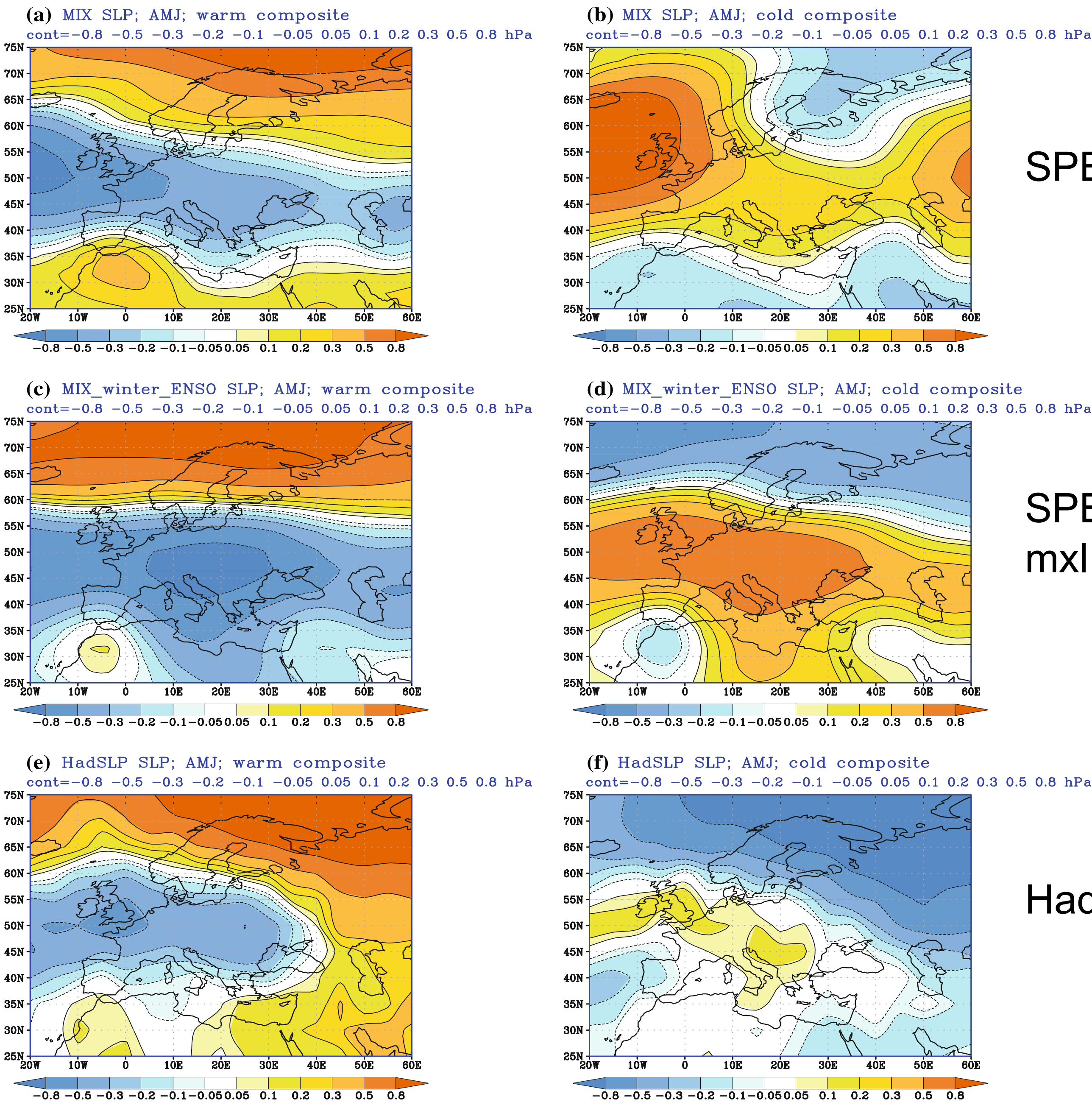

SPEEDY + presc SST +mxl

SPEEDY + prec SST winter + mxl

HadISST obs

prec comp

CRU obs

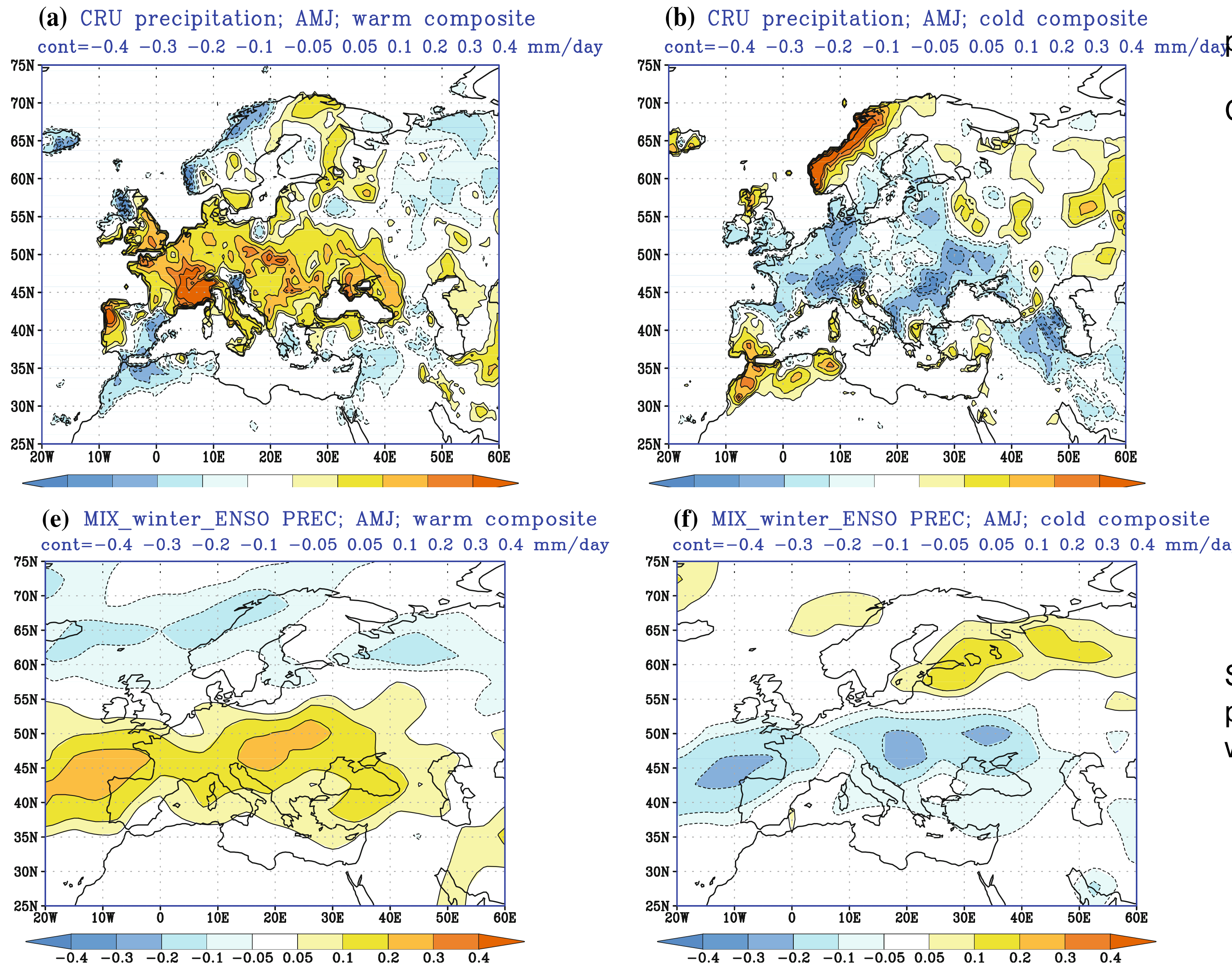

SPEEDY +
prec SST
winter
+ mxl

Warm event

Cold event

From: Herceg-Bulic' et al., 2010, Clim Dyn, DOI 10.1007/s00382-011-1151-9

SST correlation

Speedy + presc SST winter + mxl. Speedy + mxl

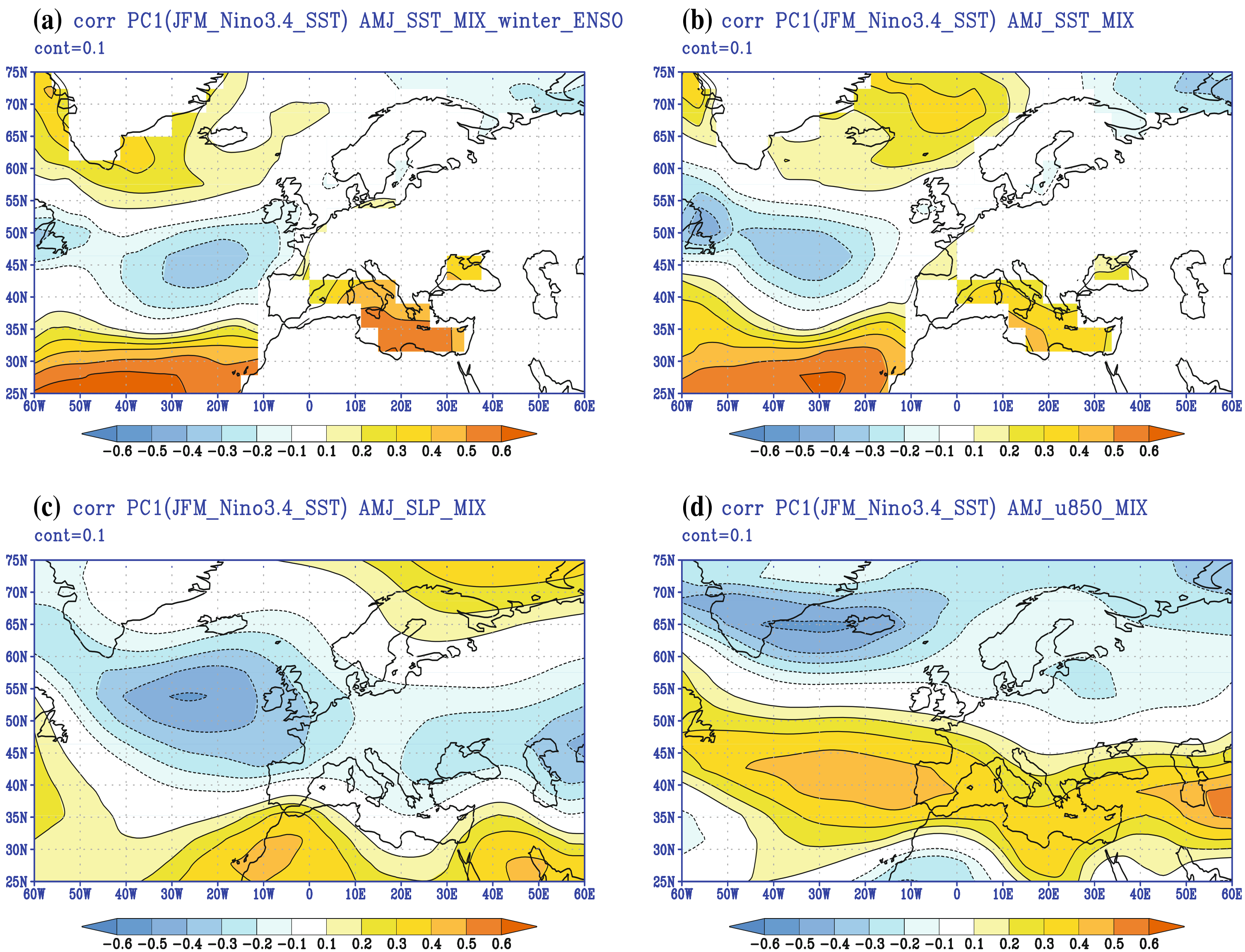

NA clim SST

NA MXL SST

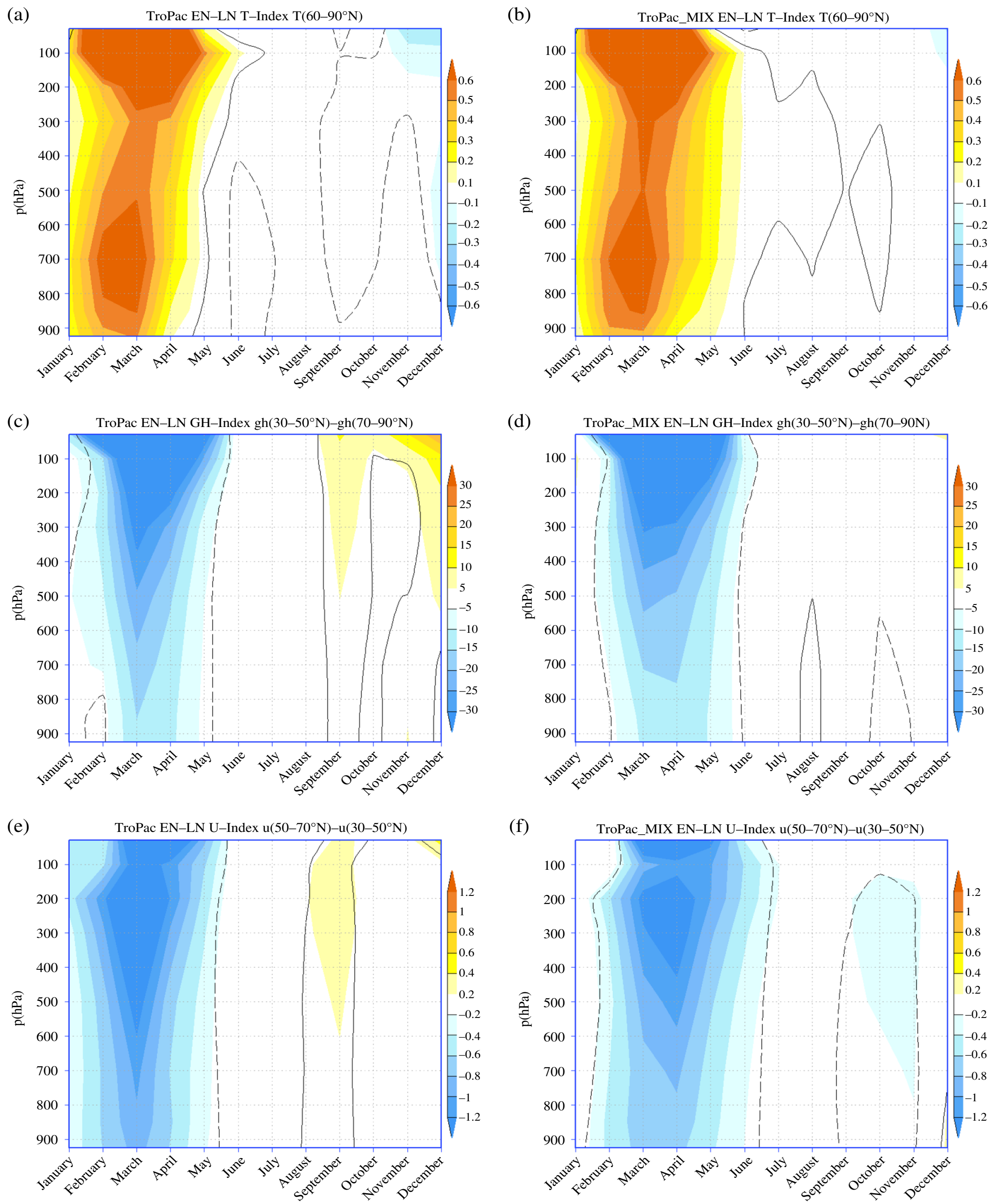

Comparing an experiment with frocing from Dec to March with clim SST and one with mxl in NA

Temperature

~ - AO index
gh (30-50) – gh(70-90)

u(50-70)-u(30-50)

From: Herceg-Bulic' et al., 2017, DOI: 10.1002/joc.4980

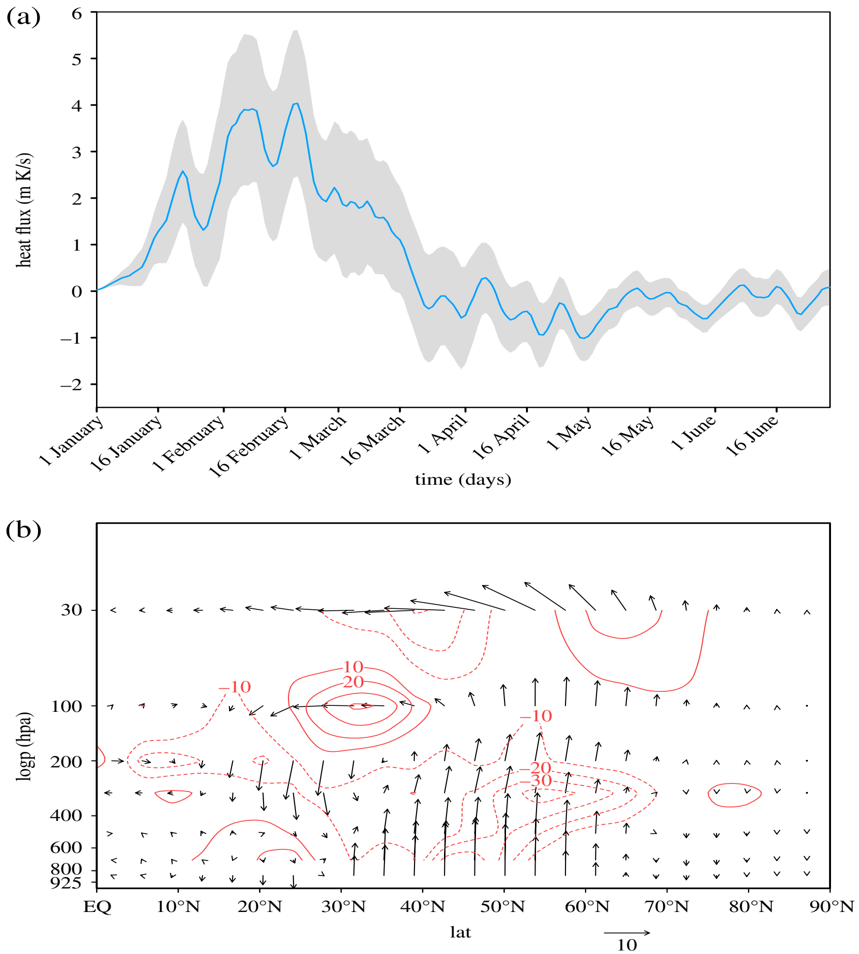

Eddy heat fluxes at 100 hPa and

Eliasse-Palm fluxes in February for an idealized El Nino forcing experiment minus control with climatoligical SSTs.

From: Herceg-Bulic' et al., 2017, DOI: 10.1002/joc.4980

Example 6: Interbasin teleconnections

What about a possible impact of tropical Atlantic on Pacific SSTs?

After all, ...

The mechanism: A Gill-type response; possibly enhanced by compensating sinking in Western Pacific

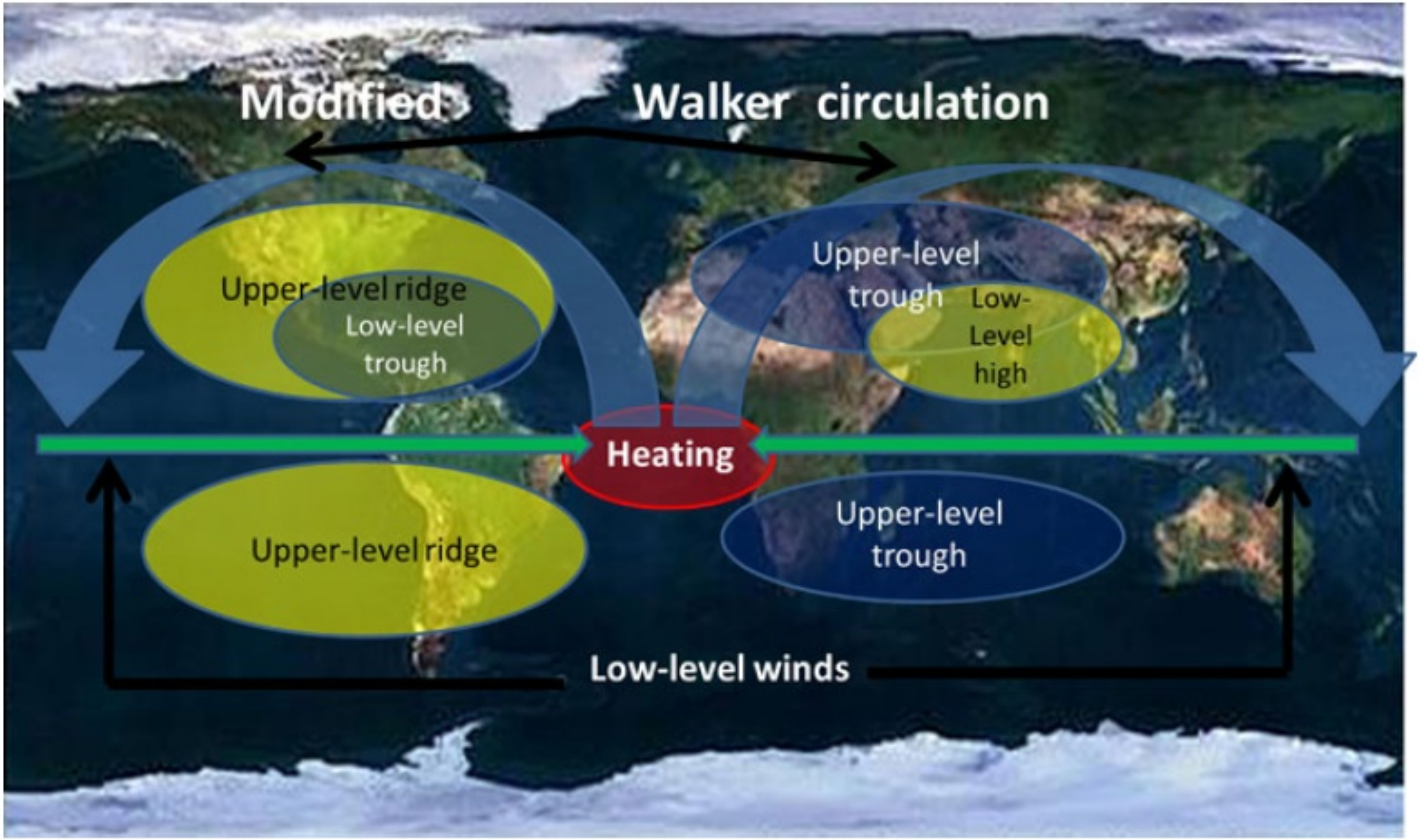

Figure from Barimalala et al., 2011

Growing literature on Atlantic impact on Pacific:

a) Interannual, for example:
Rodriguez-Fonseca et al. (2009), Jansen et al. (2009),
Martin-Rey et al. (2012, 2014, 2015), Ding et al. (2012), Frauen et al. (2012),
Keenlyside et al. (2013), Ham et al. (2013a, 2013b), Polo et al. (2014),
Kucharski et al. (2014), Sasaki et al. (2014), Terray et al. (2016), ...

b) Decadal-to-multidecadal, for example:
Timmermann et al. (2007), Zhang and Delworth (2007), Lu et al. (2008)
Kucharski et al. (2011, 2015, 2016), Chikamoto et al. (2012, 2015, 2016),
McGregor et al. (2014), Kang et al. (2014), Li et al., (2015), Sun et al. (2017),
Trascasa-Castro et al., (2021), Ruprich-Robert et al., (2021)
and surely many more....

The Abdus Salam International Centre for Theoretical Physics

How can the 'small' Atlantic Ocean impact variability in the 'big' Pacific Ocean? Probably the Atlantic Ocean can provide some initial persistent forcing that is amplified in the Pacific through positive feedback (e.g. Bjerknes feedback and others). Some catalytic effect.

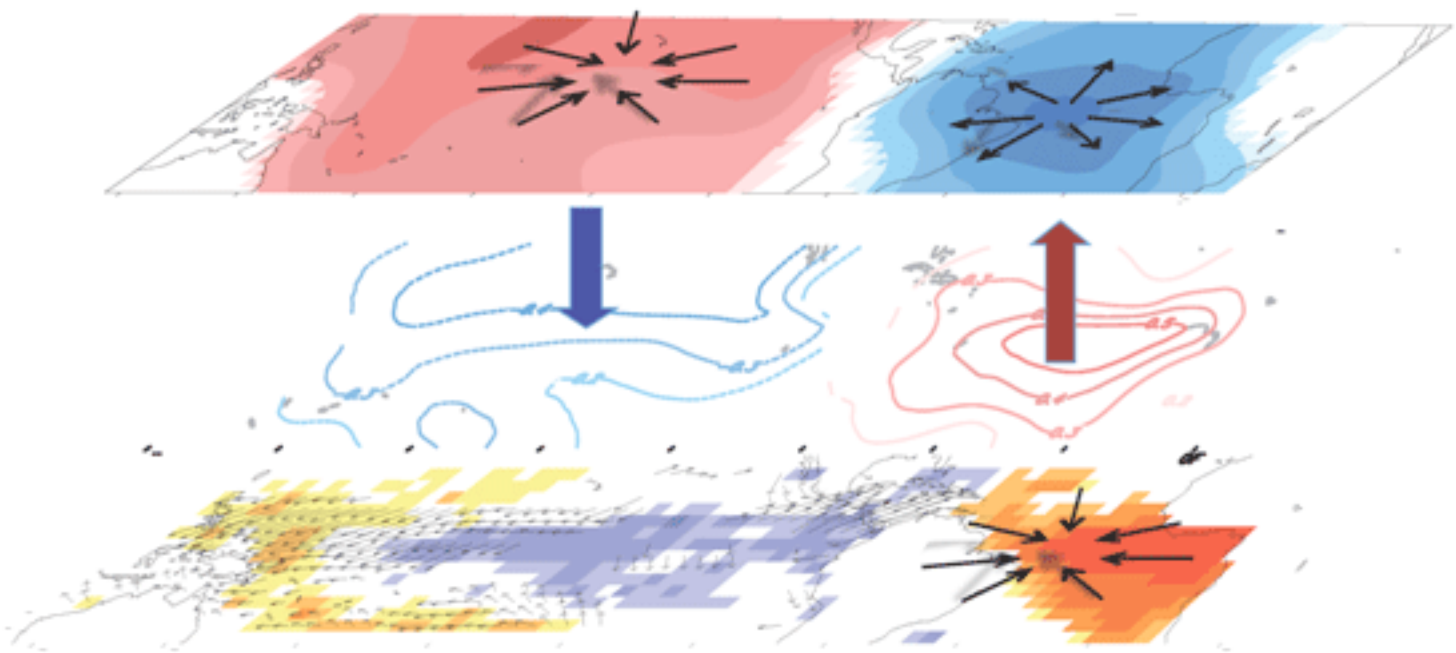

The Abdus Salam International Centre for Theoretical Physics

Atlantic Pacemaker experiments

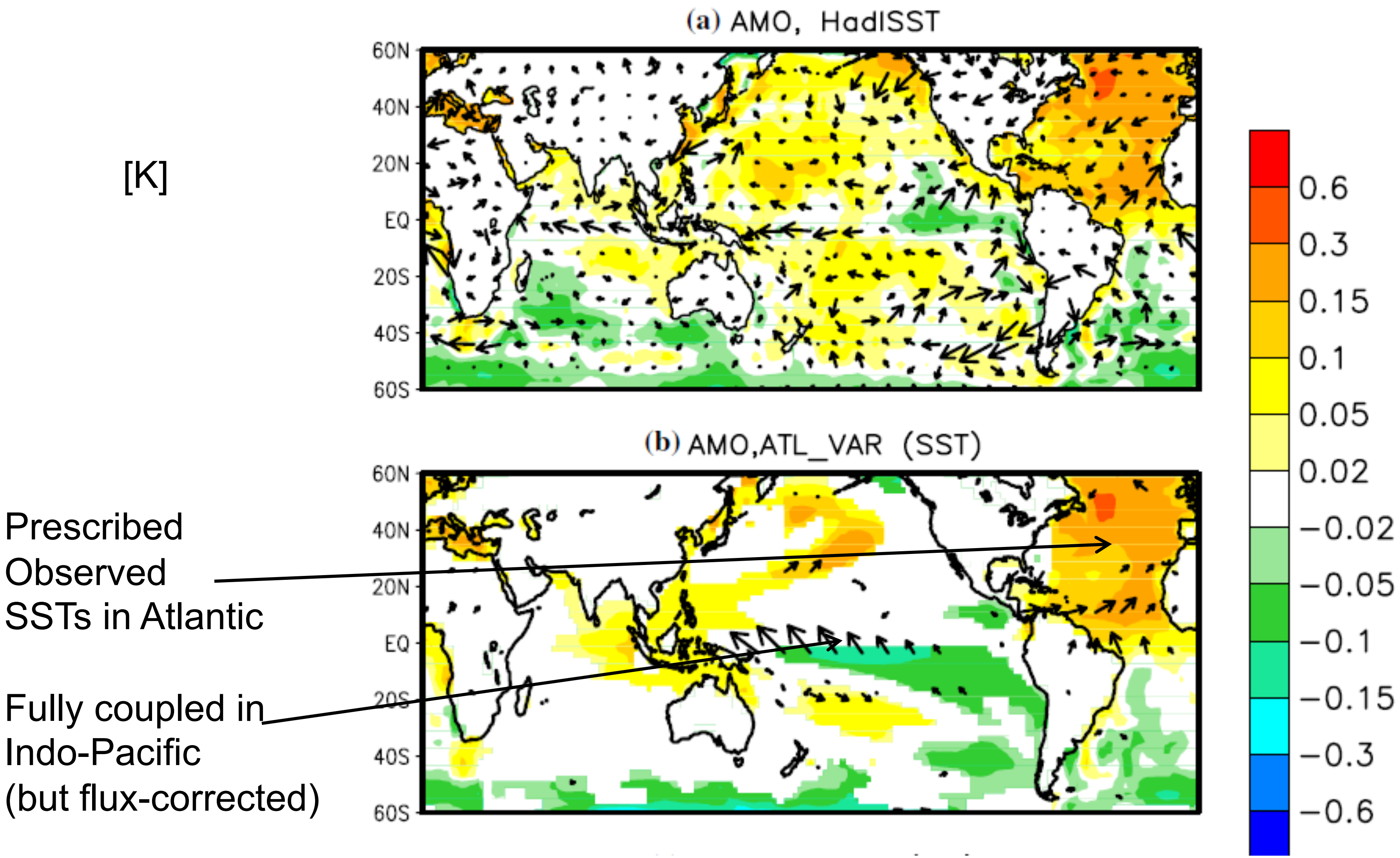

a) Atlantic zonal mode impact on ENSO

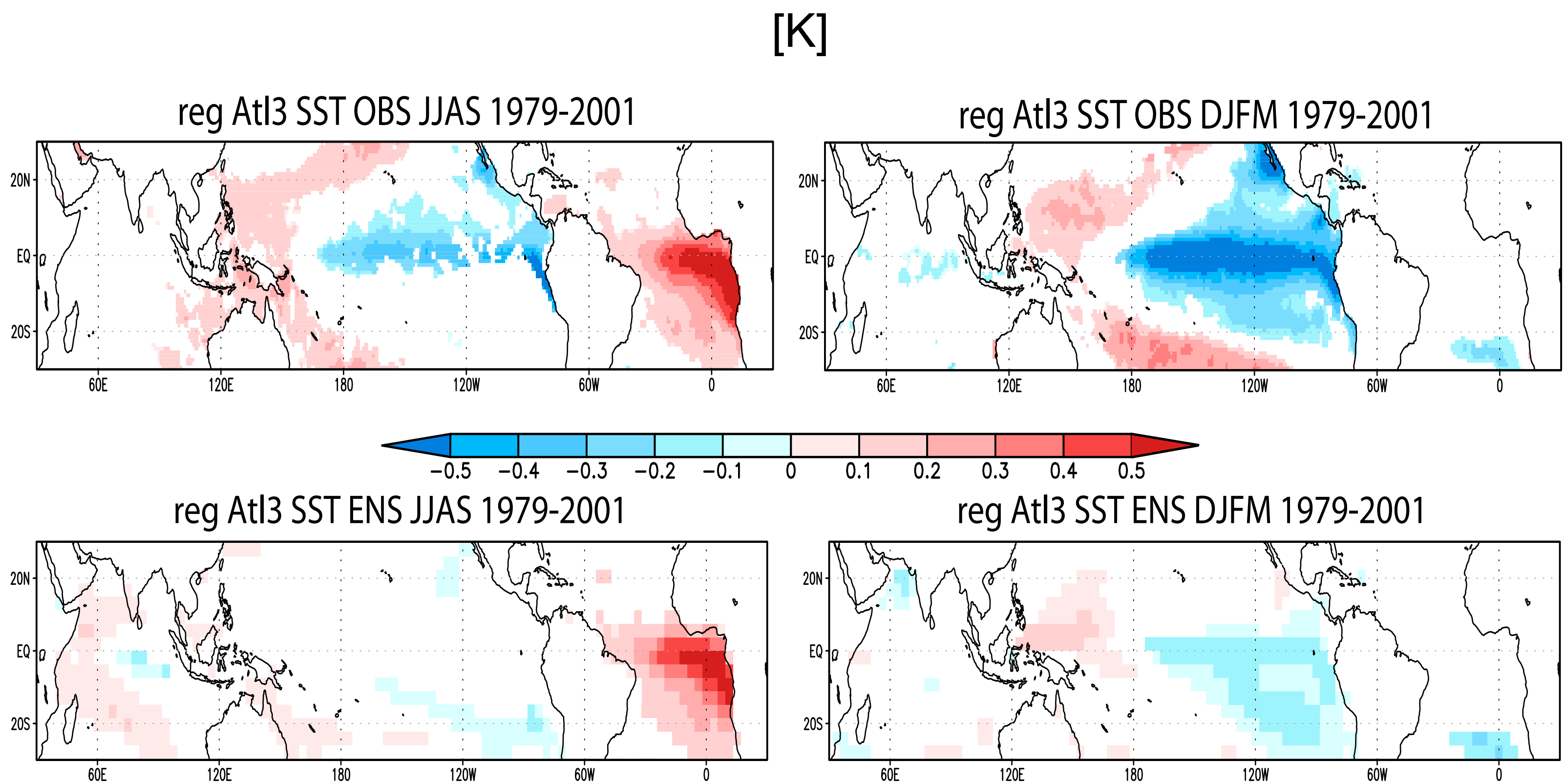

From Rodriguez-Fonseca et al. (2009) for period 1979 to 2001
Experiments done with speedy coupled to an RGO.

b) Atlantic Multidecadal Variability impact on Indo-Pacific

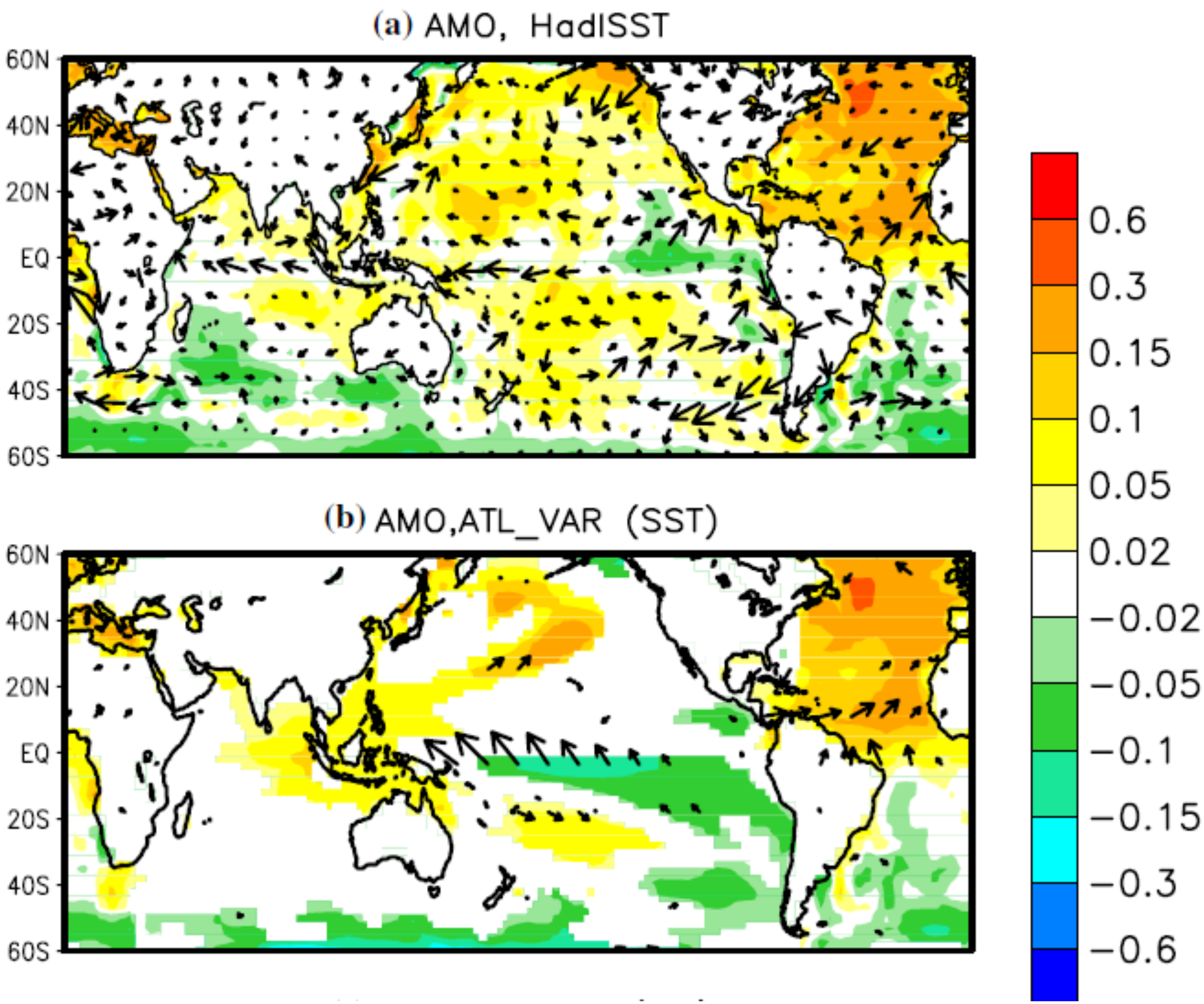

Regression of AMO index onto SSTs and low-level winds

OBS

[K]

SPEEDY-NEMO

From F. Kucharski, F. Irkam et al. (2015), Clim Dyn, DOI 10.1007/s00382-015-2705-z

b) Atlantic Multidecadal Variability impact on Indo-Pacific

Time series (low-pass filtered) of AMO index (green), central Pacific surface wind index obs (black), model (red); [m/s]

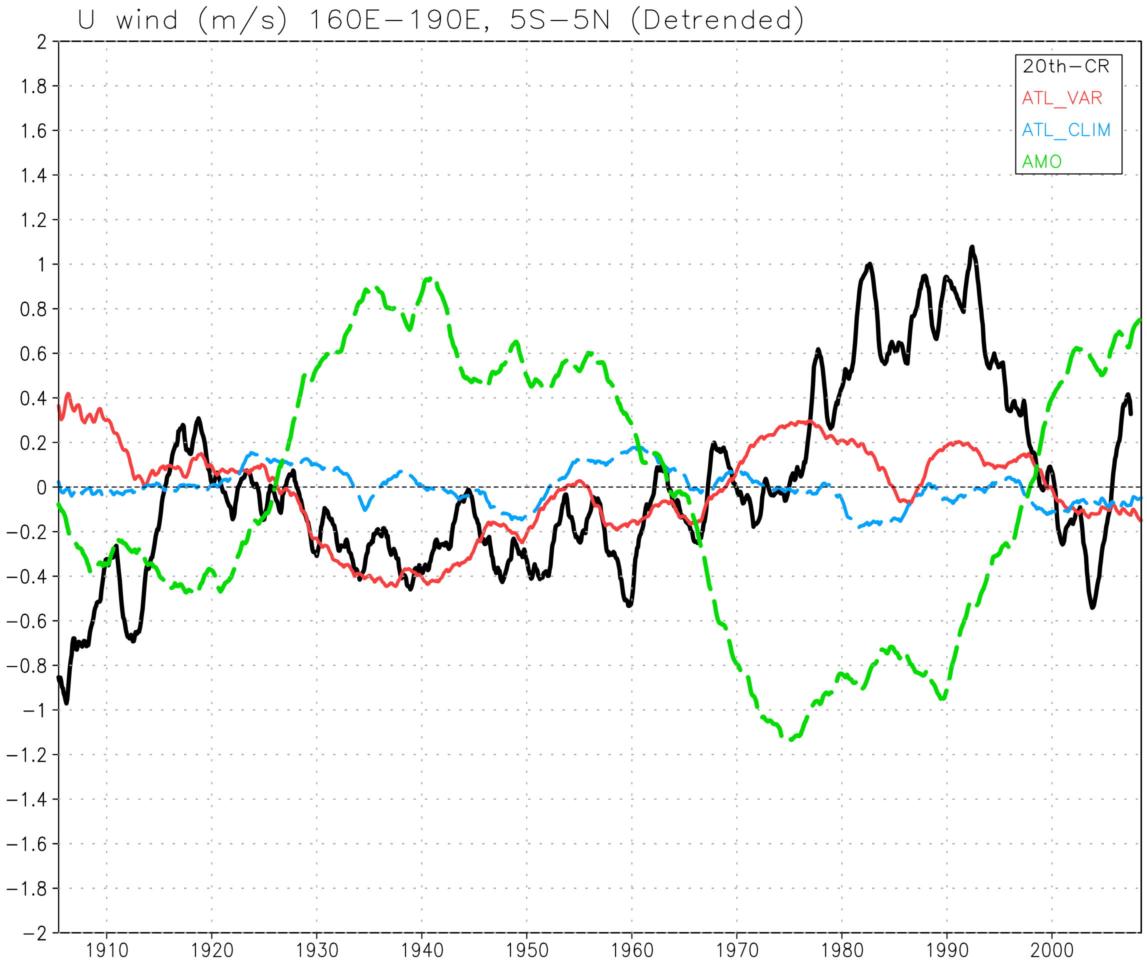

From F. Kucharski, F. Irkam et al. (2015), Clim Dyn, DOI 10.1007/s00382-015-2705-z

c) Long-term changes and trends due to Atlantic SSTs

Atlantic mean SSTs (red), global mean SSTs (black), tropical Pacific SSTs (green), SPEEDY-RGO Pacific SSTs (blue).

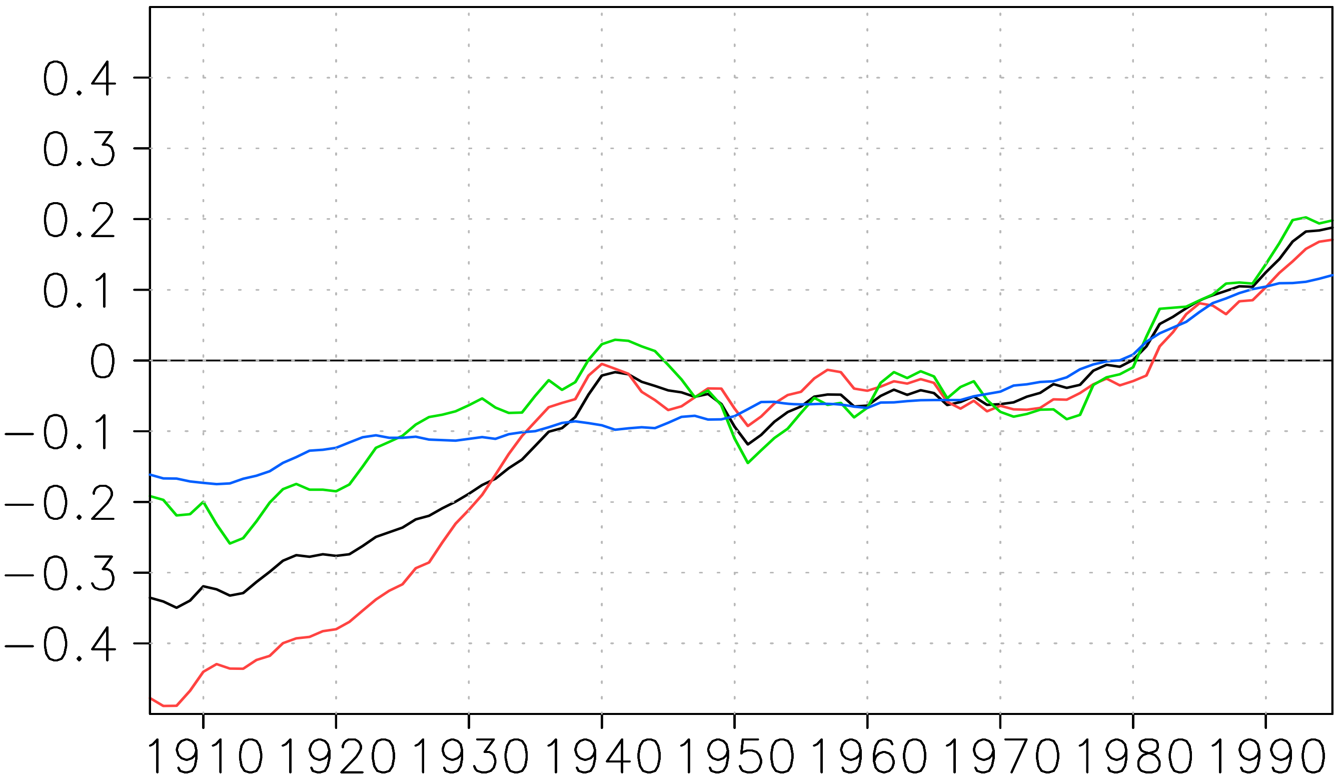

From: Kucharski et al., 2011: GRL, VOL. 38, L03702, doi:10.1029/2010GL046248

Long-term changes and trends due to Atlantic SSTs

Atlantic mean SSTs (red), global mean SSTs (black), tropical Pacific SSTs (green), SPEEDY-RGO Pacific SSTs (blue).

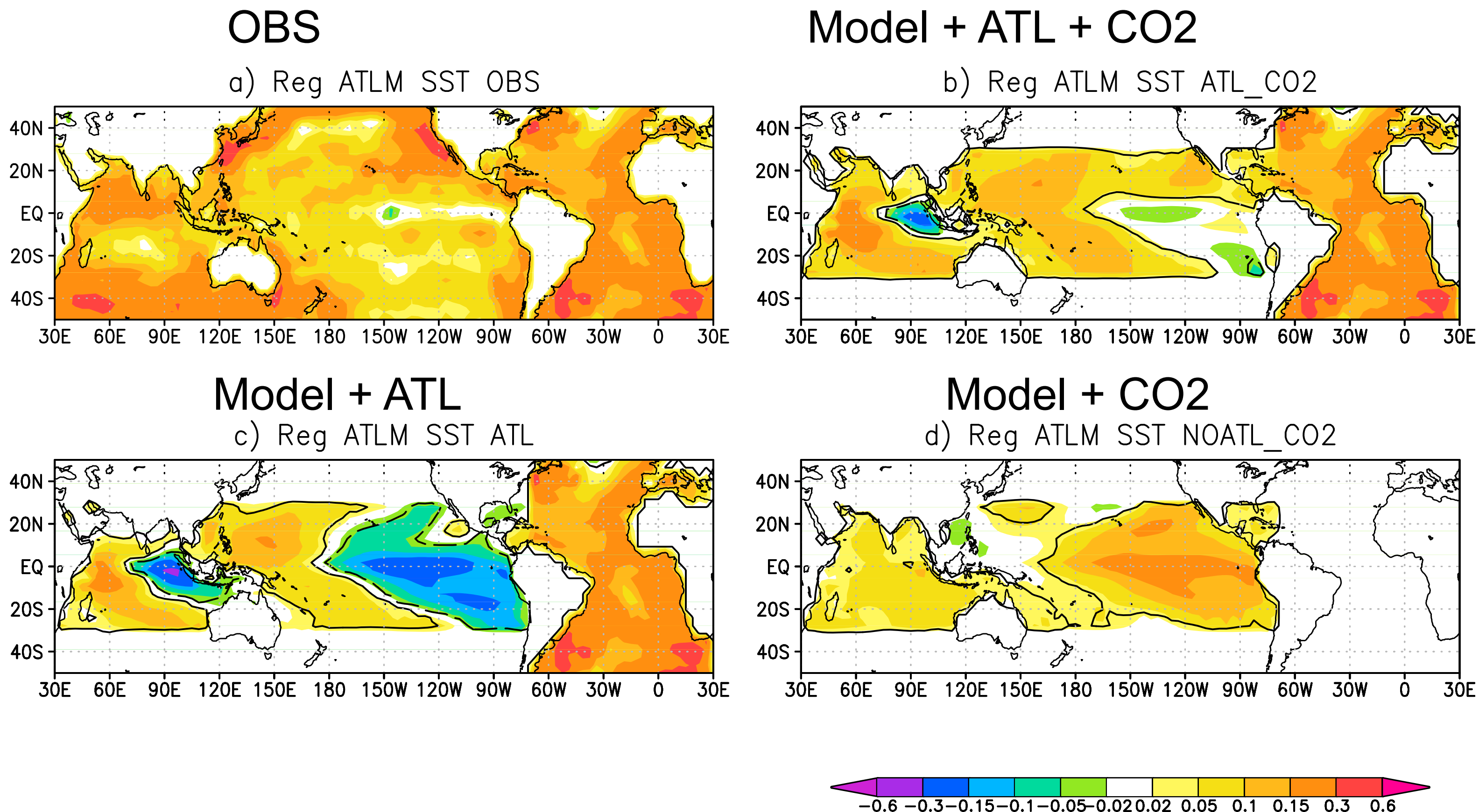

Essentially looking at trends here.

From: Kucharski et al., 2011: GRL, VOL. 38, L03702, doi:10.1029/2010GL046248

The following results published in:

Sun et al. (2017) Western tropical Pacific multidecadal variability forced by the Atlantic multidecadal oscillation, NATURE COMMUNICATIONS | 8:15998 | DOI: 10.1038/ncomms15998

The Abdus Salam International Centre for Theoretical Physics

SST variability over WTP

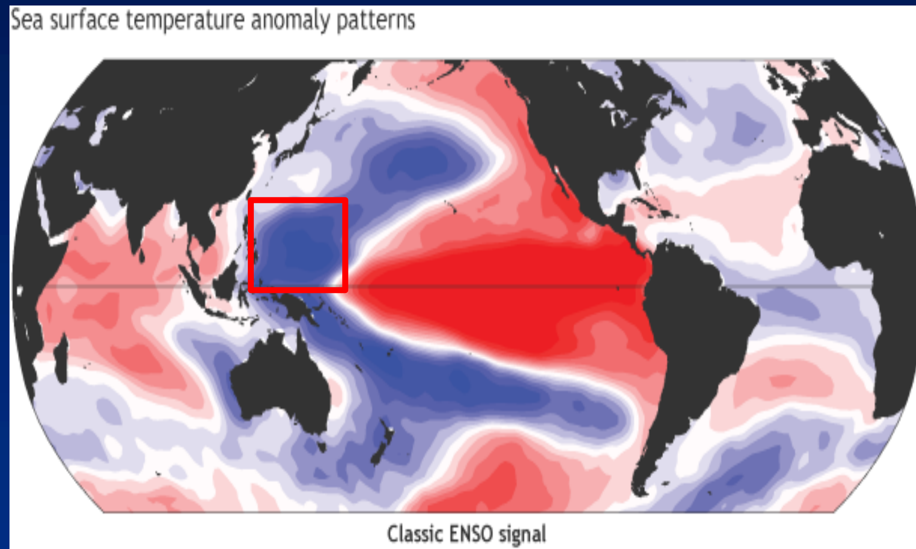

A seesaw pattern over tropical Pacific at interannual time scales, which is related to ENSO

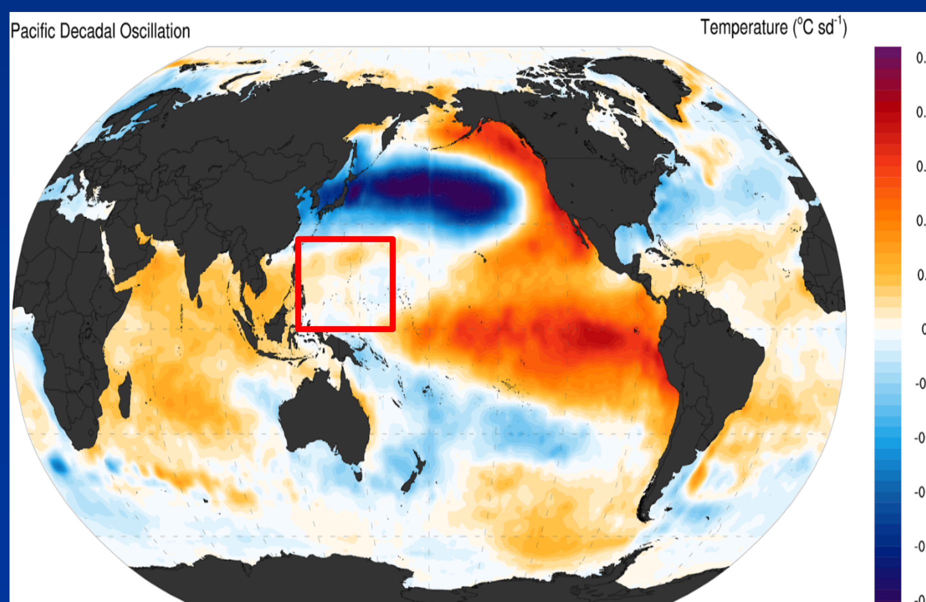

Decadal SST variability over western tropical Pacific (WTP) is unlikely to be explained by the IPO/PDO

Decadal time scales: IPO mode or ENSO-like interdecadal variability

WTP decadal SST variability and AMO

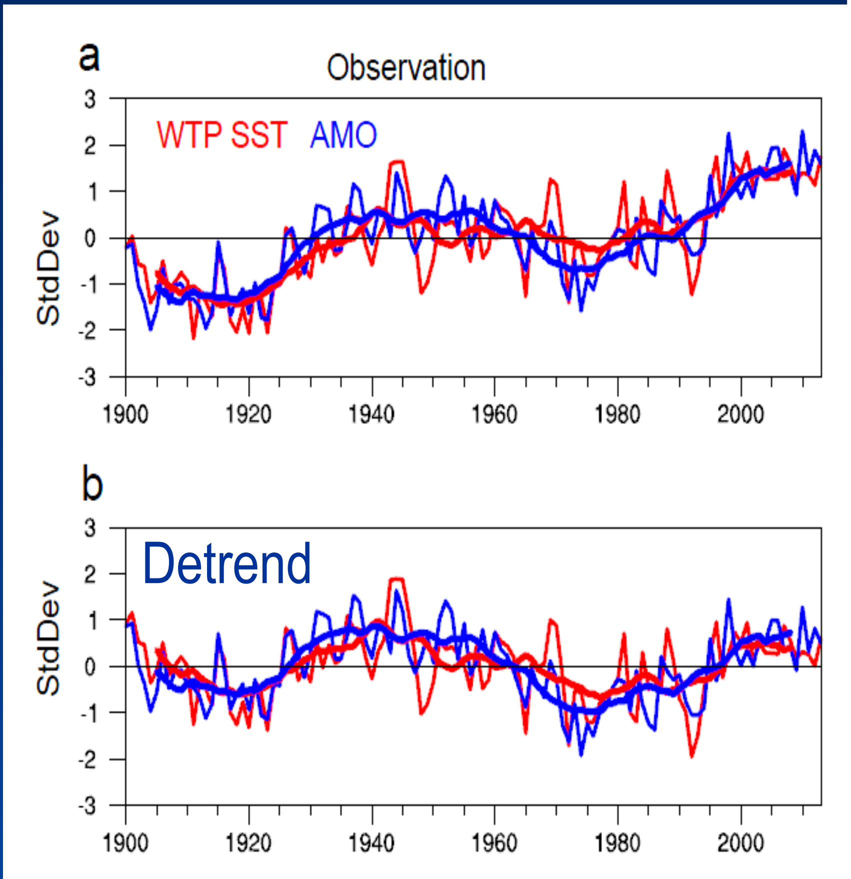

Atlantic Pacemaker experiment: ATL_VARMIX

Pacemaker

Local air-sea interaction

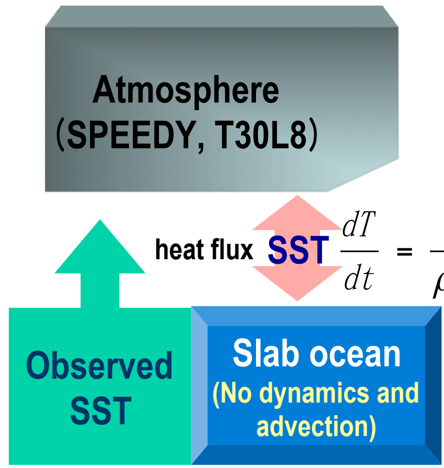

$$\frac{dT}{dt} = \frac{F_{net}}{\rho C_p H}$$

Mixed layer model + AGCM

Mixed layer depth	40 m tropics, 60 m extratropics
Ensemble Member	5
Model Period	1872-2013
Analyze period	1900-2013

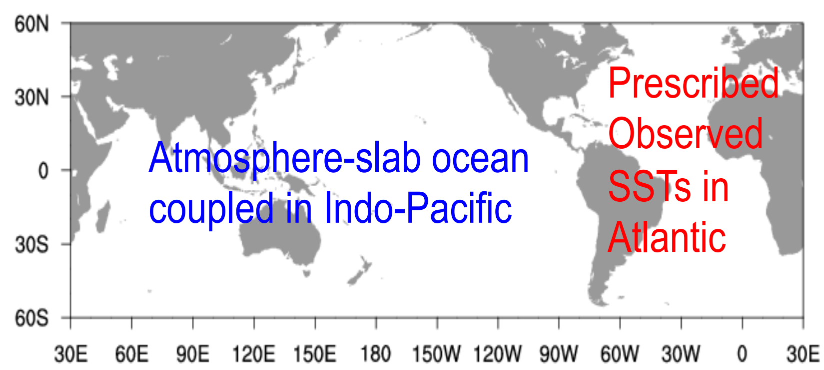

WTP decadal SST variability and AMO

ATL_VARMIX successfully reproduces the WTP-AMO connection

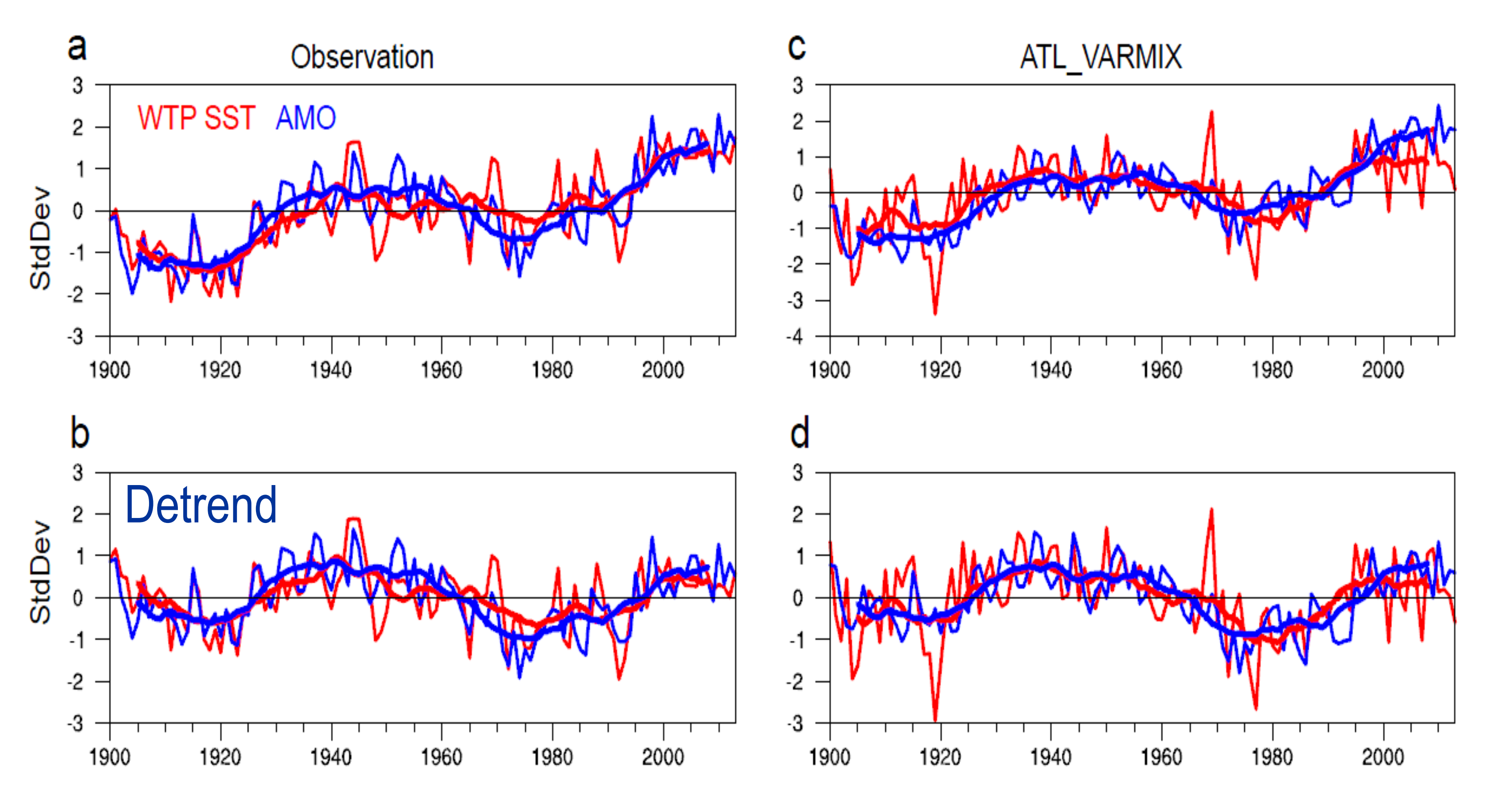

The Abdus Salam International Centre for Theoretical Physics

Lead-lag correlation between WTP SST and AMO

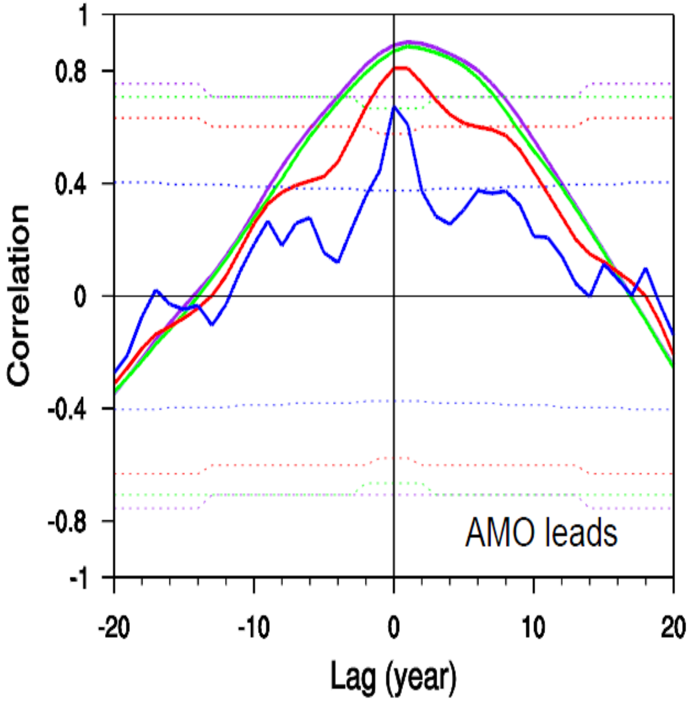

Spectral analysis of WTP SST

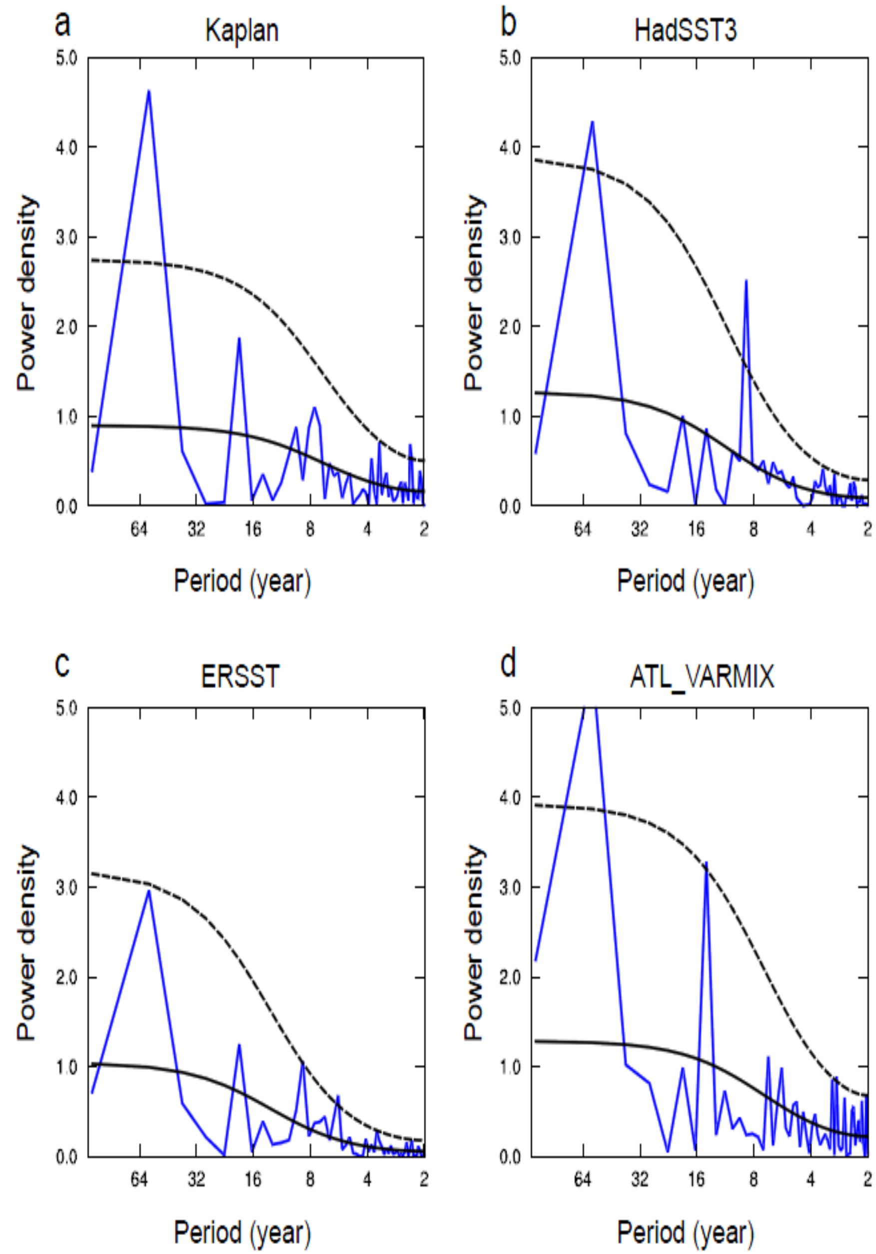

Decadal SST teleconnection: reproduced by the Atlantic Pacemaker exp.

Correlation map between WTP SST index (in box) with global SSTs

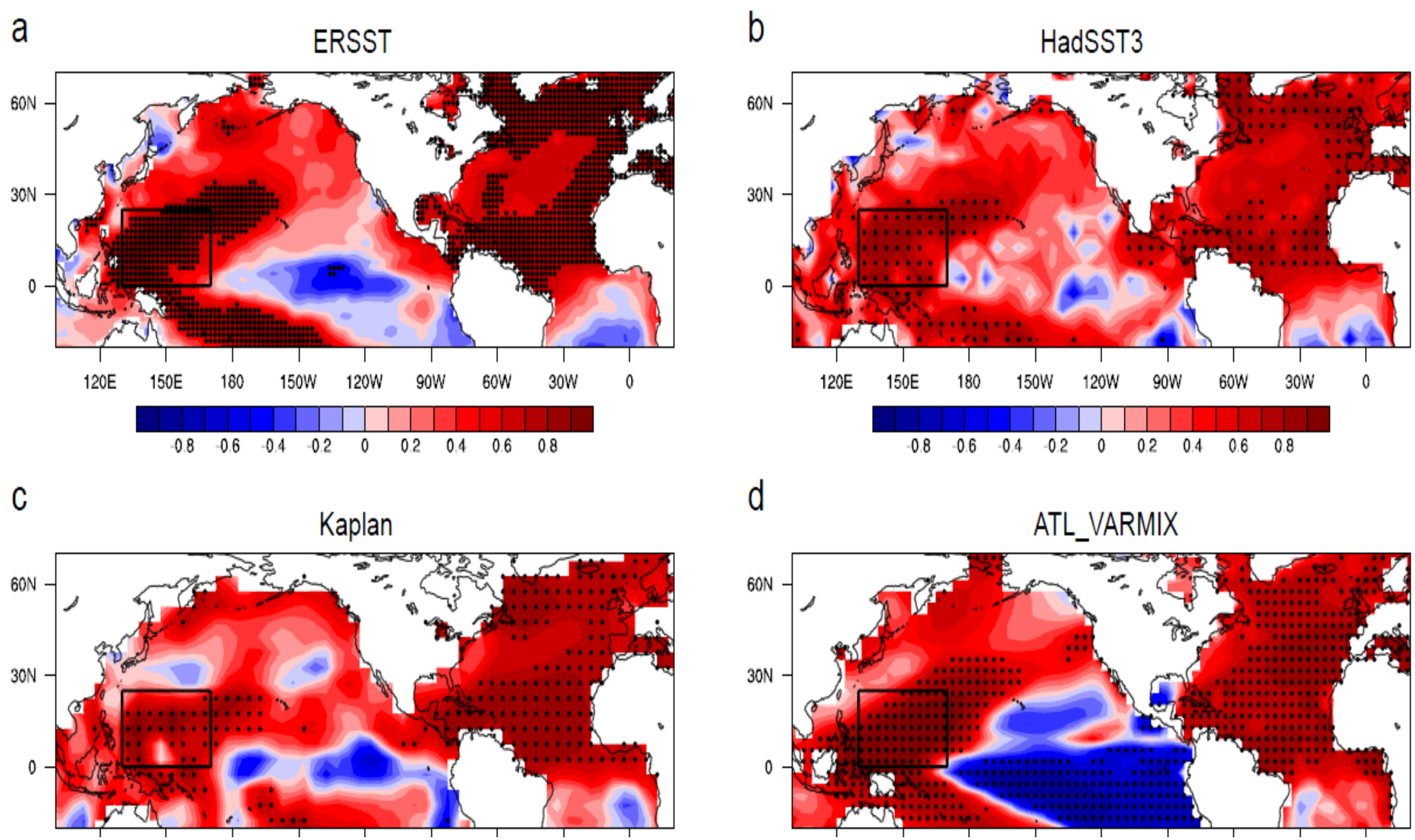

•

Schematic graph

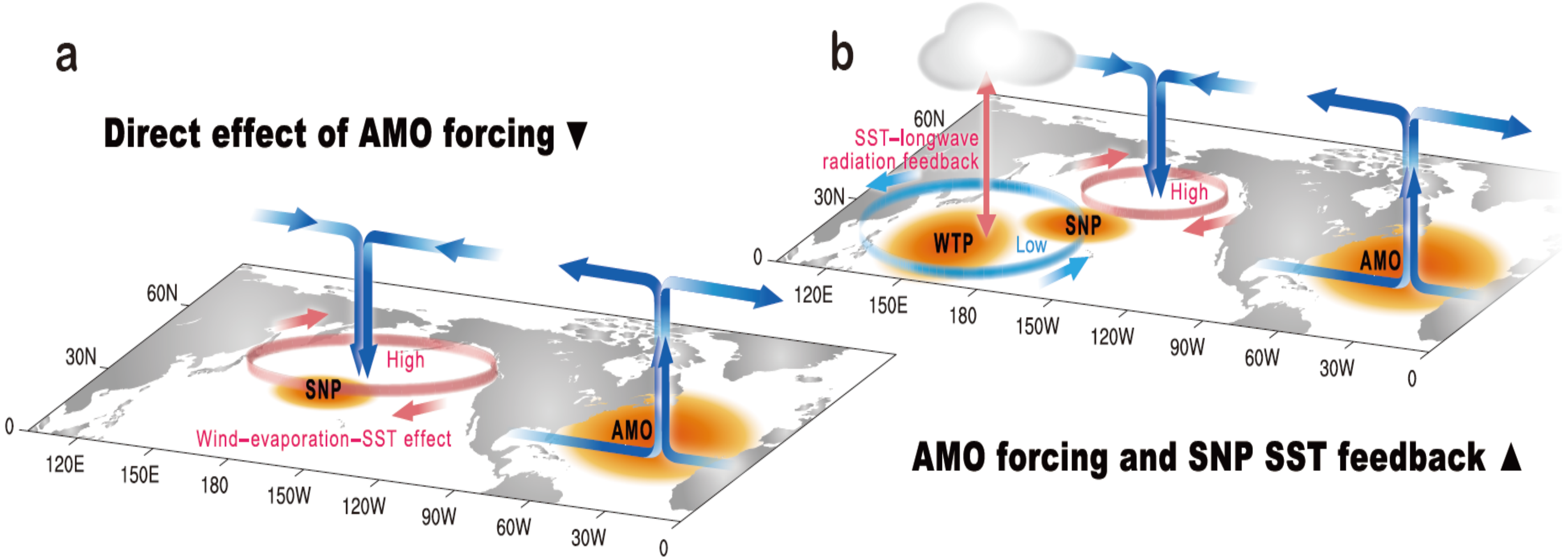

Atlantic Ocean acts as a key pacemaker for the western Pacific decadal climate variability

•

The Abdus Salam International Centre for Theoretical Physics

Example 6: Intraseasonal ENSO teleconnection changes

See Adnan M Abids talk, here just the caninical wavetrain

Rossby waves

- $\zeta = \frac{\partial v}{\partial x} - \frac{\partial u}{\partial y}$ Vertical component of relative vorticity
- $f = 2\Omega sin\phi$ Planetary vorticity

$$\frac{D(\zeta + f)}{Dt} = -(\zeta + f)\nabla \cdot \vec{v}$$

a source term!

Dispersion relation: $\nu = \overline{u}k - \beta k/K^2$

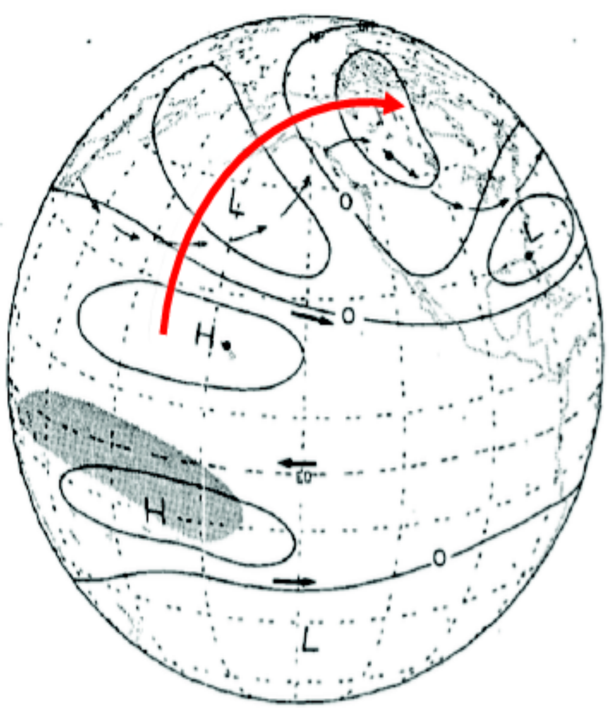

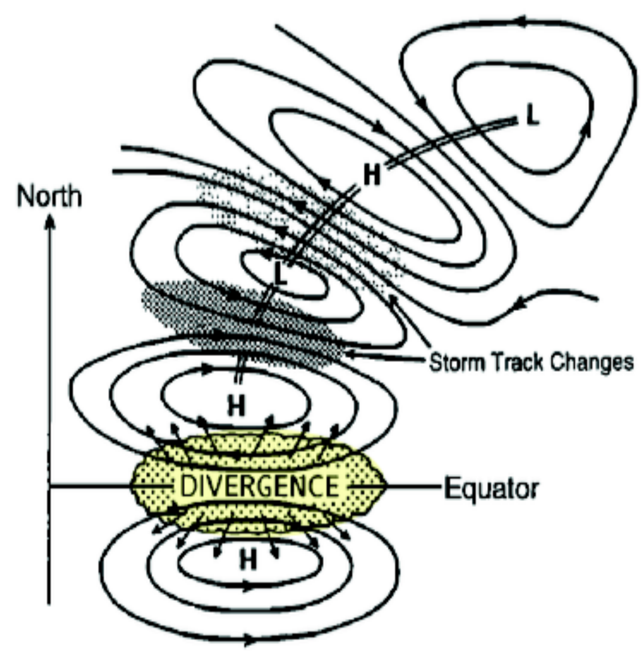

Canonical ENSO wave-train for December-to-February mean

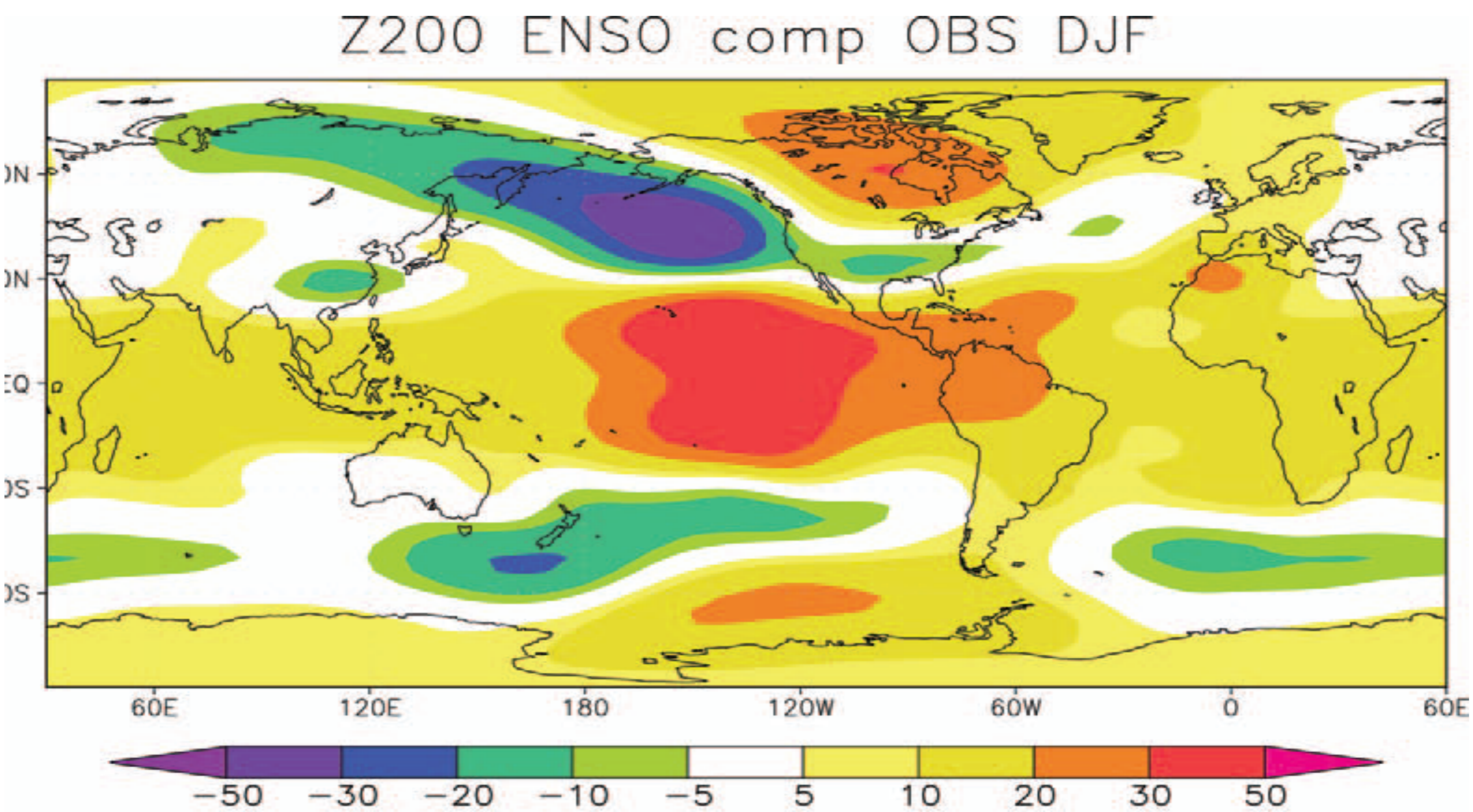

The Abdus Salam International Centre for Theoretical Physics

Another Mechanism for ENSO teleconnections

·

Typical winter El Nino composite of a field indicative for upper-level flow

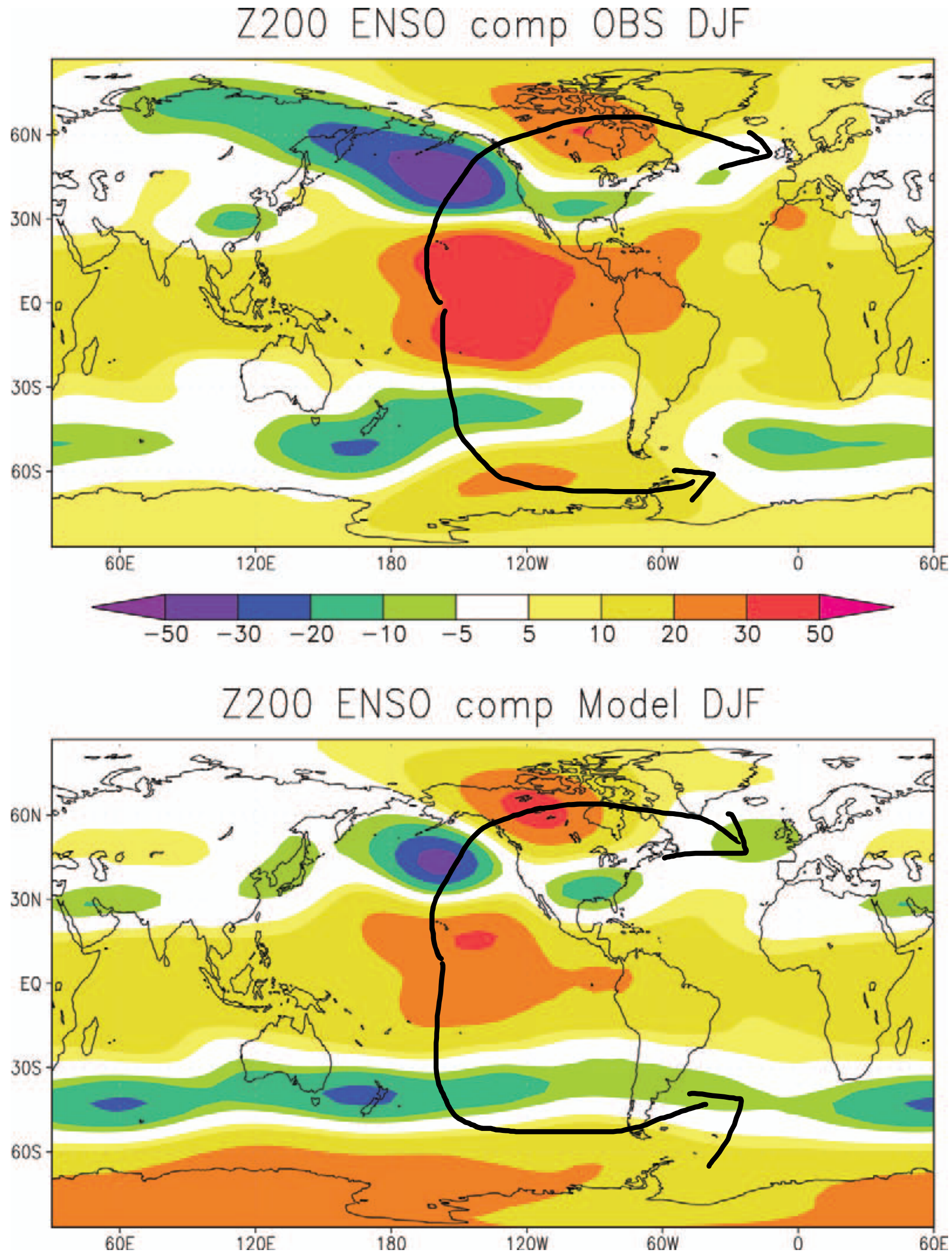

Source: Kucharski et al., 2013, BAMS, DOI:10.1175/BAMS-D-11-00238.1

Another Mechanism for ENSO teleconnections

Typical winter El Nino composite of rainfall

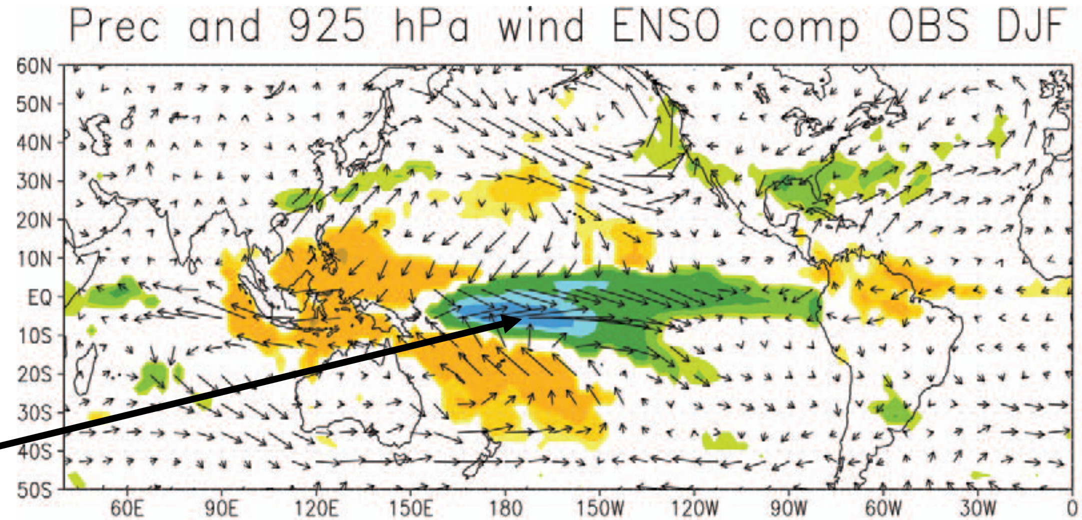

These winds in the central Pacific (related to Gill response) are important to provide the positive feedback to ENSO; they change the tilt of the 'thermocline'.

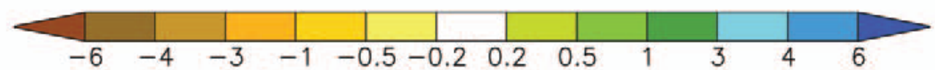

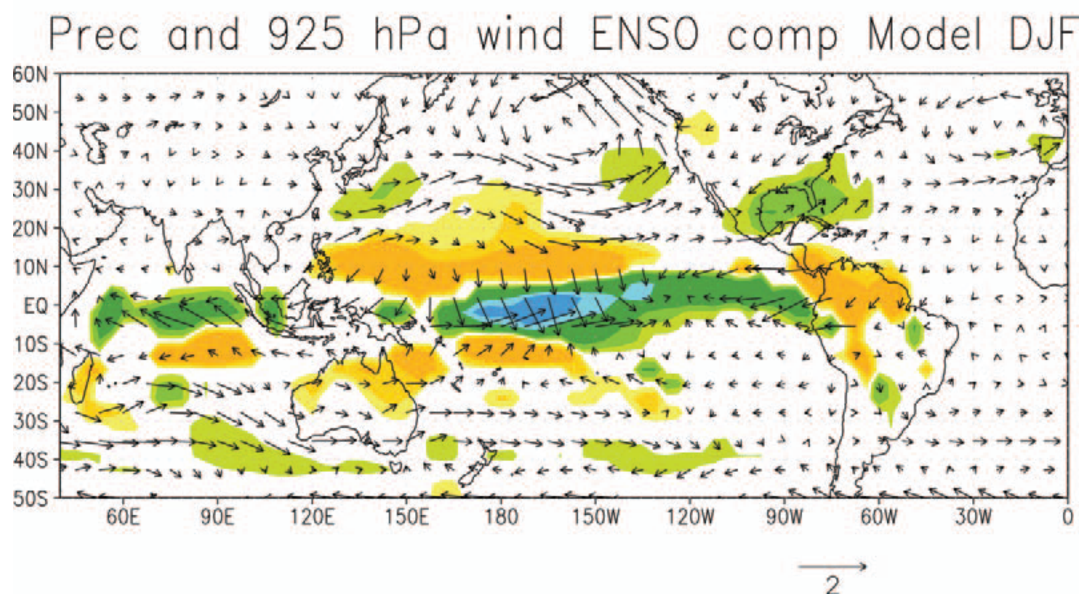

Source: Kucharski et al., 2013, BAMS, DOI:10.1175/BAMS-D-11-00238.1

Canonical ENSO wave-train; note it can also perturb meridional heatfluxes into stratosphere

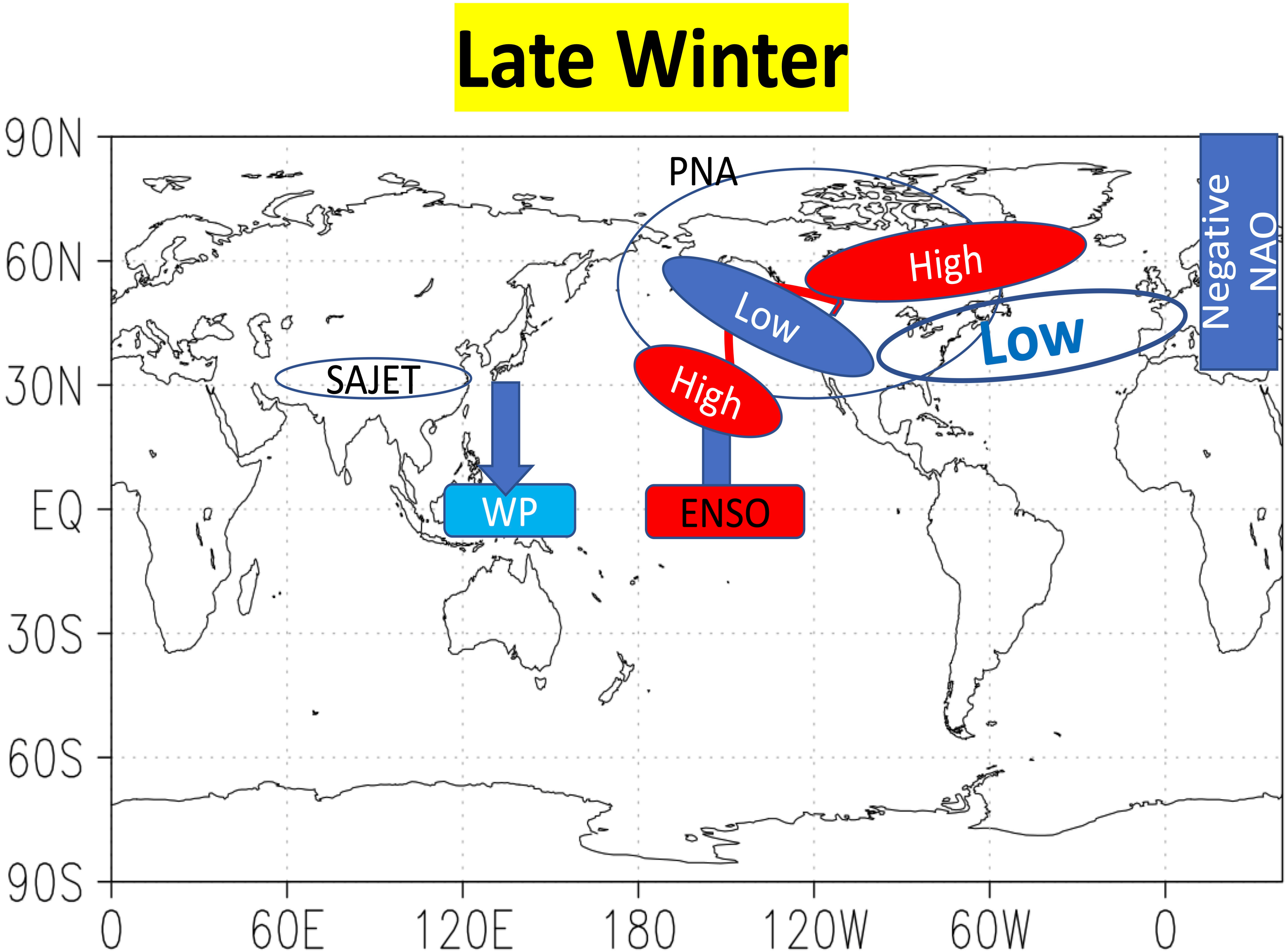

https://www.ictp.it/about-ictp/media-centre/news/2022/4/esp-postdoc-2022.aspx#close

NEWS HIGHLIGHTS

Postdoctoral Opportunity

For research in climate dynamics, climate variability and ocean-atmosphere interactions

13/04/2022

Postdoctoral Opportunity

ICTP seeks applications for one postdoctoral position from outstanding young scientists with a strong research record.

The position is in the Earth System Physics (ESP) section in the broad areas of climate dynamics, climate variability and ocean-atmosphere interactions. The ESP section provides a vibrant international research environment with an intense programme of workshops and conferences. Postdoctoral fellows are also encouraged, and supported, to participate in activities in developing countries in order to promote the mission of ICTP.

The ICTP takes seriously its commitment to equal opportunity and diversity in hiring, and in its global mission to promote science in the developing world.

Fellows must have completed a PhD in Meteorology, Oceanography, Climate Dynamics or related disciplines prior to the start of their Fellowship. Candidates who have experience in the research areas mentioned above and who obtained their PhD after 2017 will be given priority.

ICTP offers internationally competitive remuneration and a number of benefits. The appointment will be initially made for one year. Candidates should apply through the ICTP online application system.

Application deadline: 31 July 2022

Please note that only short-listed candidates will be contacted by e-mail after the selection process (mid -August).

Contact: esp@ictp.it

Apply online